

# Evaluation and Validation of Canopy Laser Radar (LIDAR) Systems for Native and Plantation Forest Inventory

David L.B. Jupp, Darius Culvenor,  
Jenny L. Lovell and Glenn Newnham

CSIRO Marine and Atmospheric Research Papers.  
Number 020.



Enquiries should be addressed to:

Dr. David Jupp

CSIRO Marine and Atmospheric Research  
GPO Box 3023  
Canberra ACT 2061  
Phone. +61 2 6246 5985  
Fax. +61 2 6246 5988  
Email. David.Jupp@csiro.au

Evaluation and validation of canopy laser radar (LIDAR)  
systems for native and plantation forest inventory.

Bibliography.  
ISBN 9781921232961 (pdf).

1. Forests and forestry - Australia - Remote sensing. 2.  
Natural resources - Australia - Management. 3. Sustainable  
forestry - Australia. I. Jupp, David L. B. II. CSIRO.  
Marine and Atmospheric Research.

333.751701526982

## **Copyright and Disclaimer**

© 2007 CSIRO To the extent permitted by law, all rights are reserved and no part of this publication covered by copyright may be reproduced or copied in any form or by any means except with the written permission of CSIRO.

## **Important Disclaimer**

CSIRO advises that the information contained in this publication comprises general statements based on scientific research. The reader is advised and needs to be aware that such information may be incomplete or unable to be used in any specific situation. No reliance or actions must therefore be made on that information without seeking prior expert professional, scientific and technical advice. To the extent permitted by law, CSIRO (including its employees and consultants) excludes all liability to any person for any consequences, including but not limited to all losses, damages, costs, expenses and any other compensation, arising directly or indirectly from using this publication (in part or in whole) and any information or material contained in it.

**Project Client:**

Forest and Wood Products Research and Development Corporation (FWPRDC)

**Project Number:**

FWPRDC PN 02.2902

**Project Title:**

Evaluation and Validation of Canopy Laser Radar (LIDAR) Systems for Native and Plantation Forest Inventory

**Project Manager:**

Dr Robert Lockwood  
Ensis

**Report Completion:**

April 2005.

**Contact:**

David L B Jupp  
CSIRO Marine and Atmospheric Science  
PO Box 3023  
Canberra ACT 2601  
[David.Jupp@csiro.au](mailto:David.Jupp@csiro.au)

**Team Members:**

David L B Jupp	CSIRO Marine and Atmospheric Science
Darius Culvenor	Ensis
Jenny Lovell	CSIRO Marine and Atmospheric Science
Glenn Newnham	Ensis
Nicholas Coops	(Formerly) CSIRO FFP (Presently) University of British Columbia, BC, Canada
Greg Saunder	ForestrySA
Murray Webster	Forests NSW

**Funding:**

The Forest and Wood Products Research and Development Corporation, CSIRO Earth Observation Centre (a unit in CSIRO Atmospheric Research) and CSIRO Forestry and Forest Products have provided direct support for this project. Forests New South Wales and ForestrySA have provided significant in-kind support and access to data and information.

# **Evaluation and Validation of Canopy Laser Radar (LIDAR) Systems for Native and Plantation Forest Inventory.**

## **ABSTRACT**

The opportunity for new technologies based on laser radar (or Lidar) to significantly improve forest measurement and contribute to improved forestry operations at similar or lower costs than current methods has been addressed by developing field assessments of current airborne Lidar and a novel CSIRO developed ground based Lidar system. The CSIRO ground-based system is called the ECHIDNA® and it is currently being tested using a prototype called the ECHIDNA® Validation Instrument or "EVI". The idea of the ECHIDNA® has attracted great interest among forest measuring groups and it has been shown that in its planned ongoing development and commercialisation, the ECHIDNA® instrument has the capability to undertake many if not all of the in-forest measurement tasks necessary for standard inventory. It has also been shown how the airborne and ground based data can be linked and matched through consistent models of canopy/Lidar interactions. The potential for new methods of forest assessment and the development of efficient allometry from both ground and airborne Lidar systems provides a pathway to future accurate and cost effective methods of forest assessment. The findings provide a strong case for making these systems available to the industry through commercialisation and product development.

Cover Picture: The cover picture shows the ECHIDNA® Validation Instrument (EVI) in the snow in Tasmania during its first deployment in the Project in July 2004.

## Table of Contents

1	Executive Summary.....	1
2	Introduction .....	2
2.1	Project Objectives.....	2
2.2	Forest Measurement practice.....	3
2.2.1	Forestry and Forest Inventory.....	3
2.2.2	Environmental and Ecological Measurements .....	4
2.2.3	The statistical basis of forest measurement .....	5
2.2.4	Commercial and Financial Basis .....	6
2.3	New Technology Options using Lidar.....	7
2.3.1	Lidar Basics .....	7
2.3.2	Remote Sensing .....	10
2.3.3	Ground Based Technologies.....	12
2.4	Report Outcomes and Structure.....	12
3	The CSIRO ECHIDNA® Validation Instrument (EVI).....	15
3.1	Options for using Laser Rangefinders .....	17
3.1.1	Commercially available ground-based lidar instruments .....	17
3.1.2	Rangefinder Prototype ECHIDNA® (RPE).....	20
3.2	ECHIDNA® Validation Instrument (EVI).....	25
3.2.1	Motivation behind build .....	25
3.2.2	Hardware description.....	26
3.2.3	Operation .....	36
3.3	ECHIDNA® processing algorithms using EVI.....	37
3.3.1	EVI Base Data .....	38
3.3.2	Data Re-Projections.....	41
3.3.3	Statistical Analysis of ECHIDNA® Waveforms .....	44
3.3.4	Trunk density and size distribution .....	54
4	Best Practice Airborne Lidar Processing.....	56
4.1	Introduction .....	56
4.2	Airborne Lidar Systems.....	56
4.3	Analysis of Discrete Point Data .....	58
4.3.1	Digital Elevation Model .....	59
4.3.2	Canopy Height.....	59
4.4	Foliage Analysis .....	61
4.4.1	Canopy Cover .....	62
4.4.2	Vertical structure .....	62
4.5	Scaling up ground-based measurements .....	64
5	Research Outcomes .....	66
5.1	Introduction .....	66
5.2	Field sites.....	67
5.3	Hemispherical photography.....	68
5.3.1	Principles and applications .....	68
5.3.2	Mast system .....	69
5.3.3	Photograph processing and modelling.....	70
5.4	ECHIDNA® processing results.....	72
5.4.1	Pgap Method.....	73
5.4.2	Waveform Modelling Method.....	74
5.5	Comparisons between ground and airborne data.....	76
5.5.1	ALS Canopy height .....	76
5.5.2	Foliage profiles from ALS, EVI and field data .....	79
5.6	Trunks and Counting methods.....	85

5.6.1	EVI Data Processing.....	86
5.6.2	Tree Counting by range .....	87
5.6.3	Using EVI as a “Relaskop” .....	89
6	Potential Commercial Applications.....	94
6.1	Commercial opportunities in forest measurement.....	94
6.2	Industry uptake arising from the FWPRDC Project.....	97
6.2.1	Increased Industry Adoption .....	98
6.2.2	Commercialisation of ECHIDNA® .....	98
6.3	Future R&D .....	99
7	Conclusions .....	100
7.1	Modelling and Measuring Canopy Structure.....	100
7.2	Tree Counting and Trunks.....	100
7.3	Accuracy and Value of the Data.....	101
7.4	Commercialisation and Adoption.....	102
8	Acknowledgements .....	103
9	References .....	104
9.1	CLI Journal Papers .....	104
9.2	CLI Conference Papers.....	104
9.3	CLI Reports .....	104
9.4	CLI Patents and Applications.....	104
9.5	General References.....	105
10	Appendix 1: Field Sites and Data Collected.....	109
10.1	Site Selection Criteria.....	109
10.2	Tumbarumba.....	109
10.3	Mt Gambier .....	109
10.4	Florentine Valley .....	110
10.5	Wedding Bells .....	110
10.6	Summary Tables.....	111
10.6.1	Details of Demonstration Sites.....	111
10.6.2	Airborne LIDAR Data Specifications .....	112
10.6.3	Summary of Ground Validation Measurements.....	113
11	Appendix 2: Angle Count methods used at Field sites.....	115
11.1	Theory.....	115
11.2	Units .....	118
11.3	Site Protocols for EVI validation .....	119
11.4	Output site statistics.....	119
12	Appendix 3: The Lidar Equation .....	122
13	Appendix 4: tree size, basal area, form factor & volume .....	124
13.1	Basics and Summary .....	124
13.2	Identifying the angular spans of trees.....	128
13.2.1	Lidar return model.....	128
13.2.2	Measuring the angular span.....	129
13.2.3	EVI “Relaskop” methods.....	134
13.3	Computing the Basal Area estimates.....	135
13.3.1	The standard “Relaskop” method.....	135
13.3.2	Obscuring and a model for its effect .....	137
13.3.3	Estimating other parameters and complexities.....	143
13.4	Basal area by size class.....	144
13.5	Taper and stem form.....	146
13.6	Deriving Form Factor from EVI data.....	148

# 1 EXECUTIVE SUMMARY

The CSIRO Canopy Lidar Initiative (CLI) has had strong support over the past three years from the FWPRDC, CSIRO and industry partners from ForestrySA and Forests NSW. The FWPRDC project has aimed to evaluate the potential of advanced forest inventory and mapping tools based on Lidar technologies. A significant aspect of this work was proving the value of ground based Lidar as a plot measurement tool. After evaluating existing and commercially available ground based Lidar technology, CSIRO decided that such instruments could not fulfil the demanding requirements of forest assessment and that access to a prototype of the CSIRO designed system called “ECHIDNA®” would significantly enhance the project outcomes. The ECHIDNA® idea had previously attracted great interest from forest measuring groups. The Australian engineered prototype, the “ECHIDNA® Validation Instrument” (EVI), has been shown to produce advanced 3-D image information of forests, and provide the means to retrieve standard forest structural parameters and advanced descriptions of forest structure not previously available through any other practical means.

CSIRO has used standard forest measurements as validation for Lidar based estimates of forest structure at a range of forest sites in Eastern Australia. These structural descriptions included both standard inventory and environmental aspects of forest structure such as cover, height, basal area, leaf area index (LAI), bole height and foliage profiles. Both airborne and ground based systems were able to measure many of these parameters in an efficient and repeatable manner. The combination of both airborne and ground based Lidar systems are able to work together to provide complementary data sets working at different scales of forest mapping.

At the forest floor, the EVI data has demonstrated the methods by which future commercial ECHIDNA® instruments will measure pre-harvest information such as tree size distributions and stem properties at both individual tree and stand scales that will be linked to estimates of timber volume by size class. The next step is to undertake an assessment of operational accuracy and cost-effectiveness in the context of commercial operations. This requires a comparison of pre-harvest assessment with post-harvest measures of delivered timber products and quantification of added value in terms of information accuracy, cost and timeliness based on minimal field activity. This is the next stage in the process of promoting adoption of a technology that offers objective and reliable information to underpin resource management decisions. It is planned for this to occur over the coming year in the form of pilot projects with industry partners. It will also occur in parallel with commercialisation activities for equipment and software to provide future access to the technology and with a growing activity in R&D to exploit the opportunities that have now been uncovered.

A significant issue for the uptake of new technology such as Lidar is the availability of instruments, suitable software and project support. The level of hardware and software validation of the airborne and ground based systems undertaken in this project has significantly reduced the technology risk previously associated with the commercial and operational use of lidar in Australian forestry and will help enable local commercialisation of the ECHIDNA® concept and other advanced Lidar systems in the future providing the means for industry to access both the hardware and its operational support.

## 2 INTRODUCTION

### 2.1 Project Objectives

In mid-2002, CSIRO Earth Observation Centre (or EOC, a unit in CSIRO Atmospheric Research) and CSIRO Forestry & Forest Products, in company with ForestrySA and Forests NSW embarked on a major project with the support of the Forest and Wood Products Research and Development Corporation (FWPRDC). The project is now complete and this document is its Final Report.

The Objectives planned for the project were:

- Validate and characterise new CSIRO methods for forest inventory measurements in Australian native and plantation forests which use airborne and ground based Lidar data;
- Demonstrate and validate ECHIDNA® Lidar measurements using available hardware with patented algorithms and methods;
- Test the accuracy and value of data obtained by this technology against conventional forestry and other field measurements; and
- Develop strategies for the widespread adoption of the technology and the methods for Australian and international forest inventory.

A “Lidar” (or Light/Laser Radar or Light/Laser Detection And Ranging) is an instrument in which a beam of laser energy in the optical or adjacent region is transmitted in a specific direction and the time (or phase) and intensity of any return signals from materials and objects are used to measure the distance to and amount of scattering materials encountered by the beam. Lasers have, in recent times, become highly developed and affordable instruments with many applications.

CSIRO has, since mid-2000, promoted the development of Lidar technology, instrumentation and applications in forestry with the purpose of seeing the emergence of both a supporting (potentially Australian) industry developing and using the technology as well as the wide-spread use of the technology in forest operations throughout the world.

The areas of potential application encompass both airborne Lidar technology, including currently available Terrain Lidar systems and currently experimental Canopy Lidars, and ground based Lidars for measurements within forests as an extension of traditional plot-based inventory. As a result of the CSIRO studies, two system specifications were promoted – one for an airborne technology (called “VSIS”) and one for a ground based technology (called “ECHIDNA®”). The specifications included hardware and software for forest information extraction.

Since Canopy Lidars are not available to be flown in Australia even at this time, and since at the time the project was started, the ECHIDNA® was a developing CSIRO innovation and not yet a commercially available instrument (nor even a prototype), the original project aim was to use available systems in a way that simulated the outputs of the proposed systems. In the case of the airborne data this has been done to the extent that it is possible and how best use of current airborne technology can be made is discussed later in the Report.

In the case of the ground-based system, it was decided (for reasons presented in Section 3) that simulations based on commercially available systems would not be adequate to demonstrate the potential of the ideas for forest assessment. The project was therefore revised to take advantage of the build of a prototype of the proposed instrument that CSIRO has (now) assembled. The prototype system is called the ECHIDNA® Validation Instrument (EVI) and its description, use and validation forms a major part of the Report.

The Project Objectives have therefore only been modified in that the ground-based data were collected using the EVI and thereby took the study a step beyond what was originally proposed. In this way, the applications and commercial potentials of the technology have been much more extensively studied and the outcomes of the Project provide an excellent base for ongoing commercialisation and industry adoption in the future.

The Project was developed with a clear view of the potential for ground and airborne Lidar technology to improve the outcomes of forest inventory and also reduce the costs of inventory. However, all new technology carries risk that can make it hard to find investment or partners while the risk is still high. A key objective of the project was to undertake validation to reduce the technology risk as a means to promote investment and uptake in the Forestry industry. Future adoption by the industry will follow both from demonstrations of value and also from commercial availability of the tools. We believe that the prospects for both have been significantly improved by the work and outcomes that follow in this Final Report.

## **2.2 Forest Measurement practice**

### **2.2.1 Forestry and Forest Inventory**

The basic tool of forest measurement for the timber industry is Forest Mensuration. This area of forest science is well covered by available texts (e.g. Brack and Wood, 1998 and its references) and does not need to be repeated here. However, for the purposes of placing our work in context and structuring our assessments of the project we will briefly outline some of the most important aspects.

The forest industry and other industries involving management of vegetation depend on accurate information for planning and making sound management decisions. Among foresters the needs for measurement will depend on the purpose of the activity. For example, the needs will be different between activities such as:

- Early prediction of likely final yields;
- Ongoing management (such as for pruning or fertilizing) and
- Pre-harvest assessment for accurate estimates of delivered product.

The type of activity can obviously change the emphases of the measurements taken. Measurements for both the prediction of future yields (possibly 20-30 years into the future) and pre-harvest assessment will also differ depending on the product objectives or mix. Saw logs and milled timber products may be only one of the

products involved and in some cases the forest is grown for pulp alone. The requirements on information and measurement will clearly be different in these cases.

However, a common characteristic of situations where at least some of the forest is to be delivered to mills is that measurements of trunk and stem size, form and quality feature strongly in the measurements. In most cases, estimated timber volume by size class, and estimates of the likely timber quality are key outputs. Among the kind of parameters that are needed to achieve this over forest blocks are:

- Size distribution of Diameter at Breast Height (DBH);
- Tree height and its variation;
- Green level or bole height and its variation;
- Form Factors or taper;
- Trunk shape at various scales (sweep and defect).

The tree “shape” at the general scale relates to how “straight” the trees are and at the finer scale to how many “lumps and bumps” there are on the trunk. The existence of multi-stems and the height at which branching occurs are all significant factors in the quality of the timber delivered to the mill. However, size by itself is also important and extreme variation can cause as many problems as lack of larger trees.

Despite this variation, the main emphasis in forest inventory by the Forest Industry involves the structure of the forest and particularly the amounts and variations in stem sizes. Foliage and leaf are secondary factors in this activity. In operational forestry these data are integrated into management systems and provide basic information for business planning and operations management.

## **2.2.2 Environmental and Ecological Measurements**

The need to measure vegetation occurs much more widely than to meet the specific needs of foresters to manage and estimate the delivery of trees to mills. However, even in the forestry industry, many modern forestry operations are increasingly adding environmental measurements to their inventory data as information on tree function and health is incorporated into forest management operations and decision support systems.

Plant function, health and growth involve the use of light, water and nutrients as well as plant competition and succession as forests grow and interact. The overall growth of all tree components (leaves, stems, trunks, root etc) and their functioning in photosynthesis, transpiration and respiration generally place an emphasis on tree canopy, forest structure (the way leaves and stems are allocated vertically and horizontally) and leaf functioning that can be absent in activities aimed only at assessment of harvestable timber.

Increasingly, the forest industry is making use of growth models to forecast yields from early inventory data, and recognising the need to be aware of the “off-site” impacts of forestry and its interactions with cities, farms and native forests in national reserves. The need to assess potential impacts and threats both from outside and from inside a forest block has also led to greater need for measurements of vertical canopy

profiles (including the development of under-storey) and leaf amount. Leaf amount is usually expressed as Leaf Area Index (LAI).

Among the parameters needed to derive this type of information can be listed:

- Projective cover;
- Crown cover, size and openness;
- Stem density;
- Branching structure;
- LAI (per crown or per plot);
- Canopy profile (or vertical leaf area density);
- Leaf health (spectral or biochemical data).

There is considerable overlap between these measurements and those traditionally carried out by foresters. Many of the additional measurements needed for environmental needs can, with suitable field instruments, be incorporated in forestry field procedures with only the added marginal overheads in time and cost.

### **2.2.3 The statistical basis of forest measurement**

Because of the costly nature and large area involved in forest operations, the assessment of resources is normally carried out by sampling. However, because of the highly variable nature of forests – even plantation forests – the accuracy of the assessments can be poor unless sampling is well designed and extensive. As we will discuss later, this leads to a critical trade-off between cost and accuracy that drives many decisions in forest assessment.

Most current inventory is based on collecting information at a few intensive sites and extending this information with lower intensity plots or transects (sometimes called “cruising”) within the forest. The plots may be fixed in size and (possibly) position or they may be “plotless” and may be chosen independently on each occasion of measurement. The efficiency and representativeness of the data collected at the intensive sites are important factors in the effectiveness of the final estimates as is the efficiency of transect design. However, one of the most important factors in this equation is the nature of the forest and its variation.

Plantation forests are generally “simpler” to assess than native forests and in many cases inventory (especially in the early stages of growth) makes use of established relationships between the parameters for the type of tree being grown and its age to reduce the task of site measurement and the extent of cruising needed for a satisfactory result. These types of inference are generally known as “allometry”.

For example, ForestrySA make use of established relationships between key parameters to assess sites in terms of a relatively small number of “Site Quality” (SQ) classes. The classes are based on a key set of forest measurements of which only a few, because of the relationships found or assumed to exist in the forests, may be taken. Through many years of records and research, an established average relationship between SQ at one date (perhaps after 9½ years of growth) and final timber yield is used to estimate potential harvest and to identify areas which are not performing well and may be in need of attention. However, even in well-studied areas

these methods are not always accurate. In this situation, better alternatives that were no higher in cost will be very attractive.

In other areas, where new species are being used in new environments and possibly with different requirements (such as shorter growing period) there is not a strong base of existing information or research about how growth form and tree performance may change over time in that new environment and about how various parameters are related. In these areas, people may make use of growth models but are then faced with the need for more extensive measurements. The added need for measurements can sit rather uncomfortably with the higher start-up costs that new areas may also have.

To pursue an example that will be of specific interest in our evaluation of the EVI technology, a common estimate for timber volume over a stand or block can have the general form:

$$V = BA \times h \times FF$$

In this equation,  $BA$  is the basal area (or tree density ( $\lambda$ ) by mean area at breast height ( $\bar{A}$ ) leading to the expression  $BA = \lambda \bar{A}$ ),  $h$  is the mean height of a stand and  $FF$  is called the Form Factor. If the tree stems were cones with diameter DBH at the base and tapering to a point at the tree height ( $h$ ) then we would have the simple relationship  $FF = 1/3$ . However, tree shapes are not so simple and the stand Form Factor is the product of a set of complex factors that are combined into a stand characteristic for the type of tree in the particular environment and at the particular age.

The provision of sufficient individual tree measurements to scale up to this type of stand level equation can be very time consuming and involve measuring tree height, BA, DBH distributions at varying levels and other information taken for sufficiently many samples that the relationship stabilizes to a value suitable for the stand. However, once there exist established and stable statistical relationships between forest variables such as height, BA, DBH and FF then the requirements for site measurements reduce significantly. The development of allometric relationships is therefore important for sampling efficiency and to minimise costs. The corollary is that using inappropriate relationships may make the accuracy much worse and waste scarce resources.

Finally, it needs to be emphasised that provided the information taken at the sites is efficient and any allometry used has a proper base (and is accurate for the location) then there is no limit to the accuracy that can be achieved in forest inventory. It is simply a matter of taking a sufficient number of well-designed samples. Any limitations to the accuracy of forest information must arise elsewhere – such as in management objectives and economic constraints.

#### **2.2.4 Commercial and Financial Basis**

The principal factors defining and limiting the scope and accuracy of forest inventory are the cost and the marginal added value that the information provides for forest management and production relative to its cost. The value of the anticipated products to be harvested from the forest (sawlogs, pulp or mixed products), the extent of

current levels of investment in plant and equipment as well as current and anticipated commodity price levels can all obviously influence the precise point where added inventory becomes unprofitable.

From information on how forest operations are occurring in Australia and New Zealand it would seem that on average the limits of investment in inventory are reached at an expenditure of somewhere between \$20 and \$40 per hectare applied on at least two occasions during a standard 20-30 year rotation. At the same time, most operational forest companies recognise that the achievable accuracy this imposes on the information is too low and strongly feel the need for better and more extensive information to improve forest management and product delivery.

The added value of information can be in terms of direct impact on delivery of timber to a mill (such as decisions about whether to cut a block for pulp or sawlogs or whether to cut a non-performing block early or fertilize) or for reporting and valuations such as are required by investors and shareholders. There are an increasing number of legal and environmental reporting requirements on the industry that need adequate information levels and there is an increasing need to increase profits from marginally performing forests. Off-site aspects are also playing an increasing role in forest management – such as assessment of adjacent areas for fire risk to the forests or of the forests as fire risks to adjacent land uses and hydrological impacts of plantations on catchment water yield.

Whatever the exact level of investment accepted and value of information, the principle is the same. That is, the current state of forest inventory is capped by costs and currently perceived value of the information. Any attempt to improve the accuracy and introduce new and better information into forest management must work within the current cost levels if it is to be successful. Providing a wide range of new types of information – but at greater cost – or even providing greater accuracy for the same type of information – but at greater cost – is not likely to provide an acceptable solution. It is in this context, as well as the general measurement context outlined above, that we will frame and evaluate the potential for Lidar to improve accuracy and richness of forest information.

## **2.3 New Technology Options using Lidar**

### **2.3.1 Lidar Basics**

The term ‘LiDAR’ derives from the phrase ‘Light Detection And Ranging’, sometimes referred to as ‘LaDAR’ after ‘Laser Detection And Ranging’ and sometimes ‘Laser RADAR’. Laser radiation differs from conventional electromagnetic radiation in terms of spatial and temporal coherence. High temperature (e.g. solar) radiation results from direct thermal excitation of photons. This produces light that is spectrally broadband and incoherent (Measures, 1984). Laser radiation, conversely, is derived from stimulated (pumped) emission within a resonating chamber capable of producing spatially and temporally coherent energy. This is illustrated in Figure 2-1.

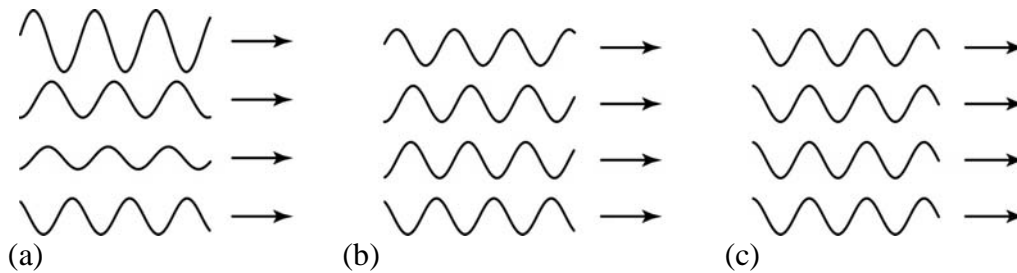


**Figure 2-1: Spatially and temporally incoherent radiation (a), temporally coherent radiation (b) and spatially and temporally coherent radiation (c).**

Lidar technology is not new. An extension of the echo-return principle applied in microwave radar systems for over half a century, one of the first laser-based rangefinders was developed in the early 1960's by Fiocco and Smullin (1963) for measuring atmospheric particulates. While both radar systems and laser rangefinders employ radiation emitted at the speed of light, laser systems have a number advantages for ranging applications,

- (i) the spatially coherent nature of laser radiation allows for excellent control over laser direction and divergence in the form of a 'beam',
- (ii) temporal coherence results in a narrow and stable wavelength output, and
- (iii) electrons in an excited state in a laser chamber can be caused to change state extremely rapidly, resulting in the emission of an intense pulse of energy within a very short duration, typically nanoseconds.

Such well collimated, monochromatic and short-pulsed lasers are ideal for remote sensing of the environment (Measures, 1984).

The essence of lidar is the time taken for an emitted pulse of light with a time variation of power of  $\Phi_0(t - t_p)$  with its peak power at  $t_p$  to be transmitted through space, reflected from an object and recorded back at the originating location. The range to the target is then calculated as (speed of light  $\times$  pulse traverse time / 2). This is illustrated in Figure 2-2.

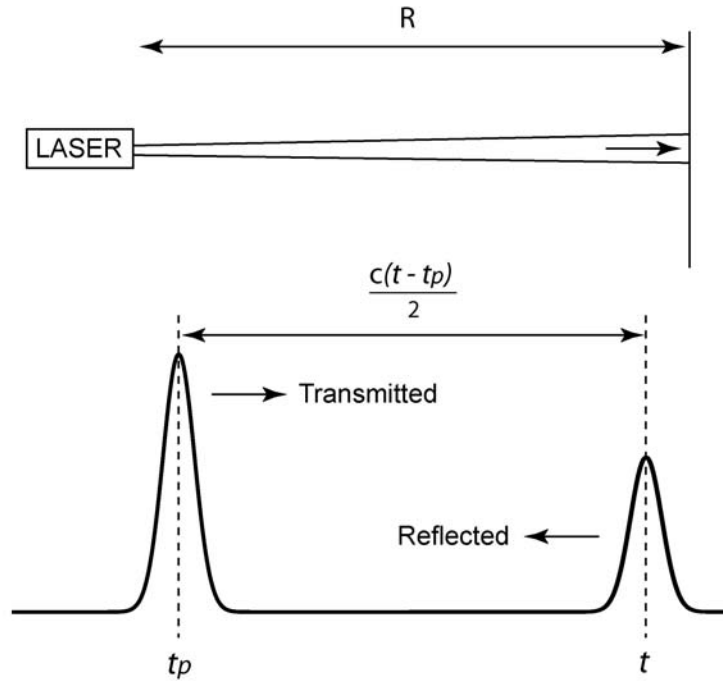


Figure 2-2: Pulsed laser rangefinding. The range,  $R$ , to the target is calculated from the time difference between the transmitted and reflected laser pulses.

Written symbolically, the returning signal from a flat solid target (a “wall”) will be sensed at a shifted time and with reduced intensity due to possible absorption by the wall and by the dissipation of the energy with distance. That is:

$$I(t) = \Phi_0 \left( t - t_p - \frac{2R}{c} \right) \frac{\rho_t}{R^2}$$

where  $I(t)$  is the time varying return signal,  $\rho_t$  is the reflectivity of the target (wall) and  $R$  is the distance to the wall. The factor “ $2R$ ” is present due to the laser pulse travelling to the target and back to the receiver. By measuring the time at the peak of the outgoing pulse ( $t_p$ ) and the time difference to the recorded peak of the return pulse the range ( $R$ ) can be measured as:

$$R = \frac{c(t - t_p)}{2}$$

A basic lidar instrument to record this returning “waveform” comprises a pulsed laser, a precise clock and a detector. In an ideal case such as that shown in Figure 2-2, the single return pulse is fully intercepted after being reflected from the flat surface perpendicular to the direction of propagation. However in real world environments, varying reflectance properties, partial beam interception and diverse surface orientations relative to the direction of the beam may result in a complex array of reflections for a single transmitted pulse. The shape and structure of the return signal is called its “waveform”.

There are basically three types of information available from a Lidar waveform. They are:

- Range
- Intensity
- Waveform shape and structure

Instruments using only the first are called Rangefinders. The range and bearing to events (usually just the first) returning a signal above a threshold are recorded and used to build up a 3D image of the most reflective targets in the operational field of the instrument. Instruments using the full waveform and its (calibrated) intensity are rare; however, they include the types of instrument that have best potential in forest measurement. Basically, we can regard targets as being “hard” if the returns are single pulses with simple modification (such as due to angle of incidence at a wall) and “soft” when the signal is dispersed and the waveform more complex. Vegetation components, especially foliage, twigs and branches, are generally a “soft” target for a Lidar. Rangefinders tend to find one or a few “hard” targets while the full waveform is a more desirable thing to measure when targets are “soft”. The modifications this adds to the simple Lidar equation above are described briefly in Appendix 3.

By tracing a pattern across the landscape, a tree, a rock-wall, a forest or any region, it is possible to build up a 3D view of the objects and arrangements that occur within it as well as the background terrain height when the scanning is from above. This report is about scanning Lidars. Some of the examples discussed are Rangefinders and some use all three types of information listed above from the Lidar waveform as well as the image structure to measure and map.

### **2.3.2 Remote Sensing**

The present FWPRDC Canopy Lidar Project and this Final Report concern an evaluation of the opportunities for forest measurement provided by Lidar technology based on the principles outlined above. One of these is the use of Lidar instruments in aircraft (or, in the future, on satellites) to remotely sense vegetation. However, since a Lidar is only a particular type of instrument carried on an aircraft or a satellite, the role of Lidar is best looked at in the more general context of remote sensing.

Remote sensing from airborne or spaceborne platforms provides a significant cost advantage for measurements that are needed covering large areas quickly, consistently and regularly. Satellite based instruments can also provide information worldwide and enable planning and monitoring information to be accessed from any part of the world. This “platform advantage” is realised only if the instrument(s) and data processing provide products that answer the questions users need to answer. While this may seem an obvious statement it so often turns out that available instruments provide a great deal of very interesting and novel data and information – but perhaps not the exact parameters or estimates familiar to the user. The user must then either adopt the new types of information or not use the data.

Remote sensing has been used in Forestry for many years. Stereo-pairs of aerial photography have been used to sample tree heights and to estimate stem density,

crown size and crown cover. Satellite images have been used to map cover, to assess crown health (leaf condition) and to provide general maps at the familiar “Landsat” scale. Unfortunately, the vertical view from the air or space makes it very difficult in this case to map the trunk and stem factors that are essential for forest inventory in forestry operations. The degree to which the crown size distribution and cover can surrogate for DBH to provide BA is very limited. To rectify the situation needs either accepting lower accuracy or undertaking collateral ground based measurements to “calibrate” the remotely sensed data. Such additional ground based work generally reduces or removes the cost advantages of the platform.

The use of airborne Lidars for forest mapping does not overcome the problem of the vertical view. But it does provide a technology that can measure ranges and distances and provide both a useful map of the position of the ground surface and estimates of the way the foliage and stems are arranged vertically above the ground. Airborne Lidar has also been investigated for many years as a tool for forest mapping. For a historical perspective it is interesting to read the paper by Aldred and Bonner (1985) and its discussion of Lidar developments in Canada from the mid-1960’s and the paper by Maclean and Krabill (1986). Unpublished accounts of the early days of the Australian LADS (Laser Airborne Depth Sounder) recount how the original instrument was seen as a land mapping tool but a flight over a dam in the Adelaide hills in the 1970’s showed the value of the data for depth mapping and the LADS project moved “off-shore”. As shown by the papers of Nelson *et al.* (1984), Bufton, (1989), Nilsson, (1996), Naesset, (1997a,b) and Magnussen *et al.*, (1999) the potential to use airborne Lidars to measure height had been well established by the year 2000.

It is clear that for data *taken with sufficient Lidar shot density*, such Lidars can provide tree height and even individual tree crown properties of interest and value for forest mapping. The data value is thereby potentially greater than stereo-pairs of aerial photography in its use of direct inputs of parameters into current allometric relationships. The most obvious of these is tree height. The opportunities provided by airborne Lidar are presented in detail in Section 4 of this report where both the capacity of effective processing to extract forest information and the potential for the ECHIDNA® data to be used with the airborne data are covered.

To go beyond this level of information, airborne Lidar data need an additional type of generalised “form factor” to scale from the height, cover and profile information to stand based estimates of the outputs foresters need – such as timber volume, BA or DBH variation. It may not be possible to derive such factors with high accuracy and the investigation of what is possible and its accuracy is itself important but very difficult to carry out. The issue of “calibration” is therefore critical to the use of remote sensing for forest inventory. Other issues that need to be discussed in this context involve differences between currently available Terrain Lidars (with their separate market in terrain measurement) and the experimental Canopy Lidars that are developing with forest mapping as their primary focus. These will be discussed later in Section 4.

### **2.3.3 Ground Based Technologies**

The forest industry has been energetic in its search for newer technology to improve the accuracy and reduce the costs associated with forest inventory. Equipment such as the Relaskop, enhanced with rangefinders and GPS allow plots to be measured and recorded accurately, consistently and quickly. Ranging and angle-measuring devices make tree range, tree height and other factors simpler and quicker to measure by a relatively small field crew. Advanced surveying methods are now a part of forest measurement.

The project has been undertaken to explore the idea that ground based Lidar data, in which the Laser beam scans the whole hemisphere and with full waveform digitizing and variable beam sizes (that ensure complete sensing of the hemisphere) provides a major advance in technology of special value to forest inventory. There are a number of commercially available laser systems designed for scanning from the ground and information about them, as well as a comprehensive description of the ECHIDNA® Validation Instrument (EVI) as built by CSIRO are included in Section 3.

This report provides an extensive discussion and investigation of the capacity of a ground based Lidar to measure forest parameters of immediate interest at both individual tree and stand scales and also provides a number of measurements that have been difficult or not reasonable to measure before. With such promising feasibility established there is a discussion of the potential for commercialisation and adoption in the forest industry in Section 6. It also addresses the issue of how best to “calibrate” airborne data – with a ground based Lidar.

Since the remote sensing platform advantage has so many attractions for large area coverage and easy repeat times the issue of linking ground and airborne Lidar data has also been investigated. Provided the EVI data are compatible with airborne for the same set of view angles the potential for assessing stem and basal area data for the whole stand from the airborne data seem good. Basically the information is “transferred” or “carried” via the compatible ground system to provide allometric measures for the airborne data while the airborne data “carries” the detailed ground information to larger areas. Such synergistic use adds value to both the ground and airborne systems and is a primary idea behind the CSIRO development of the EVI. Sections 4 and 5 and the commercialisation section (Section 6) take this further when the results and outcomes have been summarised.

## **2.4 Report Outcomes and Structure**

The principles that emerged from the previous CSIRO studies into the potential for Lidar data to provide forest information and to form the basis of a successful commercialisation of the technology for this purpose were basically three. They were:

1. Airborne canopy Lidar provides products more in tune with forest measurement needs than other remote sensing technologies but still retains the “platform advantage”;

2. Ground based Lidar provides information compatible with airborne sensors, as well as key in-forest data required for forest survey;
3. The combination of these two approaches can deliver the information required for forest surveys, covering large forested areas at an accuracy as high as or higher than current ground based techniques at a competitive overall cost and price structure.

The fundamental need in making this package an attractive option for company and other investment was defined as the “risk” level inherent in a new technology project. The level of internal rate of return (IRR) needed before a company will decide to invest is much higher for new technology and Australian investors are among the more conservative. The FWPRDC Project has therefore sought to reduce the technology risk by validation and provide evidence that will enable future investment and eventual production of the technology in response to demand for the data from the Industry. It has also sought to build that demand through the industry links implicit in the involvement of the FWPRDC to identify and contact industry leaders in the uptake of new technology.

In this Final Report we particularly describe how CSIRO have:

1. Used the CSIRO prototype EVI as the primary tool for the validation of ground based methods;
2. Shown how, based on field data, the methods provide effective information for forest inventory as well as added information of added value (e.g. form factors);
3. Made best use of currently available terrain Lidar data to map forest information;
4. Matched EVI and airborne data and discussed the pathway to combined analysis and “calibration” of airborne Lidar by ground based Lidar;
5. Provided (as best we can) comparisons of accuracy of the results;
6. Provided a plan for continuing technology transfer and technology uptake in the Forest Industry based on commercialisation of the ECHIDNA® idea.

These are discussed in detail in the following Sections.

- Section 3 describes the EVI instrument, its selection over current rangefinder instruments, its innovative data and the way its data are processed;
- Section 4 describes how it is possible to extract effective information from terrain Lidar data;
- Section 5 discusses the work outcomes in detail. The discussion includes:
  - Sites and partner interaction
  - Hemispherical image data
  - EVI Processing results
  - Comparisons – airborne, EVI & field data
  - Stems and counting methods
- Section 6 discusses potential commercial applications
- Section 7 concludes the Project work and summarises the key findings.

We claim that as a result of the project outcomes the path to commercialisation and the adoption of the technology by the forest industry has been well advanced. Some of

the plans for the steps being taken to commercialisation are also discussed. In the short term, these involve working with industry partners to test the data and technology against forest inventory at pre-harvest stage. This work will proceed at the same time as a search for a commercial partner to exploit the technology. Provided each is successful it seems that an Australian industry in the provision of the technology as well as Australian and New Zealand use of the initial systems produced is possible and likely.

In addition, the time over which the project has been completed has seen the emergence of an instrument that has not existed before and its provision of data that has also never been available before. The outcomes have created many ideas and a great potential for innovative research that will advance the activity into new areas of application and thereby support ongoing product and market development for the commercial offshoots of this initial work. This R&D may well be the most significant longer-term outcome.

### 3 THE CSIRO ECHIDNA® VALIDATION INSTRUMENT (EVI)

The CSIRO Canopy Lidar Initiative (CLI) aims to promote the use of Lidar technology in forestry and in the forest industry and has developed ideas and novel IP for its efficient realisation. The FWPRDC project has been pursued to validate these ideas, reduce the technology risk associated with commercialising the ideas and promote uptake in the industry.

The CLI developed two specific ideas for types of hardware that, together with effective processing, can achieve the goals to best effect. In previous documentation, of which the CSIRO EOC Report by Jupp and Lovell (2005) is a publicly available example<sup>1</sup>, the instruments described consisted of a ground based Lidar called “ECHIDNA®” and an airborne system called “VSIS”. In this report it is the ECHIDNA® technology that is of prime interest. ECHIDNA® is a Trade Marked and patented technology and the patenting is listed among the references. The priority date for the patenting is February 2001. Based on those documents the range of IP may be summarised and merged as follows:

The patented CLI IP relates specifically to a ground based forest survey system using multi-angle sounding, controlled, variable beam width and shape and recording the return waveform with calibration to provide apparent reflectance as a function of range for each choice of angle and beam size and shape. Some important aspects of the design include:

- Controlling and utilising beam size and ranging in combination with degree of angle flexibility in scanning to resolve the "blind spot" effect of clumping of foliage.
- Utilising degree of angle flexibility, beam size and shape and ranging separately or in combination to resolve the "blind spot" effect of object orientation and angle distributions.
- Controlling and utilising beam size with ranging plus the combination of high rate sampling of return pulse intensity, small pulse width and suitable signal to noise ratio (SNR) to resolve the "blind spot" effect of the trade-off between scatterer density and reflectivity.

The CLI IP description also outlines the value of the combination of ground based information with airborne data to provide large area information from the airborne system not available from the airborne system alone. Both the ground and airborne systems would need to:

- Obtain signals with high SNR from vegetation at depth in canopies;
- Sound with variable beam width and shape, and
- Scan in multiple directions and varying scan patterns;

And optionally;

- Capture and store data at RF rate;

---

<sup>1</sup> This report was originally written in 2000 but has been updated, externally reviewed and is now publicly available from the EOC web site.

- Measure calibrated outgoing pulse intensity;
- Measure calibrated intensity of return trace to nanosecond sampling;
- Provide accurate range to target by pulse deconvolution; and
- Process data in situ.

The IP descriptions also include methods and systems for the interpretation of the various data from the two systems to provide forest products over small and large areas utilising one, some, or all of the following inventive methods or algorithms:

- Calculation and use of apparent reflectance;
- Combination of the convolved differential equation for  $P_{gap}$  and advanced geometric probability models;
- Advanced deconvolution algorithms to sharpen data and remove the ground effect and measure effects of rough terrain on the ground pulse using calibrated pulse model;
- Multi-layer interpretation by modelling;
- Determination of actual foliage profile with ground based system and extended to the airborne system;
- Separation of foliage amount and angle distribution profiles in ground-based system data for interpretation of airborne system data;
- Determination and use of foliage variance profile for clumping measurement;
- Use of Steiner's Theorem, weighted dilation and Geometric Probability to measure tree and canopy size and shape information (e.g. Diameter at Breast height (DBH), basal area, height, timber volume, size distributions, Leaf Area Index (LAI), crown length ratio etc);
- Stratification of forests based on calibration of airborne data using layering, foliage angles and allometric relations derived from a ground-based system.

In principle, the type of information discussed could be assembled from a very high density of Lidar shots covering the whole hemisphere in which the full waveform is digitised and recorded at RF rates. The use of variable size and shape in beams is an optical or hardware version of the software processing needed in the case of a high density of narrow width shots. When the FWPRDC project plan was formulated we felt that currently available rangefinder instruments configured to cover the hemisphere could provide a base data set to simulate and validate the ECHIDNA® proposal. It turned out that this was not the case. It is very hard to get the kind of density and control needed for such a task and at the time, as now, the available systems were rangefinders and did not record the full return waveform. Based on this experience it was then felt that the existing CSIRO system specifications (most of which are included as background technology in the patent applications) could be revised and an instrument built to enable the validation to occur and also advance the commercialisation through experience and reduction of technology risk.

The system that was built was called the ECHIDNA® Validation Instrument or "EVI". While the EVI has not implemented all of the ideas originally outlined for ECHIDNA® it does realise the primary characteristics and provides effective validation for the ideas. It has also provided practical experience and a test bed for the final specification of the planned commercial prototype ECHIDNA®.

In this Section, our experiences with rangefinder options are first outlined and information about some of the newer systems that have since become available are reviewed. The rangefinder technology is continuing to improve but was not pursued then and is not being reconsidered both because it was not able to provide effective simulation of an ECHIDNA® and also because it has fundamental limitations for forest mapping and assessment. These are discussed in Section 3.1. Section 3.2 outlines the technology that makes up the EVI. The EVI has developed to be a highly advanced and powerful instrument that is unique among options available at this time. It is the product of contracts with Australian engineers and Companies based on CSIRO specifications. Finally, Section 3.3 outlines the range of processing algorithms from the above list producing products that are validated in this Report. These algorithms make up the selected ECHIDNA® processing options as realised by the EVI.

### **3.1 Options for using Laser Rangefinders**

The majority of commercial lidar instruments are Rangefinders, providing the range to a single target for each transmitted pulse based on the principles described in Section 2.3.1. Consequently, the design of the detector and signal processing algorithm is a significant factor in determining which return, in complex environments with many “soft” targets, is selected for the range calculation. A common approach is to identify the peak intensity of the largest return above a given threshold. Alternative strategies include identifying the first or last returns above a given threshold, or supplying the range to the average of all returns.

#### **3.1.1 Commercially available ground-based lidar instruments**

A variety of ground-based lidar instruments are commercially available. These instruments have generally been aimed at the engineering and surveying markets and are ideally suited to ranging in ‘built’ environments.

Instruments of particular interest for forestry applications involve some form of scanning mechanism for rapid sampling of tree and vegetation and the generation of statistics describing the structure of the plot or stand. In reviewing scanning lidar instruments for application in forest assessment, a number of relevant specifications were examined, including scanning resolution, scan field of view (FOV), range limitations and laser wavelength.

**Table 3-1: Specifications for commercial ground-based scanning lidars undertaken as an early review of available technology.**

Manufacturer	Instrument name	Scanning resolution <sup>o</sup>	Field of view horizontal <sup>o</sup>	Field of view vertical <sup>o</sup>	Beam diameter and/or divergence	Recommended operating range min – max (m)	Range precision	Laser wavelength (nm)
Callidus	CP 3200	0.0625 – 1.0	360	180	unknown	unknown – 32	5 mm	unknown
Cyra	Cyrax 2500	0.0003	40	40	<6 mm	1.5 – 50	±6 mm @ 50 m	532
iQSun	iQSun	0.009 – 0.018	360	320	3 mm / 0.1 mrad	unknown – 80	<6 mm @ 10 m	785
Maptek	I-Site	unknown	340	80	unknown	2 – 350	25 mm	unknown
Optech	ILRIS-3D	0.00115	40	40	3 mrad	5 – 50	4 mm	IR and vis
Riegl	LMS-Q140	0.16	80	none	3 mrad	2 – 350	25 mm	905
Riegl	LMS Z210	0.24	340	80	3 mrad	2 – 350	25 mm	905
Riegl	LPM-2K	0.02	360	+135 – -60	1.2 mrad	unknown – 800	25 mm	905
Riegl	LPM-VHS	0.02	360	300	3 mrad	2 – 200	±25 mm	905
UK Robotics	LFM	unknown	360	60	unknown	0.5 – 60	10 mm	680
Metric Vision	100B	0.0003	350	120	<4 mm	2 – 60	±0.2 mm	IR

Specific parameters considered necessary to undertake a scientific validation of lidar technology for forest assessment were:

1. computer control and data logging
2. flexibility in software control (particularly scan configuration and data logging) without proprietary software restrictions
3. full hemispherical scanning capability
4. ranging capability from 50 cm to over 100 metres
5. laser wavelength and energy that is highly reflected in vegetation environments and does not pose an eye safety hazard

Table 3-1 lists some of the commercially available scanning lidars reviewed in 2001 when systems were being examined for use in field trials. The broad category of military and atmospheric lidar systems were considered to be grossly incompatible with the proposed application and are not included.

All of the instruments identified in the above Table are single-return scanning lidar systems. A number of these are capable of full hemispherical scanning at fine angular resolution. The greatest limitation apparent from the listed specifications is the minimum and maximum ranging capability. Established work on canopy structural analysis (for a discussion of the extensive literature on this area see Jupp and Lovell, 2005) identified the zenith angle of  $57.5^\circ$  from the forest floor as the angle at which foliage profile estimates are invariant to leaf angle distribution. Consequently, to exploit this property for canopy leaf area description, maximum lidar range should be at least twice the maximum tree height at the sample location to ensure full lidar beam penetration through the canopy at  $57.5^\circ$ . A maximum range of at least 100 m should therefore suffice for most forest and plantation environments.

Of equal importance is the ability to measure distance to objects in the near field. Use of a scanning lidar for forest measurement may involve operation in densely vegetated environments or at random sample locations. The presence of near-field objects can result in significant occlusion of sectors of the hemisphere. Only one instrument originally reviewed (UK Robotics, LFM) had an acceptable near-field ranging capability, however the instrument's far-field ranging capacity was inadequate, as was its scanning field of view.

Based on these considerations, of the various commercial lidar instruments and laser based forest assessment tools available, none of the systems met the requirements of the validation study in terms of technical capabilities and/or cost-effectiveness for evaluation.

In addition to these instruments have been some developments intended specifically for forestry applications. Although not a true lidar instrument, Tanaka *et al.* (1998, 2004) reconstructed 3D forest information by triangulation using images from a scanning planar laser beam and optical imaging as it is intercepted by canopy elements. The system is used either on the ground or elevated to a platform on a scaffold tower. The ground-based measurements provide hemispherical coverage and allow LAI to be estimated. The performance of this system depends critically on the sensitivity, resolution and noise characteristics of the CCD camera used to capture the images. Both visible (red) and near-infrared laser wavelengths are used. This enables separation of stem and leaf components when combined with image segmentation

algorithms. To achieve optimum imaging conditions the system must be operated at night. A hemispherical scan takes approximately 90 minutes.

The recently deployed Tree Attribute Profiler (TAP) has been designed to scan individual trees for description of stem size, stem form and branching structure. The hardware follows a design similar to the Riegl LPM-VHS scanner with data interpretation software developed specifically for forestry applications. A single tree is scanned in 2-4 minutes and post-processed to retrieve stem attributes relating to log quality. While not commercially available at the time of the initial instrument review, the specifications of the instrument are still not ideally suited to the minimum and maximum ranging requirements for the work undertaken in this study.

Perhaps of more relevance to the proposed evaluation work than ranging and scanning capability is the common single-return mode of operation of the instruments investigated. Theoretical knowledge of lidar operation and prior experience with lidar instruments raised some uncertainties about the suitability of threshold-based rangefinding instruments for vegetation assessment. In particular, the diffuse or 'soft' targets often encountered in forested environments were likely to result in many partial interceptions of an emitted lidar pulse, producing weak return pulses dispersed through time. Such returns are problematic to identify using lidar systems optimised for 'hard' targets in (for example) a built environment.

Given these technical risks and the considerable investment required to purchase or lease scanning lidar equipment, an interim study for technology evaluation was undertaken. This evaluation activity is described in Section 3.1.2.

### **3.1.2 Rangefinder Prototype ECHIDNA® (RPE)**

As an initial evaluation of currently available Lidar technology as a means to realise the ECHIDNA® ideas and (more generally) for forest assessment, the CSIRO Canopy Lidar Initiative constructed, from off-the-shelf components, a scanning laser rangefinder capable of scanning the upper hemisphere. The instrument was termed the Rangefinder Prototype ECHIDNA® (RPE). The RPE build was initiated to meet scientific validation requirements that were not immediately obtainable from complete commercial systems in view of unexplored technical risks.

#### **3.1.2.1 RPE description**

The RPE was constructed from three separate commercially available components – a lidar unit, a pan-tilt platform and a laptop computer. The Lidar unit is a Class 1 LaserTech Impulse rangefinder model LR 200. It has separate transmit and receive apertures, an initial beam diameter of 40 mm and fixed divergence of approximately 3 mrad. The Impulse has a data port that allows the laser to be remotely triggered and the range data recorded. A built-in inclinometer records inclination of the instrument to an accuracy of 0.1°. Standard operating range is from close to zero to 100 m although ranging up to 500 m is possible where the target is solid and highly reflective.

The Impulse rangefinder was attached to a pan-tilt platform which was in turn supported on a sturdy camera tripod. The pan-tilt platform used was model PTU-46 manufactured by Directed Perception. The unit consists of two computer controlled stepper motors capable of achieving azimuth and zenith angular positioning accuracy to within 0.013° with the capacity for hemispherical coverage.

RPE control software written<sup>2</sup> in LabView<sup>®</sup> was run from a laptop computer. The software was used to control the pan-tilt platform (scan configuration), trigger the laser after each pan-tilt platform increment, and record a string of ASCII data from the Impulse and pan-tilt unit. An example RPE dataset is given in Table 3-2 where each row represents the data collected for each laser trigger event.

Table 3-2: Example RPE data records

Laser shot number	Range (m)	Pan angle (azimuth)	Tilt angle (zenith)	Impulse inclination
1	0.00	180.0	54.0	90.11
2	8.97	176.4	54.0	90.20
3	8.85	172.8	54.0	90.24
4	8.97	169.2	54.0	90.17
5	9.08	165.6	54.0	90.19
6	9.24	162.0	54.0	90.28
...	...	...	...	...

A range of zero is taken to represent a gap in the canopy. The sequence of data in Table 3-2 shows that data are acquired by scanning at a fixed zenith angle for a full azimuth sweep before incrementing the zenith position and repeating. The custom control software allows great flexibility over hemispherical scan density, however, due to the relatively slow laser trigger and data recording rate, each scan typically involved angular increments of 3-4 degrees in azimuth and zenith. Approximately 1,000 – 2,000 laser firing positions were achieved per hemisphere. The RPE instrument is shown in operation in Figure 3-1.

---

<sup>2</sup> Design, advice and a software operating environment were provided for the RPE by Phil Connor of CSIRO MMTG.



**Figure 3-1: Rangefinder Prototype ECHIDNA® (RPE)**

Field operation of the RPE involved careful levelling of the pan-tilt platform and stabilisation of the supporting tripod using weights. The computer and pan-tilt unit were run on 240V power using a truck battery and a 12VDC-240VAC inverter.

### **3.1.2.2 RPE field evaluation**

The RPE was assessed in a number of forest environments and compared against equivalent forest measurement techniques for plot-scale structural description. Specifically, the RPE was evaluated as a potential instrument for assessing:

1. mean stem diameter at breast height ( $D$ )
2. stem number density ( $\lambda$ )
3. canopy height ( $H$ )
4. canopy gap probability ( $P_{gap}$ ) and leaf area index (LAI)

The field assessment methodology used for RPE evaluation is consistent with field methodologies used for ECHIDNA® Validation Instrument evaluation, described in Section 5.

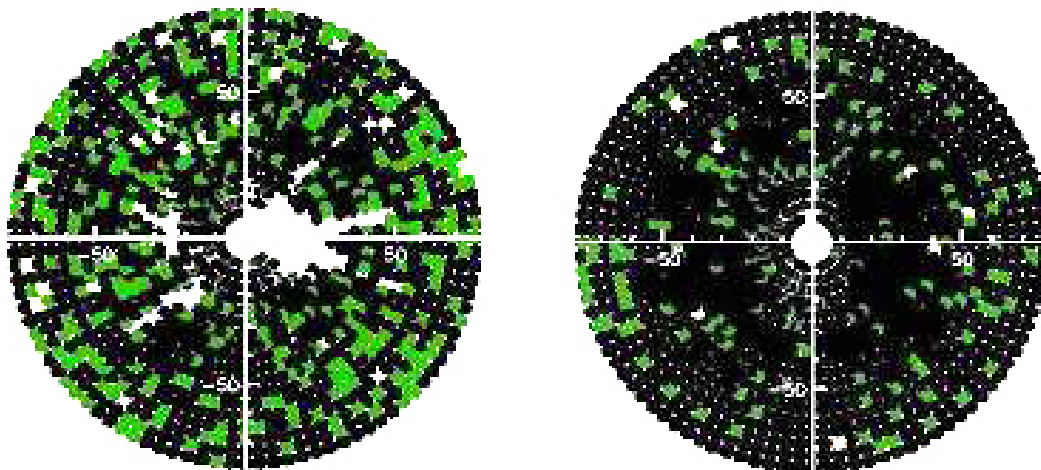
Table 3-3 shows the forest types and structures assessed as part of the RPE evaluation.

Table 3-3: RPE evaluation field sites

Location	Number of plots	Species	Age Class
Tumbarumba, NSW	1	<i>Eucalyptus delegatensis</i>	Mature
Tumbarumba, NSW	1	<i>E. pauciflora</i>	Mature
Tumbarumba, NSW	1	<i>E. globulus</i>	Mature
Tumbarumba, NSW	1	<i>Pinus ponderosa</i>	Mature
Mt Gambier, SA	3	<i>P. radiata</i>	9 years
Mt Gambier, SA	3	<i>P. radiata</i>	20 years

Initial trials with the RPE at Tumbarumba confirmed suspected difficulties of simple threshold rangefinder operation in a soft target environment. A telescopic sight mounted on top of the rangefinder allowed the operator to observe the target(s) within the beam as the RPE performed a hemispherical scan. Audible tones indicated when the laser was triggered and whether a target was successfully or unsuccessfully acquired. In many instances the laser was clearly observed firing at a vegetation target but no range was returned. This was typically the case with fine branches and foliage.

Following initial RPE field trials the control software was modified to repeatedly attempt to acquire a target in a given scan direction before scanning to the next position. The number of repeat attempts was operator-specified and typically varied between 1 and 3.



(a) (b)  
Figure 3-2: RPE results in 20 year old (a) and 9 year old (b) *P. radiata* plantation plotted in a 2D polar projection where the zenith is at the centre and the horizon is at the edge of the circle. Light-green spots required more attempts to successfully acquire a target than the dark green spots.

Figure 3-2 shows RPE results from Mt Gambier plotted in a 2D polar projection where the zenith is at the centre and the horizon is at the edge of the circle. White regions indicate gaps in the canopy. Dark green spots indicate dense needles or woody material and light-green spots represent sparser canopy elements – estimated as the

inverse of the number of repeat attempts to acquire a valid target in a given direction. Dense targets require fewer attempts than sparse targets.

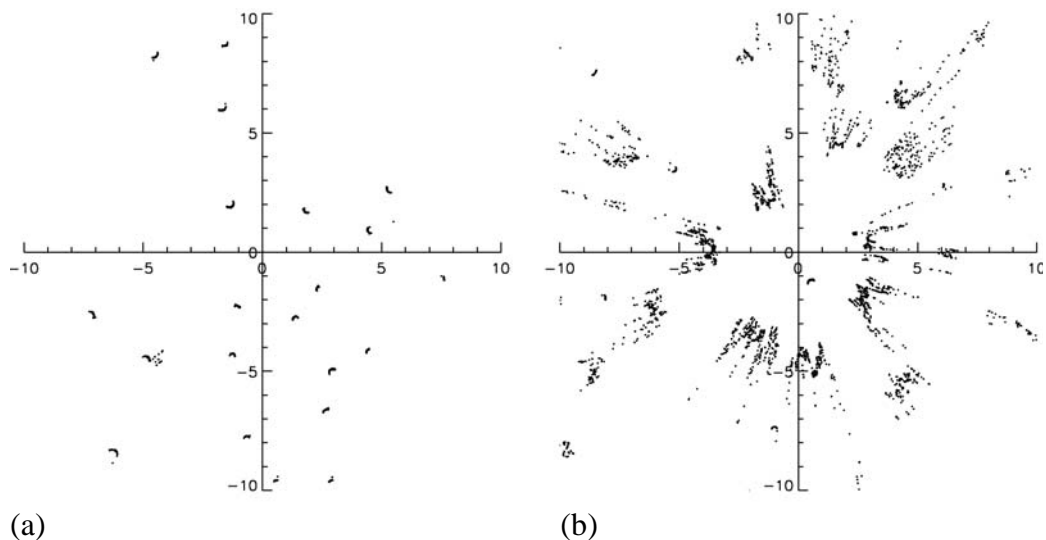
While the potential for unrecognised targets implies a propensity to over-estimate canopy gaps, this is outweighed by the more significant single-return limitation of the instrument. If the beam is completely unobstructed by the canopy, then the instrument correctly records a canopy gap for the beam area. However, if any part of the beam is obstructed by a canopy component large enough to return a signal above the instrument noise threshold, then the assumption must be made that the complete beam area has been intercepted. This also restricts the detected range to foliage in close proximity to the instrument, since it is only the first return above the noise threshold that is recorded. This leads to an overestimated foliage density profile that is biased toward the base of the canopy.

Results from Mt Gambier trials found that the RPE underestimated predominant height in young (9 year old) *P. radiata* plantations by approximately 30%. This was attributed to the limited number of targets found in the upper canopy due to interception by dense lower foliage. Conversely, predominant height in the more mature, thinned plantation, was measured by the RPE to within 1% of field measured values.

This range-foreshortening effect in dense canopies may be less significant if the beam diameter and divergence was very low. This would allow a beam to pass through small gaps in the canopy unattenuated. However, with a simple thresholding system, any canopy gaps less than the beam cross sectional area are still indistinguishable from the canopy components surrounding them.

Parker *et al.* (2004) trialled several rangefinders for use in a canopy profiling system. Their field experiment involved two instruments: the Impulse LR 200 and Riegl LD90-3100HS. The rangefinders were mounted on a platform carried through the forest by the operator as a substitute for scanning operation. Returns from vertically directed pulses were recorded in a transect through the forest. This produces a canopy height model similar to that derived from optical point quadrats (OPQ). Accurately locating canopy hits along the transect depends on the stability of the platform and the ability of the operator to walk at a constant speed. Comparisons against OPQ sampling were in keeping with RPE findings in that the method consistently overestimated cover due to the finite beam size and divergence. The Riegl, with its narrower beam, was found to perform slightly better than the Impulse.

A number of algorithms were developed for the retrieval of stem number density ( $\lambda$ ) and mean diameters at breast height ( $D$ ) from RPE data. Estimates of both  $\lambda$  and  $D$  were shown to be meaningful when data were acquired in open stands with clean boles and no understorey. However, both  $\lambda$  and  $D$  were overestimated in forests where foliage and branches are dense in the plane of the breast height scan. This was again attributed to the single return nature of the instrument and the inability to distinguish (from the intensity of the reflected signal) the nature of the target, e.g. foliage, branch or stem. Figure 3-3 shows the location of targets identified in a horizontal scan at breast height at two different sites – a mature and open stand with a clear view to trees (a), and a stand with understorey and prevalent branching on the stems (b).



(a) (b)  
 Figure 3-3: Location of targets in a horizontal RPE scan at breast height in a mature and open stand with a clear view to trees (a), and a stand with understorey and prevalent low branching (b)

The open stand is well characterised. Both tree locations and stem curvature are apparent. The alternate stand (Figure 3-3 (b)) shows a scattered horizontal profile that is insufficient for extraction of stem location and diameter. The provision of additional information such as reflected pulse energy and multiple returns may enable target discrimination and acceptable basal area estimates in these forest types.

The RPE proved to be a useful experimental instrument for investigating the performance of single-return, threshold-based rangefinders in a vegetated environment. In addition to limitations already discussed, as a practical instrument the RPE's low sampling rate and slow measurement speed were found to be insufficient to capture the density of measurements required to characterise the typically high spatial variation in forest structure.

## 3.2 ECHIDNA® Validation Instrument (EVI)

### 3.2.1 Motivation behind build

Findings from the RPE field evaluations provided valuable information on the performance of single-return, threshold-based lidar instruments in vegetated environments. While showing great potential, significant limitations were identified. These were:

- Range foreshortening
- Overestimation of cover
- Soft target problems
- Limited sampling density in reasonable time

These outcomes, and the lack of suitable commercial solutions, led to the conclusion that current rangefinder technology was not suitable to validate the ECHIDNA® ideas and were also likely to have inherent limitations for forest assessment. They were also

a key driver in the decision to bring forward the implementation of parts of the ECHIDNA® design and specifications (that had been developed previously by CSIRO) and build the prototype “ECHIDNA® Validation Instrument” (EVI). The EVI is a precision-engineered scientific instrument suitable for investigating the potential of terrestrial lidar in forest assessment and for refining the final engineering specifications for an ECHIDNA® commercial prototype.

In designing the EVI, two added ECHIDNA® specifications were identified to address the RPE limitations:

- detection of range to single-returns for each transmitted pulse should be replaced by a full intensity waveform digitising system, i.e. *all* the energy from a laser pulse should be recorded as it is reflected from objects along the laser path
- divergence of the transmit beam should be variable to allow investigation of cross-sectional beam area on forest structure measurement and the efficiency of operations.

Hemispherical scanning, as implemented in the RPE, was still considered to be an essential component for acquiring structural information about forests. A single scan configuration can then capture stem size and location information in the cross-sectional view, tree height and canopy structure in the vertical view, and everything from stem form, taper and branching structure at scan angles in-between. Consequently, hemispherical scanning remained a key design criterion in the new instrument.

### **3.2.2 Hardware description**

#### **3.2.2.1 General overview**

The EVI build was initiated and managed by CSIRO in association with two specialist contractors. Optical Engineering Associates Pty Ltd oversaw optical and mechanical engineering tasks, and Laser Integrated Technologies Pty Ltd was responsible for the laser and electronics engineering. CSIRO specified design criteria, provided ongoing scientific input, developed the control and data acquisition software and managed the eye safety certification. The interpretation algorithms for converting raw data into meaningful forest attributes are arguably as important as hardware design. Underlying principles of these algorithms are discussed in Section 3.3.

The EVI is broadly divided into four main components:

- tripod
- rotary table
- sensor head
- control box

The tripod is used to support the instrument in a fixed and stable position during operation, the rotary table provides scanning motion in the horizontal (azimuthal) plane as well as a structural interface between the tripod and sensor head. The sensor head encapsulates the laser, detector and optics, the scan head which affords scanning motion in the vertical (zenith) plane, and embedded logic control for implementing

commands and monitoring system status. The control box contains various power supplies a communication interface and a rack-mounted computer for issuing commands and recording data. The four primary components of the EVI are illustrated in Figure 3-4.

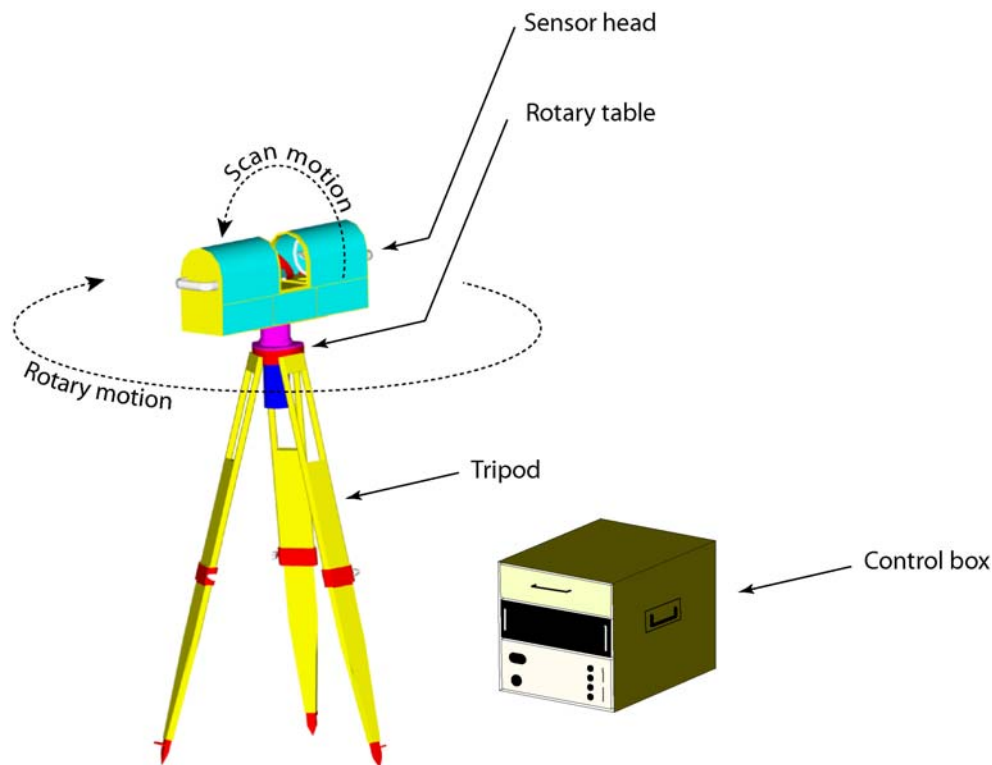


Figure 3-4: Primary components of the ECHIDNA® Validation Instrument (EVI)

The physical configuration of the transmitter and receiver in a lidar system is a decision that has significant impact on the overall design of the instrument. Modern instruments employ either a coaxial or biaxial design (Measures, 1984). In a coaxial system the transmitter and receiver paths are co-aligned. Biaxial systems, in contrast, have a physically displaced transmitter and receiver. Biaxial systems tend to be optically less efficient than coaxial systems but have the advantage of avoiding backscatter saturation of the receiver system when the laser is triggered. This is achieved by deliberately directing the laser beam outside the receiver FOV in the near field. This results in minimum detectable range limitations that may be undesirable in some applications and was one of the factors that led to the choice of a coaxial design for the EVI. Other benefits include good signal recovery and compact assembly.

### 3.2.2.2 Laser characteristics

The EVI uses a diode pumped solid state 1064 nm Nd:YAG laser. The output beam diameter is reported by the manufacturer as approximately 1.5 mm with a nominal half angle divergence of 0.8 mrad. The laser can be configured to operate at pulse frequencies ranging from 1 kHz to 10 kHz. Changes in pulse repetition frequencies have corresponding effects on pulse length (duration) and pulse energy. The laser was set to operate at a fixed repetition frequency of 2 kHz resulting in a quoted nominal pulse width of 11 ns and raw pulse energy of approximately 40  $\mu$ J according to manufacturer specifications.

Empirical tests of pulse shape (see Figure 3-5) have determined that the pulse width is actually a stable value of 14.9 ns at full-width-half-maximum (FWHM) which corresponds to an effective width in “range” of about 2.4 metres. Despite the width of the pulse the peak is sharp and well defined. The tests also showed stable and consistent pulse-to-pulse shape and a low level of shot to shot variation in output pulse power. In Figure 5 most of the remaining variation at the “base” of the data is not due to the pulse but to other electronic effects that are discussed later.

As discussed previously, the stability of pulse shape and magnitude is important because assumptions about the nature of reflecting objects and the determination of range are based on the shape of the transmitted and reflected pulse shapes. The mathematical pulse model developed and its use in pre-processing are described in detail in Section 3.3.

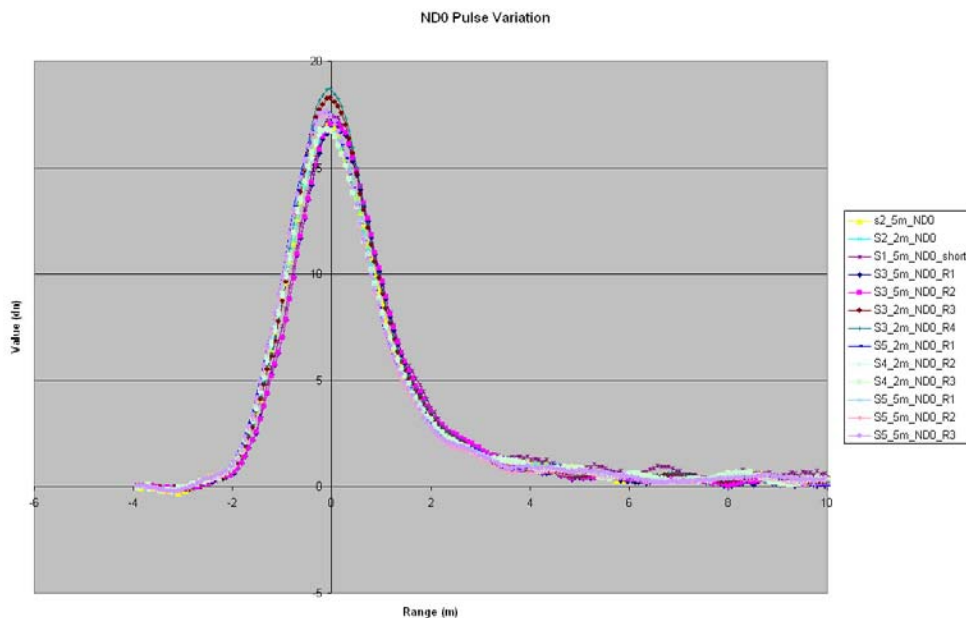


Figure 3-5: Empirical measurements of laser pulse shape from various scans at various sites at Coffs Harbour. Variation at the baseline is not related to the pulse. The pulse shape (FWHM) is very stable. Its magnitude varies a little from case to case.

### 3.2.2.3 Optical modification of laser beam

Prior to exiting the transmit aperture of the EVI, the raw laser beam is modified in terms of diameter, divergence, density and direction. Combined beam expansion (20x) and divergence optics expand the raw laser beam to a diameter of 29 mm with a manual variable divergence of between 2 – 15 mrad. Including the initial expanded beam diameter of 29 mm, a beam divergence setting of 2 mrad will result in a beam diameter of approximately 23 cm at 100 m from the EVI. A beam divergence setting of 15 mrad will result in a beam diameter of approximately 153 cm at 100 m from the EVI. This is illustrated in Figure 3-6.

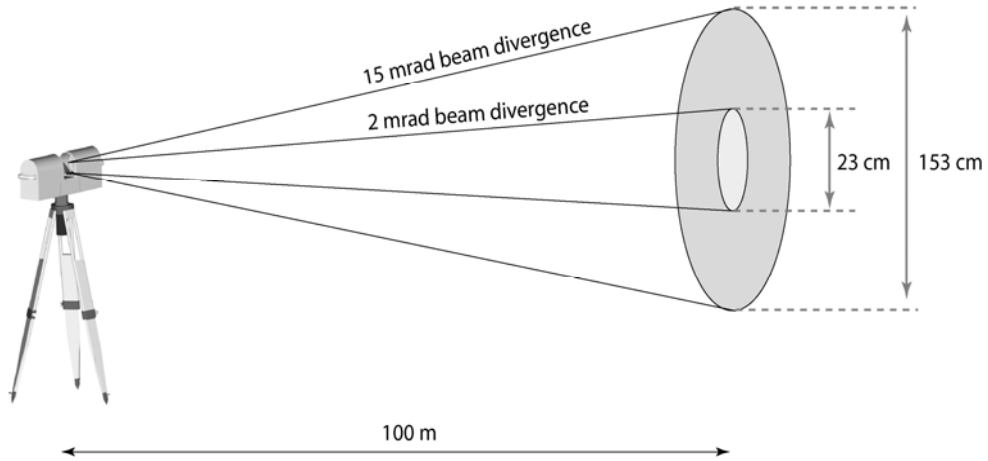


Figure 3-6: Effect of beam divergence setting on beam diameter (not to scale)

Following expansion and divergence, the laser beam passes through an apodizing filter to modify the beam density profile from Gaussian to ‘top-hat’. This reduces the peak power of the beam and produces a more uniform power distribution across the full 29 mm expanded beam diameter. Figure 3-7 shows empirical measurements of relative beam intensity after attenuation with the apodizing filter. The profile is clearly non-Gaussian with distinct edges and a moderately flat within-beam intensity.

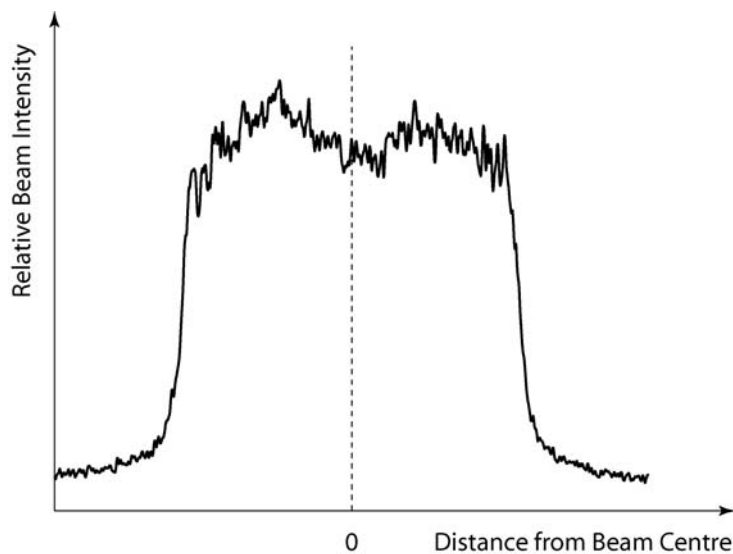


Figure 3-7: EVI beam intensity profile

Primary modification of the laser beam direction occurs by reflection from a 45° rotating mirror (referred to hereafter as the ‘scan head’). Secondary modification of the laser beam direction occurs through mechanical rotation of the entire EVI instrument by the rotary table. Figure 3-8 shows the arrangement of the transmit optical components.

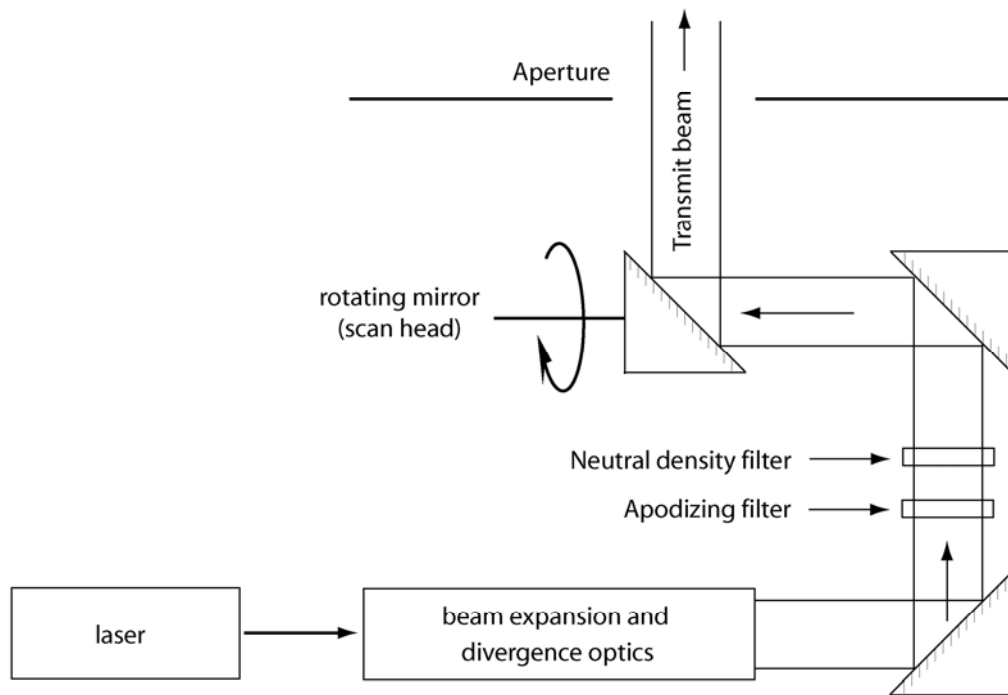


Figure 3-8: Optical modification of laser beam

The neutral density filter shown in Figure 3-8 was included to further attenuate the laser pulse energy and achieve eye safe operation. The combined effect of the apodizing and neutral density filters reduced the pulse energy from approximately 40  $\mu\text{J}$  to  $< 4 \mu\text{J}$ . Details of the eye safety analysis are given in Section 3.2.2.6.

The scanning motion of the EVI occurs through the combined movement of the scan head and rotary table. Both the scan head and rotary table motion are achieved through the use of stepper motors capable of being driven at a resolution of approximately 1.6 mrad ( $0.09^\circ$ ). The stepper motors are driven by on-board hardware and motion is effectively continuous. Stepper motor position is monitored by shaft encoders independent of the stepper motors. The shaft encoders have a resolution of 0.7 mrad ( $0.04^\circ$ ). The rate of rotation of the scan head and rotary table is designed to result in the contiguous placement of laser pulses vertically (within a scan head rotation) and horizontally (between scan head rotations). This configuration results in spatially adjacent beam placement on the horizon, with progressive over-sampling towards the zenith.

Because the rotary table is moving continually, successive pulses are not aligned vertically within the scan direction, but are slightly offset. This effect is illustrated in Figure 3-9.

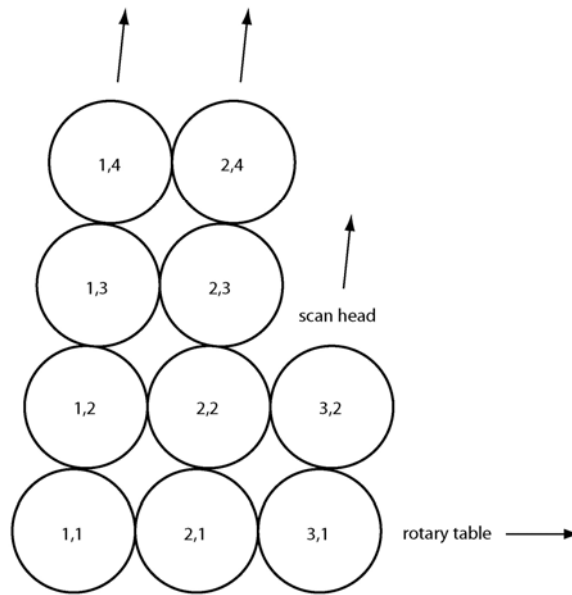


Figure 3-9: Laser pulse placement based on scan head and rotary table movement. Specified x,y coordinates indicate rotary table and scan head increment, respectively. Note that x-axis offset is exaggerated for illustration purposes.

To ensure contiguous beam placement on the hemisphere, the speed of the scan head and rotary table motion is determined by the laser pulse repetition frequency (2 kHz) and the beam divergence. Table 3-4 shows the hardware-implemented scan head and rotary table rotation specification as a function of beam divergence.

Table 3-4: Scan head and rotary table motion between laser pulses as a function of beam divergence. Laser pulse repetition frequency is 2 kHz.

Beam divergence setting (mrad)	Scan head rotation frequency (Hz)	Scan head step angle between pulses (mrad)	Rotary table step angle per scan head rotation (mrad)
2	0.63	1.99	2.00
3	0.95	2.99	2.99
4	1.19	3.73	3.99
5	1.58	4.97	4.96
6	1.90	5.97	5.82
8	2.38	7.46	7.86
10	3.17	9.95	9.43
15	4.75	14.92	14.49

Laser pulses can potentially be transmitted and received throughout a scan head range of 208°, from approximately 108° zenith angle (18° below horizon) to 100° zenith angle (10° below horizon) on the opposite side of the zenith position. For the remaining 152° of scan head motion, the mirror is pointing towards the inside base of the instrument, referred to as the ‘dead band’ area. Figure 3-10 shows the effective transmitter and receiver field of view in the vertical plane.

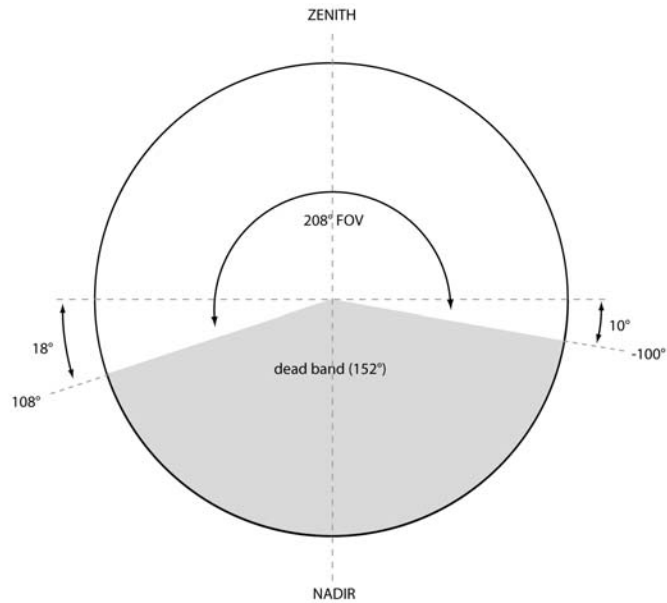


Figure 3-10: Scan head transmitter and receiver total field of view

Based on the 2 kHz laser pulse repetition frequency, the scan parameters defined in Table 3-4 and the scan head field of view, we can calculate the number of laser pulses per scan head rotation and per hemispherical scan as a function of beam divergence. This is shown in Table 3-5. Because the scan head scans from horizon-to-horizon, the rotary table need only move through 180° for the EVI to achieve full upper hemispherical coverage and down to 100° zenith angle.

Table 3-5: Number of laser pulses per scan head rotation and hemispherical scan as a function of beam divergence. Excludes dead band.

Beam divergence setting (mrad)	Scan head rotation frequency (Hz)	Number of laser pulses per scan head rotation	Number of laser pulses per hemispherical scan
2	0.63	1,889	2,971,397
3	0.95	1,259	1,321,950
4	1.19	1,008	793,296
5	1.58	756	478,548
6	1.90	630	340,200
8	2.38	504	201,600
10	3.17	378	125,874
15	4.75	252	163,800

The effect of decreasing beam divergence is to increase the effective spatial resolution of the EVI data since many more laser pulses are fired and each pulse represents a smaller spatial sample area of the canopy (smaller beam diameter). A side effect of decreasing beam divergence is an increase in data volume and a decrease in scan speed. A hemispherical scan at 15 mrad beam divergence takes approximately 2 minutes compared to a 2 mrad scan configuration of 40 minutes.

#### **3.2.2.4 Optical modification of return energy**

As discussed previously, the EVI is a coaxial monostatic lidar system. Some of the scattered laser radiation reflected from objects in the scene returns to the EVI along the same path as the outgoing pulse. This radiation is reflected by the scan head mirror through a narrow-band filter (to remove unwanted background radiation) where it is focused by a parabolic mirror onto a 1.5 mm photodetector. The photodetector generates an electrical current that is proportional to the intensity of the incident energy.

#### **3.2.2.5 Recording the data**

Photodetector current generated from reflected laser radiation is converted into a voltage signal and amplified within the EVI sensor head. The voltage signal is then conveyed via a coaxial cable to the control computer where it is digitised and recorded on the computer's hard disk.

As described in Section 3.2.1, one of the key design specifications that makes the EVI a unique terrestrial lidar is the manner in which range data are recorded. Instead of a single range value being recorded for each transmitted pulse, all the energy is recorded as it is reflected from objects along the laser path. This is known as a 'waveform', depicting the intensity of reflected laser energy as a function of time (Ni-Meister *et al.* 2001).

The waveform is recorded for each laser pulse using an 8-bit digitiser card in the control computer. The digitiser has a maximum sample rate of 2 GS/s (one sample per  $5 \times 10^{-10}$  seconds or every half-nanosecond). This equates to one sample every 15 cm in terms of the propagation velocity of a lightwave or one sample every 7.5 cm of range from the instrument (due to the dual path length of the returning beam).

The range over which a waveform is recorded is user-defined but is restricted to less than 100 m at the maximum sampling rate due to data handling limitations (data volume versus hard disk transfer speed). In addition to the core waveform data, a range of ancillary information is also recorded continually throughout a scan sequence to facilitate data interpretation and calibration, where necessary. These are described in Table 3-6.

Waveform data and related ancillary information are recorded to a binary file on the control computer 'on-the-fly'. Assuming a digitiser sample range of 80 m and a sample rate of 2 GS/s, a hemispherical scan at 15 mrad beam divergence produces approximately 200 MB of data, whereas a comparable 2 mrad scan produces approximately 3,600 MB of data.

Table 3-6: Data recorded by EVI during a scan sequence.

Information / data	Description	Sample frequency
date and time	current date and time	once per hemispherical scan
descriptive string	description of plot/site (user-defined)	
beam divergence	beam divergence setting (mrad)	
digitiser sample rate	digitiser sample rate (GS/s)	
digitiser sample range	waveform range (metres)	
platform inclination	x- and y-axis sensor head inclination (degrees) recorded from in-built inclinometer – used to detect changes in platform level during a scan or for off-level operation.	every scan head revolution
detector temperature	calibration utility – detector sensitivity varies as a function of temperature	
waveform	record of the intensity of reflected laser energy as a function of time	every laser pulse
sun sensor status	a built-in sun sensor disables signal amplification to avoid overload – sun sensor activation is recorded to identify invalid data	
scan head encoder	defines scan head zenith angle for calculating laser pointing direction on hemisphere	
rotary table encoder	defines rotary table azimuth angle for calculating laser pointing direction on hemisphere	
laser energy	calibration utility – reading from a laser pulse energy monitor	

At the completion of a hemispherical scan a simple data quality check is performed by projecting the cumulative waveform intensity for each laser pulse at its appropriate position on a 2D hemispherical plot. The resulting image is much like a hemispherical photograph. Although it is an extremely basic representation of the EVI data, the operation takes less than a minute and is a useful in-field validation procedure, e.g. to identify human shaped objects or vehicles parked too close the field site! An example hemispherical plot from an EVI scan in mature *P. radiata* plantation near Mt Gambier is given in Figure 3-11.



Figure 3-11: Example 2D data validation plot of EVI data in mature *P. radiata* plantation.

Comprehensive processing of EVI data for retrieval of quantitative forest attributes is described in Section 3.3. In the initial research phase, this is undertaken after the field data are collected. It is anticipated that future commercial versions of ECHIDNA® will perform significant parts of this processing in near real time, providing key results shortly after completion of a scan.

#### 3.2.2.6 ARPANSA & eye safety certification

Throughout the EVI design and engineering process the CSIRO was acutely aware of the potential eye safety hazard posed by lasers. Consequently, thorough testing and validation was undertaken at all stages of development to ensure that the EVI posed no hazard to the operator, bystanders or the environment. This was achieved by demonstrating that the EVI met or exceeded the stringent safety requirements of the CSIRO, the Australian Radiation Protection and Nuclear Safety Agency (ARPANSA) and relevant Australian standards. Laser safety controls included:

- Empirical measurement of laser pulse repetition frequency and accessible laser energy by the National Measurement Institute;
- Two eye safety reports prepared by independent experts in the field;
- Operational approval from ARPANSA;

- Laser safety training and standard operating procedures;
- Safety interlocks.

The extensive work undertaken has ensured that the EVI does not pose an ocular hazard to unaided viewing (i.e. to the naked eye), however, it was determined that an ocular hazard did exist if viewing the instrument through binoculars within a distance of 30 m from the instrument. Although such a case is extreme unlikely, warning signs are placed at a distance of 30 m from the EVI as a precautionary measure. A commercial version of the ECHIDNA® will undergo similarly stringent assessment and certification and will be designed to ensure that no ocular hazard exists under either aided or unaided viewing conditions.

### **3.2.2.7 Relevant technological advances**

Rapid advances in technology mean that more advanced components or new engineering techniques become available within the lifespan of many engineering projects. Where feasible, relevant and demonstrated advances in technology identified during the EVI build were adopted. However, some advances are only now appearing that may be relevant to ongoing EVI trials and commercial prototype development. In particular, high speed digitisers capable of recording waveforms at over 2 GS/s are available. Perhaps of more interest is the ability to digitise at up to 10 and 12-bit resolution at over 2 GS/s in next generation digitisers. Optimum digitisation rate for forest assessment from lidar is a matter of ongoing research that will be a compromise between technological capabilities, industry needs, data volume and processing speed. Other, relevant, technological advances are being monitored with a view to next generation ECHIDNA® instruments, particularly with respect to accuracy, reliability, cost, weight, size, speed and power efficiency.

### **3.2.3 Operation**

Field operation of the EVI was performed as consistently as possible between field sites to facilitate intercomparisons by forest types and structure. For each EVI scan location, the tripod, rotary table and sensor head were assembled and connected to the control box via interface cables. The sensor head was precisely levelled and rotary table oriented such that the start of the scan was aligned with magnetic North. The EVI and control box were powered from a small petrol generator. Figure 3-12 shows the EVI in operation in the field.



Figure 3-12: EVI in operation in the field.

All scans were acquired at a digitiser sample rate of 2 GS/s to a range of at least 50 m but typically 80 m. A variety of scan configurations were used to collect data at each location. These varied in terms of (i) beam divergence (and therefore scan speed) and (ii) the addition of a neutral density (ND) filter over the laser transmit aperture. The ND filters were used to reduce laser output power to investigate and overcome receiver saturation resulting from near-field objects. Three filters were tested – ND1, ND2 and ND3 with measured transmission properties at 1064 nm of 9.1%, 5.4% and 1.4% respectively.

The majority of field trials involved acquiring nine separate EVI scans at each scan location. These comprised three different beam divergence settings (3, 5 and 10 mrad) and three different attenuation filters (ND1, ND2 and ND3).

### **3.3 ECHIDNA® processing algorithms using EVI**

The primary objective of the CSIRO designed ECHIDNA<sup>TM</sup> instrument is to provide a means by which forest structure for forestry and environmental applications can be characterised in a quantitative and repeatable way. Optimising the extraction of specific structural parameters requires a wide variety of processing algorithms. The EVI is a research prototype for the ECHIDNA® and has been shown to be able to perform many (if not most) of the desired operations. It has, however, been configured for research and for testing engineering ideas rather than for operational use. Because of this, there were pre-processing and data handling activities that will not be part of a commercial system.

A fundamental objective in the design of the EVI was to maximise the flexibility of the instrument for research purposes. This meant, for example, constant monitoring

and recording of various instrument and environmental effects with the goal of data calibration and instrument diagnostics. Despite this, the EVI has provided very rich and detailed data for the sites visited. This section provides an outline of the processing applied to the data to obtain the results described in Section 5.

### 3.3.1 EVI Base Data

As a research prototype, the EVI instrument monitored a large number of instrumental and environmental factors that may have influence on the data recorded and enabled detailed investigations of any limitations or problems found in the field. This has led to the data sets being structured for investigation rather than operation. The EVI also has many extra settings and its data were recorded in many ways to investigate the potential of the data and to assess its ability to characterise forest structure. Because it was built to investigate both hardware and software specifications for an operational system the data have also needed some extra processing that will not be part of an operational system. Nevertheless, with this in place the EVI has provided excellent data to test the methods designated for forest mapping in the CSIRO patent applications.

#### 3.3.1.1 The EVI Data Cube

The basic data element recorded by EVI is a ‘waveform’ depicting the return intensity for a given laser pulse, fired in a particular direction as a function of time. Waveforms are the basis for our inferences of forest structure in the direction of a laser pulse through the forest.

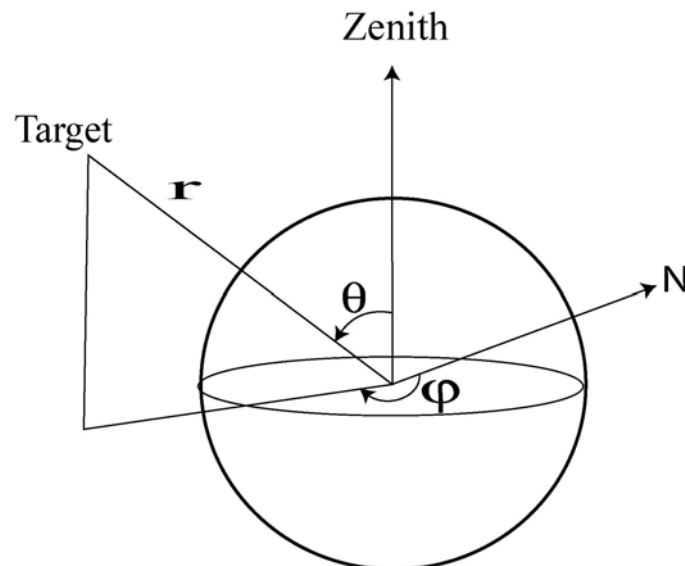


Figure 3-13: Geometry of the ground based Lidar scanner

The data recorded have three geometric dimensions; zenith angle ( $\theta$ ), azimuth angle ( $\varphi$ ) and range ( $r$ ) to target as illustrated in Figure 3-13. For each direction ( $\theta, \varphi$ ) on the hemisphere the recorded intensity of returns as a function of range constitutes the waveform. Image processing software is well equipped to deal with such three dimensional data when formatted in an appropriate manner.

As described in Section 3, the scan head of the EVI instrument sweeps out a vertical plane with recorded beam directions covering the whole upper hemisphere and some beyond. The EVI scan range is from +108 degrees to -100 degrees from zenith. The instrument rotary table simultaneously rotates through 180 degrees azimuth, at a speed that provides contiguous shots at the horizontal and overlapping data closer to zenith. The position of each shot is measured by two encoders – one for the scan head and one for the rotary table. Every full rotation and recording set has the same number of shots in each mirror scan and the same number of recorded returns in each shot. The data consisting of the number of positions of the rotary table by the number of shots in a mirror scan by the number of recorded return intensities in a shot forms a “data cube”.

We can arrange this three dimensional “data cube” using a band interleaved by line (BIL) format, where “band” in our case represents the full set of intensity values to a maximum range from the instrument. Figure 3-14 shows a representation of this data format where each row in the image corresponds to the scan of the instrument mirror from one horizon across the zenith to the other.

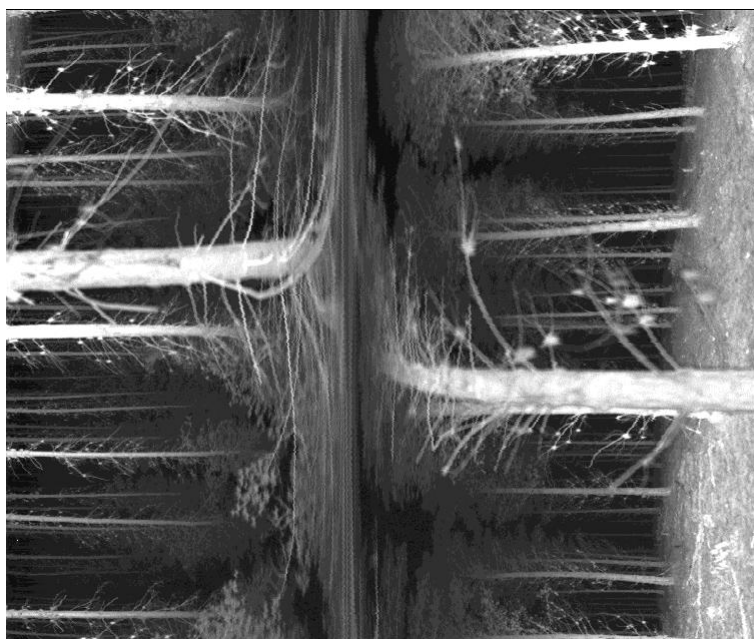


Figure 3-14: Sample data cube recorded at Springs Road Mt Gambier.

Each column in the image corresponds to a single scan head encoder position and represents the waveforms recorded for the set of rotary table positions at a single zenith angle – but on one “side” of the EVI scan. This image summarises the third (range) dimension of the data by showing the waveform totals. In effect this is the range-integrated image of the raw EVI data.

The data cube file stores all waveform information collected by the EVI. However, there are also large quantities of ancillary information that must be accessible for instrument calibration, monitoring and problem diagnosis. These data are stored in various ancillary files and all information is maintained during processing.

### 3.3.1.2 Waveform Recording

The best way to appreciate the third dimension (or the “bands”) of the EVI data cube (that are associated with range from the instrument by converting time to distance as described elsewhere) is to select specific pixels in Figure 3-14 and display the waveform associated with them. For the purpose of clarification, we can generalise the waveforms that may be recorded into two broad categories, hard target and soft target responses. Hard target responses can be thought of as a waveform resulting from the beam hitting a single object that is impervious to the beam – such as a tree trunk or a “wall”. The resulting intensity returned to the instrument will be an intense pulse with the same or very nearly the same shape as the outgoing pulse and produces a waveform like the one shown in blue in Figure 3-15.

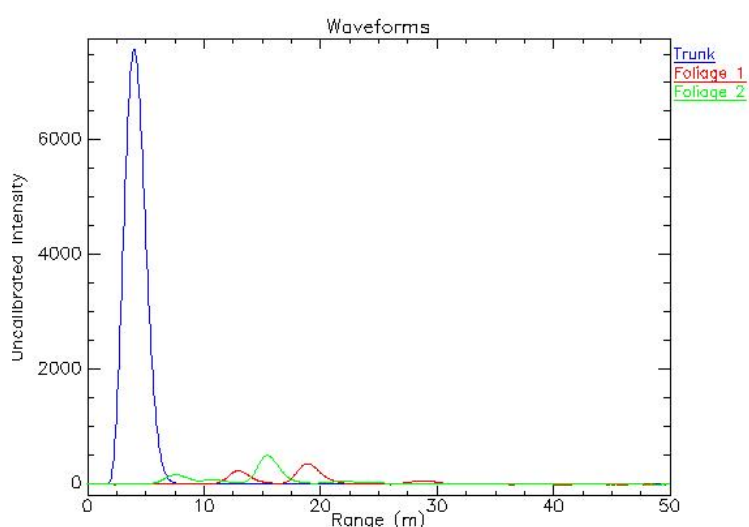


Figure 3-15: Typical waveform associated with the interception of the laser beam by a hard target such as a trunk.

A soft target response corresponds to the situation where the beam hits targets that do not fully cover the beam cross-section. This is typically the case for tree crowns where the small leaf size or small cross sectional area in the line of the beam means that it intersects a number (possibly a large number) of objects distributed over a range of distances. The typical waveform in such a case is generally composed of returns from multiple ranges. This is the case illustrated by the red and green waveforms in Figure 3-15. As the beam size increases or shots are averaged, the waveform from “soft” targets merges into a smooth, range distributed shape that contains valuable information on amount and spatial distribution of the scatterers.

The differences in intensity and spread of waveform peaks and other characteristics are important factors in extracting information from the EVI instrument. These differences allow analysis of woody components such as trunks and branches to be separated from the effects of foliage where parameters such as wood volume, yield and mean annual increment may be the primary foci. Conversely, they also allow separate analysis of foliage structure for information such as light and water interception for growth modelling.

Figure 3-15 illustrates other effects involved in the data and the data processing. In general, the returned energy from targets reduces as the reciprocal of the range squared ( $I(r) \propto r^{-2}$ ). The hard target return in Figure 3-15 is from a relatively close tree trunk while the distributed soft target returns are from foliage that is both spatially distributed and further away. Ranging systems optimised for hard targets and using an intensity threshold to detect events generally quickly lose the soft target events. Any system that aims to measure the intensity of soft targets – or hard targets from both near and distant positions – must cope with a very wide dynamic range of intensity values.

### 3.3.2 Data Re-Projections

As described above, each sample within each waveform recorded during a hemispherical scan can be located unambiguously in space relative to the instrument location using its range ( $r$ ), zenith angle ( $\theta$ ) and azimuth angle ( $\varphi$ ). This positional information also allows the data to be reprojected into a number of different formats that are visually more intuitive and can provide a superior basis for further analysis than the basic data cube described previously. For the cube format, data is arranged within the three-dimensional file structure defined by the dimensions ( $x, y, z$ ) according to scan encoder position, rotary encoder position and range.

The hemispherical re-projection (see Figure 3-16) converts the data into a form similar to a hemispherical photograph (but with an additional dimension of range) using the equations:

$$\begin{aligned}x &= \theta \cos \varphi \\y &= \theta \sin \varphi \\z &= r\end{aligned}$$

Resampling of the data is done on the basis of waveform averages but could be performed using other interpolating techniques such as nearest neighbour. Visually this is the image an observer would witness by standing at the instrument position and looking vertically upward. The intensity inverse of the waveform average image band in this projection can be used in conventional hemispherical photograph analysis software to estimate leaf area index and mean leaf angles.

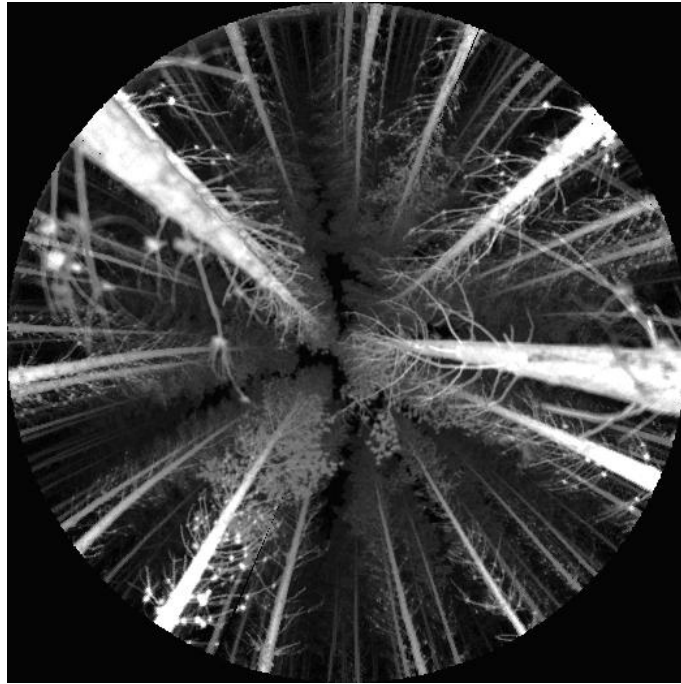


Figure 3-16: Mean waveform using a Hemispherical reprojection of the data cube recorded at Springs Road, Mt Gambier.

Often, analysis is performed using the mean of waveforms within specific angular regions. The most efficient file structure for extracting such data uses what we have called an “Andrieu<sup>3</sup> projection” (since it was used by Andrieu *et al.*, 1994 for hemispherical photographs), as shown in Figure 3-17. The equations for such a projection only require conversion between encoder values and true angles.

$$x = \theta$$

$$y = \varphi$$

$$z = r$$

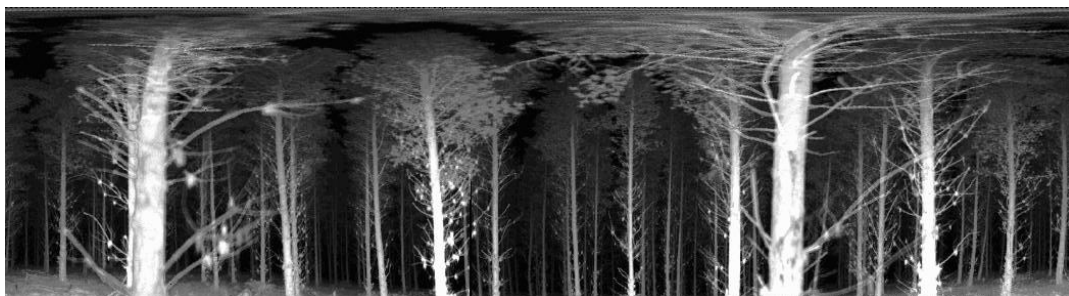


Figure 3-17: Mean waveform using an “Andrieu” reprojection of the data cube recorded at Springs Road, Mt Gambier.

It needs to be emphasised that moving from the original data cube to these projections involves reduction of data redundancy in the EVI scan pattern and the regularisation of pointing variations and other factors in the scan. The data produced are “metric” in

<sup>3</sup> This simple geometry is often used for cartographic and GIS data where it is known as the “Plate Carrée”, see Steers (1962).

the sense of having a correct viewer geometry and range to target. As such they are close to what was planned for the ECHIDNA® data.

A number of structural analysis algorithms also involve the analysis of data in terms of the more conventional dimensions of horizontal and vertical distance. In this case we describe the re-projection as cylindrical (see Figure 3-18), since a single z band corresponds to a cylinder centred on the instrument position.

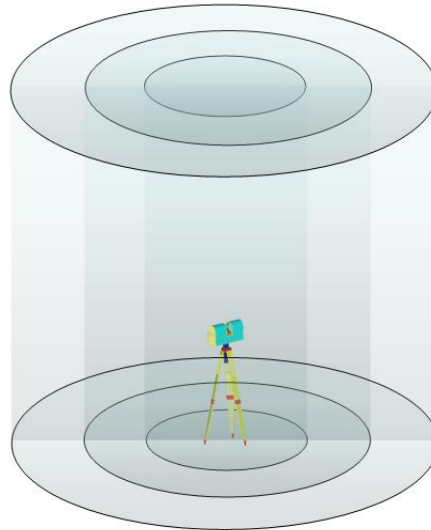


Figure 3-18: Diagram shows three cylindrical image layers (stored as bands) centred on the instrument location.

The re-projection equations used to produce these data are of the form:

$$\begin{aligned}x &= \varphi \\y &= r \cos \theta \\z &= r \sin \theta\end{aligned}$$

The advantage is that they produce images that can be analysed in terms of the true vertical structure of trees, branches and foliage. An example is shown in Figure 3-19.



Figure 3-19: Three-range colour composite using a Cylindrical projection of the data cube recorded at Springs Road, Mt Gambier.

A variant on this format is to use the height of the data as the z dimension so that each band of data corresponds to a plane of constant height above the ground, as in Figure 3-20. In this case the equations for y and z are simply reversed to give:

$$x = \rho$$

$$y = r \sin \theta$$

$$z = r \cos \theta$$

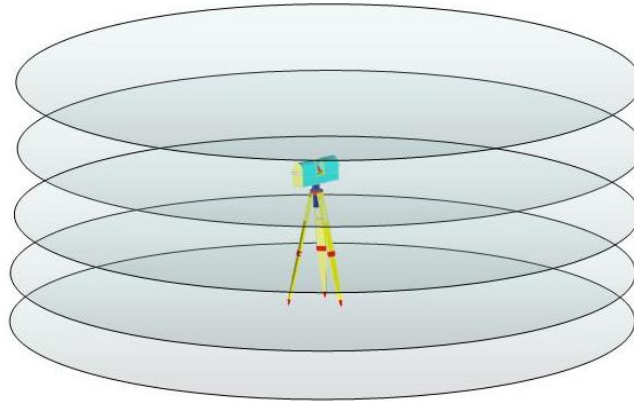


Figure 3-20: Diagram shows five planar image layers (stored as bands) of constant height above the ground.

The data in this format can be used to assess stem size and location and assess stem form as a function of height. For example, Figure 3-21 shows a colour composite of three slices just above the height of the EVI instrument at a site called Larundal in southern NSW. White areas are returns interacting with relatively straight trunks while colour and dispersion represent branches or stems that are not straight or vertical.



Figure 3-21: Three planar slices as a colour composite using the second form of Cylindrical projection of the data cube recorded at Larundal in southern NSW.

As described later, the apparent “smear” in the vertical direction is due to the laser pulse width and is taken into account during trunk size estimation and tree locating.

### 3.3.3 Statistical Analysis of ECHIDNA® Waveforms

Conventional forest structural analysis using hemispherical photography employs estimates of gap probability ( $P_{gap}$ ) within given zenith angle ranges to compute foliage area index and mean leaf inclination angle. More correctly, the foliage area index computed should be regarded as a plant area index, since different plant components (leaf, stem, branch) cannot be adequately separated in the analysis.

A corresponding technique used to analyse ECHIDNA™ data employs mean gap probability within specified zenith and azimuth sectors as a function of range and enables not only total LAI to be determined but also the foliage density to be estimated as a function of height above the canopy floor. The ECHIDNA® is designed to measure waveforms of return intensity and these can be aggregated within specific zenith and azimuth ranges and analysed in terms of a multi-angular full waveform canopy model.

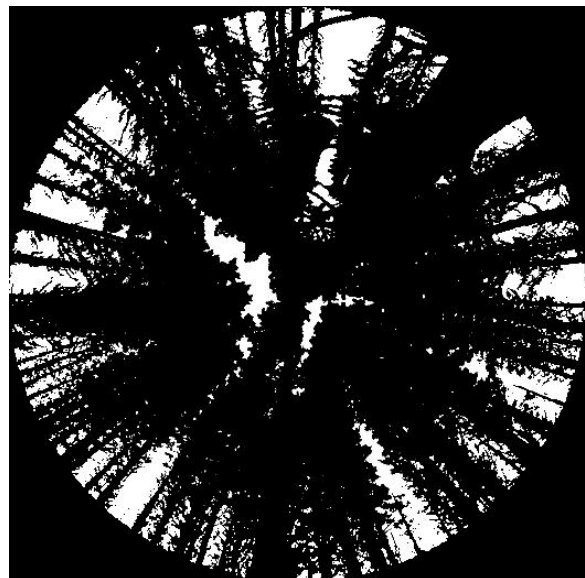
### 3.3.3.1 Pgap Method

Each range layer of ECHIDNA™ data can be separated into complete gap (from the position of the EVI instrument) out to the given range and non-gap. This is done on the basis of an initial threshold relative to a complete gap signature selected from the image. Gaps are first located in the outer layers and further analysis is performed on successively closer image layers, adjusting the initial threshold value to ensure that gaps in a given direction do not disappear at closer ranges. A typical result is shown in Figure 3-22.

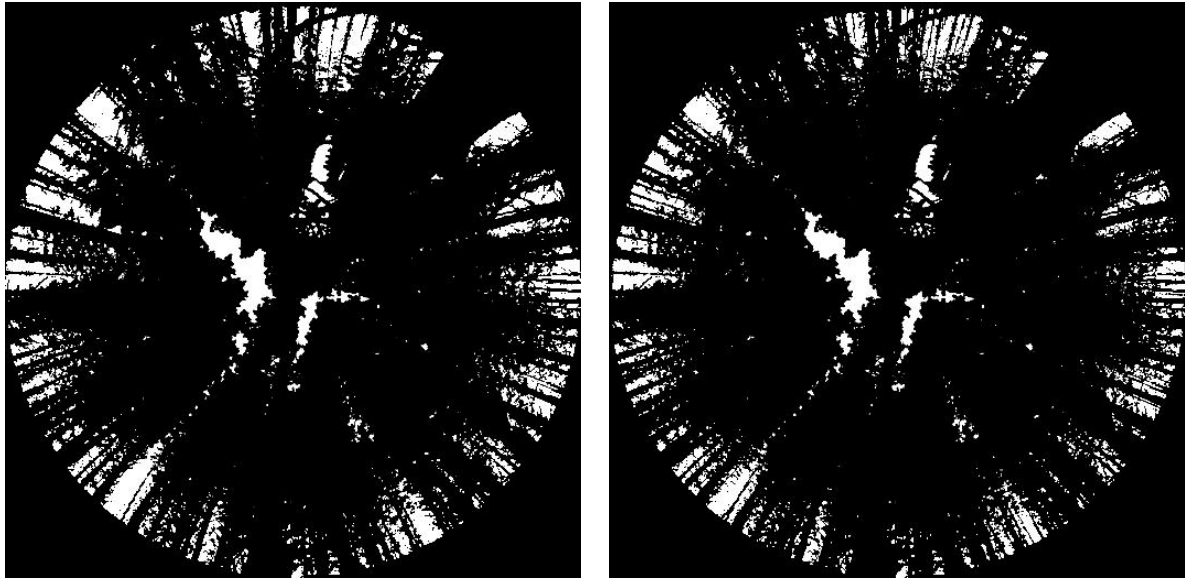
The major variations obvious in ECHIDNA® based Pgap data when compared to hemispherical photographs (other than the separation of range components) is that near the horizon the probability of a gap to the maximum range of the EVI is often larger than it is at mid-zenith angles, whereas a hemispherical photograph will rarely have gaps near the horizon. This region is where the information about the tree trunks resides.



Pgap to 20 m



Pgap to 30 m



Pgap to 40 m

Pgap to 50 m

Figure 3-22 Examples of gap probability as a function of range for the Springs Rd site. Images are presented with hits in black and gaps in white in a comparable manner to hemispherical photographs.

A mean gap probability profile can be computed for a series of zenith angle regions, based on the Pgap images. These can be used to infer structural characteristics of the canopy such as the foliage profile, leaf area index and canopy height. At the instrument (range = 0) the gap probability will be equal to unity and will fall as a function of the amount of plant material that is encountered by the outgoing pulse (Figure 3-23).

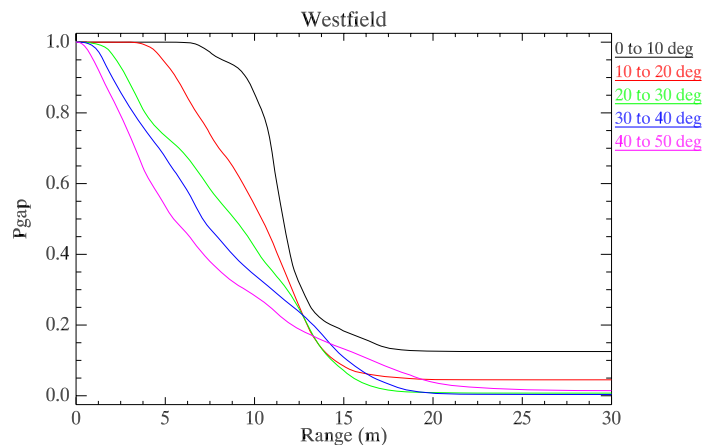


Figure 3-23: Sample Pgap profiles derived from EVI data recorded at the Westfield site in Tasmania.

Considering the influence of foliage in isolation, the mean gap probability profile for the crowns ( $P_{gap,c}$ ) as recorded at an angle close to the zenith (e.g. 10 to 20 deg in Figure 3-24) should decrease to a minimum Pgap value rapidly, due to the small distance required to reach the crowns of the trees above. With increasing zenith angle the beam must travel a greater distance before reaching tree crown, causing a delayed drop in the Pgap. This relationship can be modelled using the equation,

$$P_{gap,c}(r, \theta) = e^{-G(\theta, \theta_L)F(r \cos \theta) / \cos \theta}$$

where  $G(\theta, \theta_L)$  is the Ross (1981) foliage projection function,  $\theta$  is the zenith angle of the beam,  $\theta_L$  is the mean foliage inclination angle and  $F(z)$  is the cumulative vertical foliage area profile to height “z” such that if  $f(z)$  is the foliage density at height “z” than”

$$F(z) = \int_0^z f(z') dz'$$

The function  $F(z)$  may be approximated in this case using a Weibull distribution, similar to that used by Yang *et al.* (1999):

$$F(z) = a \left( 1 - e^{-b \left( \frac{z}{H} \right)^c} \right)$$

That is,  $F$  is the cumulative foliage density measured vertically from the ground to level  $r \cos \theta$  in the canopy,  $H$  is the canopy height,  $a$  controls the total foliage area, and  $b$  and  $c$  describe the distribution of the foliage in the vertical direction. Example curves for  $P_{gap,c}$  are shown in Figure 3-24. This distribution is a single layer approximation of the foliage profile and consequently will perform best in an even aged monoculture.

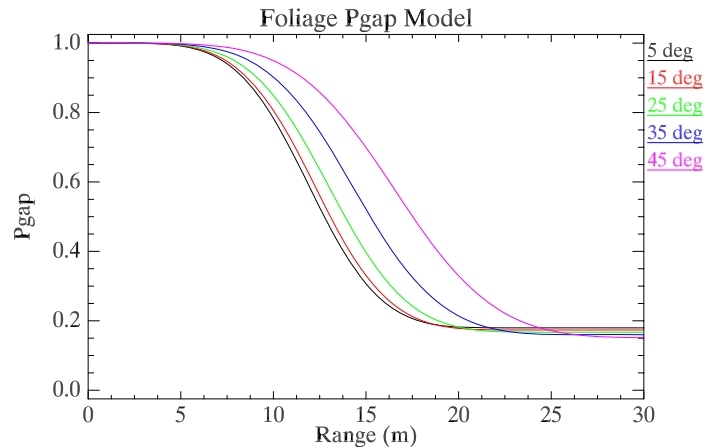


Figure 3-24: Modelled foliage gap probability curves for zenith angle ranging from 5 to 45 degrees with Weibull parameter values set at  $a = 2$   $b = 5$ ,  $c = 5$  and  $H = 15$ .

As a simple approximation, trunks can be modelled as cones with base diameter equivalent to the mean diameter at breast height  $D$  and a height equivalent to the mean tree height  $H$ . The stocking density of stems within the forest is given by  $\lambda$  and the stems are distributed randomly in the horizontal plane. The gap probability at a range  $r$  from the instrument can be thought of in terms of the number and size of shadows cast from the level of the instrument onto a horizontal plane at the level  $z = r \cos \theta$  when illuminated by the instrument beam with zenith angle  $\theta$ . This can be expressed using the equation,

$$P_{gap,t}(r, \theta) = e^{-\lambda A(r, \theta)}$$

where  $A$  is the mean shadow area cast by a trunk. The geometry of the shadow area  $A$  is shown in Figure 3-25.

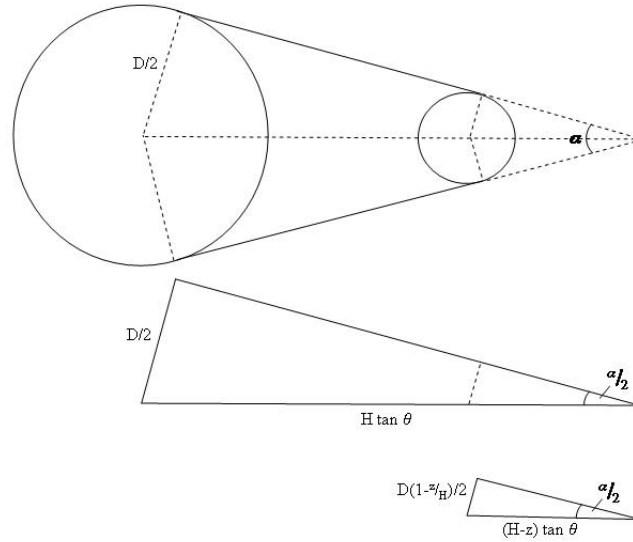


Figure 3-25: Geometry of the trunk shadows at level  $z$  in the canopy when illuminated by a beam with zenith angle  $\theta$ . The shadow is bounded by the circle defining the base of the trunk, the circle defining the trunk at level  $z$  and the tangent lines joining the two circles.

When  $z = r \cos \theta < H$  the area of the trunk shadow  $A$  is given by the equation,

$$\bar{A}(r, \theta) = \frac{1}{4} \frac{D^2 (1 - (1 - z/H)^2)}{\tan \alpha / 2} + \frac{1}{8} D^2 (\pi + \alpha) + \frac{1}{8} D^2 (1 - z/H)^2 (\pi - \alpha)$$

where

$$\sin \alpha / 2 = \frac{D}{2 H \tan \theta}$$

The set of  $P_{gap,t}$  curves in Figure 3-26 show that there is a large gap probability for a near vertical beam (zenith angle = 5 deg) when the trunks are treated in isolation and this gap probability decreases as the zenith angle of the beam increases.

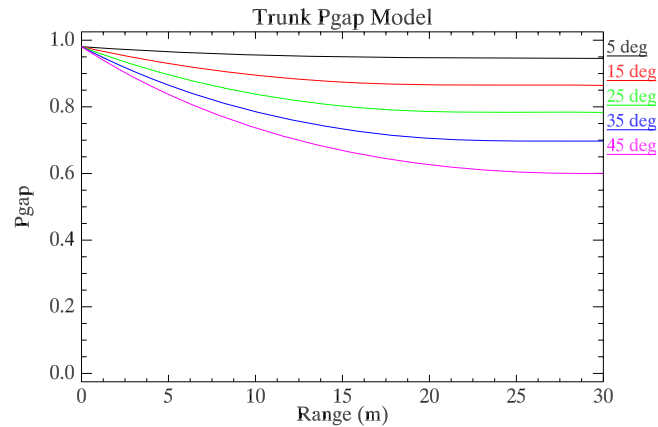


Figure 3-26: Modelled trunk gap probability curves for zenith angle ranging from 5 to 45 degrees with tree density parameter  $\lambda = 0.1$  and mean DBH = 0.5m.

The combined foliage and trunk gap model (assuming foliage and trunks form independent Boolean models) is simply the product of the two component models, giving:

$$P_{gap}(r, \theta) = e^{-(G(\theta, \theta_L)F(r, \theta)/\cos\theta + \lambda A(r, \theta))}$$

Example Pgap curves are shown in Figure 3-27 for the same parameter values as those used in Figure 3-24 and Figure 3-26. The dominance of the canopy type response in this figure is due to the low zenith angles used (5 to 45 degrees).

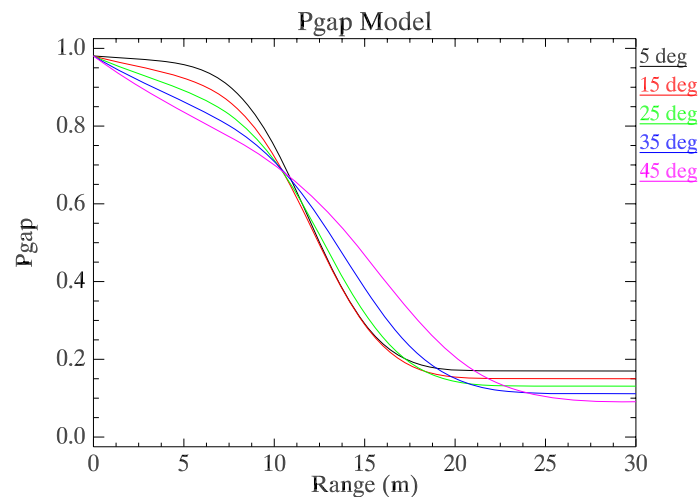


Figure 3-27: Modelled gap probability curves for zenith angle ranging from 5 to 45 degrees with parameters as set in Figure 3-24 and Figure 3-26.

As a result of this description of the forest gap probability we have a set of parameters that describe:

- stocking density;
- mean diameter at breast height;
- canopy height;

- the vertical foliage distribution (LAI and bole height).

These parameters can be estimated using non-linear optimisation on the basis of the measured gap probability profiles shown in Figure 3-23. However, in this case stocking and mean diameter at breast height are not separable, giving a parameter related to, but not the same as, basal area. Estimation of these parameters is presented in Section 5.4.

### 3.3.3.2 Waveform Modelling Method

A beam transmitted by the instrument near the vertical direction has a high probability of interception by overlaying foliage and very little probability of interception by tree trunks. As a result, a mean zenith waveform collected from a region close to the vertical shows a strong response from foliage elements, which is typically low near the ground and reaches a maximum in the region between the bole height (or height to the green level) and the top or predominant height, after which the response tapers off into the noise floor. This is shown by the black curve in Figure 3-28.

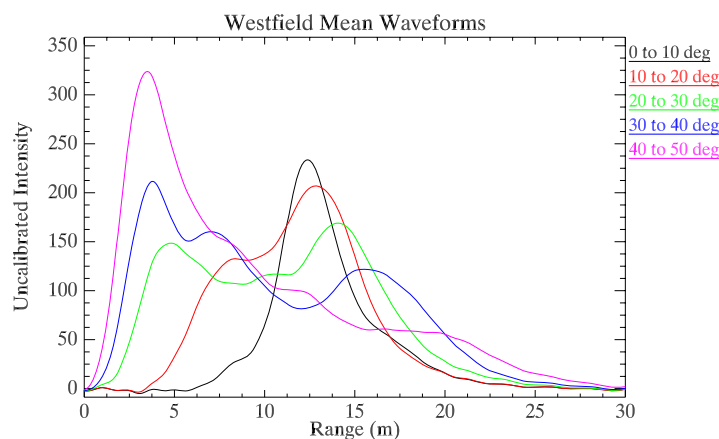


Figure 3-28: Sample zenith mean waveforms derived from EVI data recorded at the Westfield site in Tasmania.

As the zenith angle of the beam transmitted by the instrument increases, it will travel further before hitting the foliage layer and have a greater path length through this layer. Correspondingly, as the zenith angle from which the waveforms are collected increases, the location of this foliage peak increases and is spread over a greater range. This is illustrated by the gradual increase in range to and width of the foliage peak (the peak in the data occurring at a range between 12 and 20m) in Figure 3-28 as the zenith angle increases.

At the higher zenith angles are sampled, the probability of interception by trunks also increases. The effect on the waveform is the appearance of a strong close range peak in the mean waveforms, which increases in intensity with increasing zenith angle.

We can model these effects using the lidar equation (see Appendix 3):

$$I(r, \theta) = -CI_{shot} * \left[ \frac{K(r)}{r^2} p(\theta) \rho P_{Hit}(r, \theta) \right]$$

In this formulation,  $I$  is the intensity returned to the instrument as a function of range  $r$  and beam zenith angle  $\theta$ .  $C$  is a calibration factor which relates the measured data (volts, amps or counts) to the intensity of the beam,  $I_{shot}$  is the intensity of the transmitted pulse and  $K(r)$  is a close range optical efficiency function which rises from near zero at the instrument to 1.0 within a short range of a few metres. Since the transmitted pulse varies over a finite period according to a Rayleigh distribution, “\*” represents a convolution of the pulse shape and intensity with the right hand side of the equation.

The normal incidence reflectance of the plant material ( $\rho$ ) is separated from the geometric effect  $p(g, \theta)$  which influences how much of the reflected beam is scattered in the direction of the detector.  $P_{gap}$  is the gap probability of the canopy as a function of  $r$  and  $\theta$ . As stated in Appendix 3,  $P_{hit}$  is related to  $P_{gap}$  according to the equation

$$P_{hit}(\theta, r) = -\frac{\partial P_{gap}(\theta, r)}{\partial r}$$

For the foliage  $P_{gap}$  model described in the previous section,  $P_{hit}$  is then given by the equation,

$$P_{hit,c}(\theta, r) = \frac{G(\theta, \theta_L)}{\cos \theta} \frac{\partial F(r)}{\partial r} e^{-G(\theta, \theta_L)F(r \cos \theta) / \cos \theta}$$

and given that  $z = r \cos \theta$ ,

$$P_{hit,c}(\theta, r) = G(\theta, \theta_L) \frac{\partial F(z)}{\partial z} e^{-G(\theta, \theta_L)F(r \cos \theta) / \cos \theta}$$

where,

$$\frac{\partial F(z)}{\partial z} = \frac{abc}{H} \left( \frac{r \cos \theta}{H} \right)^{c-1} e^{-b \left( \frac{r \cos \theta}{H} \right)^c}$$

An illustration of the  $P_{hit,c}$  is shown in Figure 3-29

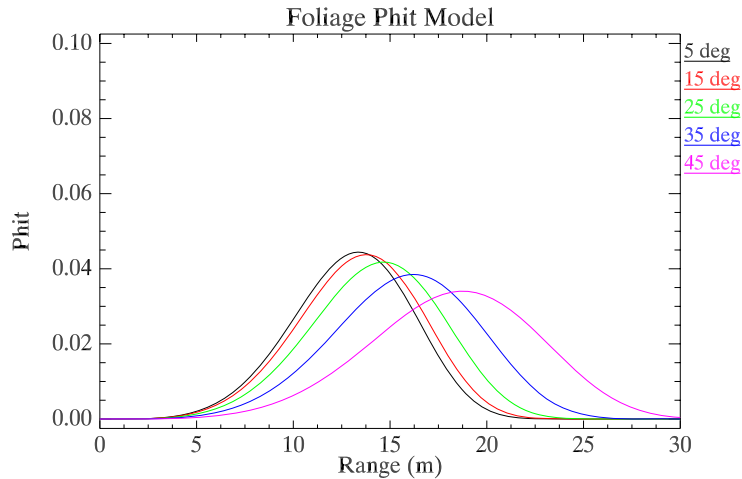


Figure 3-29: Modelled Phit,c curves for zenith angles ranging from 5 to 45 degrees with Weibull parameter values set at  $a = 2$ ,  $b = 5$ ,  $c = 5$  and  $H = 15$ .

For the previously defined trunk Pgap model, the Phit,t is given by the equation,

$$P_{hit,t}(\theta, r) = \lambda \frac{\partial A(r)}{\partial r} e^{-\lambda A(r, \theta)}$$

and an example shown in Figure 3-30.

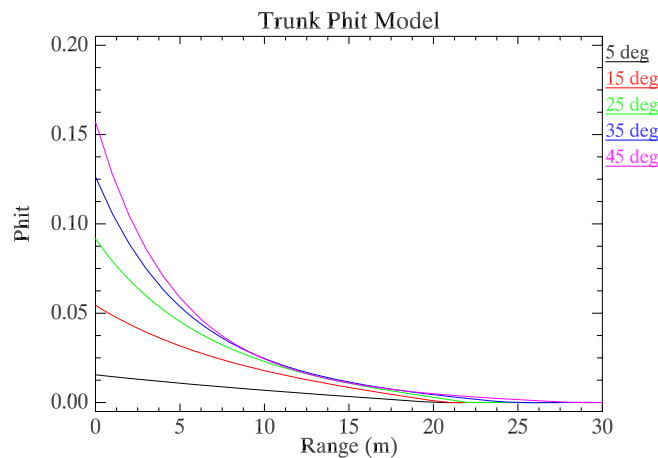


Figure 3-30: Modelled Phit,t curves for zenith angles ranging from 5 to 45 degrees with parameter values of  $\lambda = 0.1$  and  $D = 0.5$ .

For the two-component model, where crowns and trunks are treated as separate entities, Phit is given by,

$$P_{hit}(\theta, r) = \left[ G(\theta, \theta_L) \frac{\partial F(z)}{\partial z} + \lambda \frac{\partial A(r, \theta)}{\partial r} \right] e^{-(G(\theta, \theta_L) F(r \cos \theta) / \cos \theta + \lambda A(r, \theta))}$$

Example Phit curves are shown in Figure 3-31.

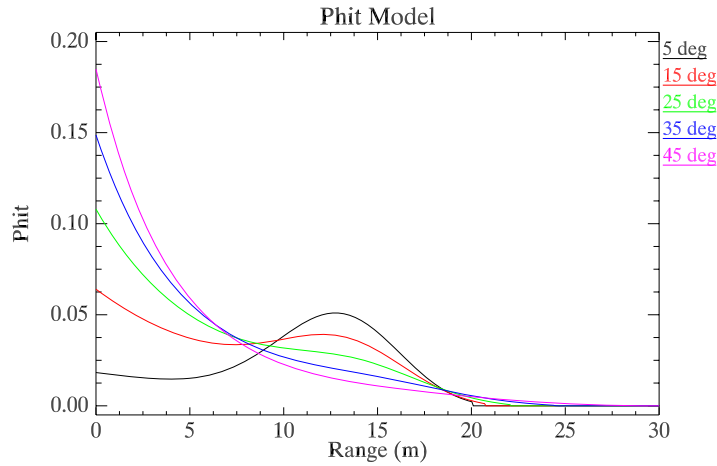


Figure 3-31: Modelled hit probability curves for zenith angle ranging from 5 to 45 degrees with parameters as set in Figure 3-27.

The lidar equation can then be stated as follows, ensuring that specific reflectance and scattering terms are assigned to the respective plant components,

$$I(r, \theta) = CI_{shot} * \frac{K(r)}{r^2} \left[ \rho_L p(g_L, \theta) G(\theta) \frac{\partial F(z)}{\partial z} + \rho_t p_t(\theta) \lambda \frac{\partial A(r, \theta)}{\partial r} \right] e^{-(G(\theta, \theta_L) F(r \cos \theta) / \cos \theta + \lambda A(r, \theta))}$$

Example waveforms produced using the model are shown in Figure 3-32 and closely resembles the form of the data shown in Figure 3-28.

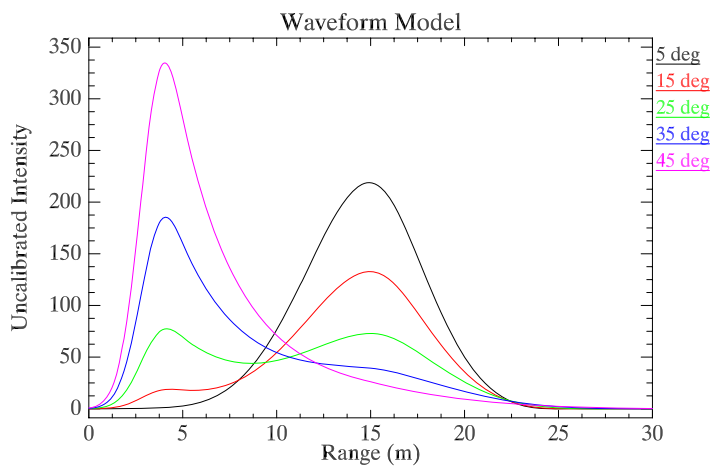


Figure 3-32: Waveform model for the data shown in Figure 3-28.

As with the Pgap method, the waveform model has a set of parameters that describe:

- stocking density;
- mean diameter at breast height;
- canopy height;
- the vertical foliage distribution (LAI and bole height).

These parameters can be estimated in a similar way to that described in 3.3.3.1 and results of this estimation are presented in Section 5.4.

### **3.3.4 Trunk density and size distribution**

The consistent geometric integrity of the EVI data and the geometric probability methods listed in the ECHIDNA® patent applications provide the opportunity for detection and measurement of individual targets such as tree trunks using range to and angular width of the object. The use of the full waveform and the intensity information also helps make this task possible. The theory behind this activity is described in Appendix 4 and will only be summarised here.

#### **3.3.4.1 Trunk identification and measurement**

The cylindrical projection of EVI data provides the most useful basis for identification and measurement of trunks. In this format, a horizontal slice can be extracted at any height (e.g. breast height) where the dimensions of the slice are azimuth (bearing) and range from the EVI to an object. The processing recognises the tree trunks from among the other components (such as branches and foliage) and assesses range and angular width at various heights above the ground. Analysis of data in this form to obtain basal area and other information is analogous to using a Relaskop to scan a variable size plot.

The reflectance of tree trunks at 1064 nm is relatively consistent (approx 0.45-0.55) even though their visual appearance may be quite variable. This provides a well-defined expected value for the intensity of returns from EVI beams that fall fully within a trunk. Thus, the primary stage of identifying trunks in the EVI data is to apply a range-adjusted threshold based on the expected intensity.

Once the location of trunks has been identified, their angular extent can be explored by considering the neighbouring EVI shots which form a scan across the tree. For a curved trunk, both the range to the surface and the returned intensity vary across the trunk. However, the range resolution of the EVI data is such that the variation across a trunk will be difficult to detect, so this method makes use of the intensity variation. For EVI beams that fall entirely on a trunk, the way the intensity changes is due to the change in angle of the target relative to the instrument (due to the trunk curvature) with the centre point returning the highest intensity. For a particular trunk, this depends on both the diameter of the trunk and its distance from the EVI, therefore an adaptive thresholding technique is used to identify the span of EVI shots that fall within a trunk. The expected ratio of intensities at the edge and centre of a trunk as a function of trunk diameter and range can also be derived. This is used to test the intensity of each return in a scan across a trunk and where the actual return falls below that expected, we can identify the trunk edge. The behaviour of the fall-off in intensity between the last within-trunk shot and the next is used to determine the edge position as a fraction of the EVI beam size.

At this point, we have identified a set of trunk centres and angular spans. Since some trees will be partially or fully obscured by those at closer range, the edges of the identified trees are classified by looking for closer targets within the neighbouring

EVI shots. If no closer targets are found, then the identified edge is the true edge of the trunk. For a tree where both edges are unobscured, the angular width is the sum of the two angular spans from the centre to the edges. If one edge is obscured, we estimate the width by doubling the angular span to the visible edge. If both edges are obscured, we place a lower-bound on the trunk width based on the span of the trunk that is visible. The data produced from this analysis is the location (bearing and range) and angular span of visible trees from which the actual diameter can be calculated. Not all trees are visible and the analysis of this data must take that into account to provide unbiased statistics on tree numbers and sizes.

#### **3.3.4.2 Tree count by range**

The measured range to the closest face of each tree can be modified to provide the range to the tree centre by addition of half the estimated trunk diameter. Using this information for each tree identified in the EVI data we have a sample of the distribution of tree numbers as a function of range. A model is used to interpret the effect of obscuration by near trees, branches and foliage and results in an expected number at a given range as a function of the tree density (number per m<sup>2</sup>) and the mean diameter. The identification of “tree hiding” and the pattern of tree stem distribution is essential to the use of angle count methods and the development of stand, as opposed to single tree, estimates of factors such as form factor and basal area.

#### **3.3.4.3 Relaskop methods**

The principle of a Relaskop is to identify the number of trees with angular size greater than a particular angle (sometimes called the “wedge” angle). These trees are referred to as the ‘in’ trees. For any given wedge size, statistical sampling theory (see Appendix 2) provides a calibration factor which relates the number of ‘in’ trees to basal area and a means to relate information about the ‘in’ trees to the unbiased sample estimates for the same information. The output of the EVI trunk-finding routines provides angular spans of all visible trees. Thus, these can be tested against standard wedge angles to determine basal area. There is modification needed to the standard Relaskop theory to account for obscuration, as modelled in the previous section.

#### **3.3.4.4 Tree diameter distributions**

The diameter of trees can be calculated from the ranges and angular spans identified in the EVI data. The distribution is incomplete since it contains only the trees visible to the instrument. The identified ‘in’ trees from the application of the Relaskop method can be used to derive unbiased estimates of the mean and variance of the diameter distribution. However, the reliability of this estimate depends on the significance of the sample on the complete distribution. This is the same method used for the analysis of measured ‘in’ trees in the field protocol based on angle count sampling and applies a weight to each measured tree according to its contribution to the basal area (see Appendices 2 and 4). The tree diameter statistics combined with the basal area results from the Relaskop method also provide a stand-based estimate of the stem density.

## 4 BEST PRACTICE AIRBORNE LIDAR PROCESSING

### 4.1 Introduction

Airborne Lidar has been demonstrated to measure useful forest properties, such as height and cover, using commercial terrain laser scanning systems (Næsset, 1997a,b; Magnussen and Boudewyn, 1998; Magnussen *et al.*, 1999; Witte *et al.*, 2000). Such studies have often included regression results with other field-derived variables (e.g. diameter at breast height) to provide large-scale mapping via relationships with the lidar data. Results are generally well correlated with field data but tend to be site dependent. Also, a high spatial density of Lidar shots is required to achieve acceptable accuracy in structural properties.

One direction of research and development in airborne Lidar systems has been to increase the beam divergence, resulting in larger footprints, and to digitise the return intensity to provide laser ‘waveforms’ – or the complete time trace of return power to the airborne platform. The best-known examples of such ‘canopy Lidars’ are the experimental SLICER (Lefsky *et al.*, 1999a,b; Harding *et al.*, 2000) and LVIS (Blair *et al.*, 1999) systems. However, since most users currently have access to commercially available terrain ranging Lidars (usually known as airborne laser scanning, or ALS systems) there is value in developing algorithms and methods that fully exploit the information content obtained from these instruments.

### 4.2 Airborne Lidar Systems

The difference between ALS systems and canopy lidars is illustrated in Figure 4-1. A canopy lidar system records the return power of the laser pulse by digitising the whole of the return and uses a relatively large footprint (such as 10-25 metres) so that signals from all reachable elements of the canopy profile are recorded in a single return trace. The time of the return of the peak of the pulse is a measure of the target range and the strength of the return an indicator of the target scattering cross section and reflectivity. By combining the digitising of the return with a larger, but variable, beam footprint and a scanning laser it is possible to cover the kinds of area needed for regional vegetation survey and retrieve canopy information that has not been obtainable by any other form of remote sensing.

In contrast, ALS systems use a high spatial density of small footprint laser pulses, to enable each shot to penetrate gaps in canopies with minimal attenuation to create a sufficient number and power of returns from the ground to sense terrain height under many levels of cover. The recorded data are the position and possibly intensity of one or more returns that exceed a threshold. Application of such data to forest measurement is enhanced in instruments that record more than one return (most current instruments record at least first and last returns) as samples of both canopy and ground can be located.

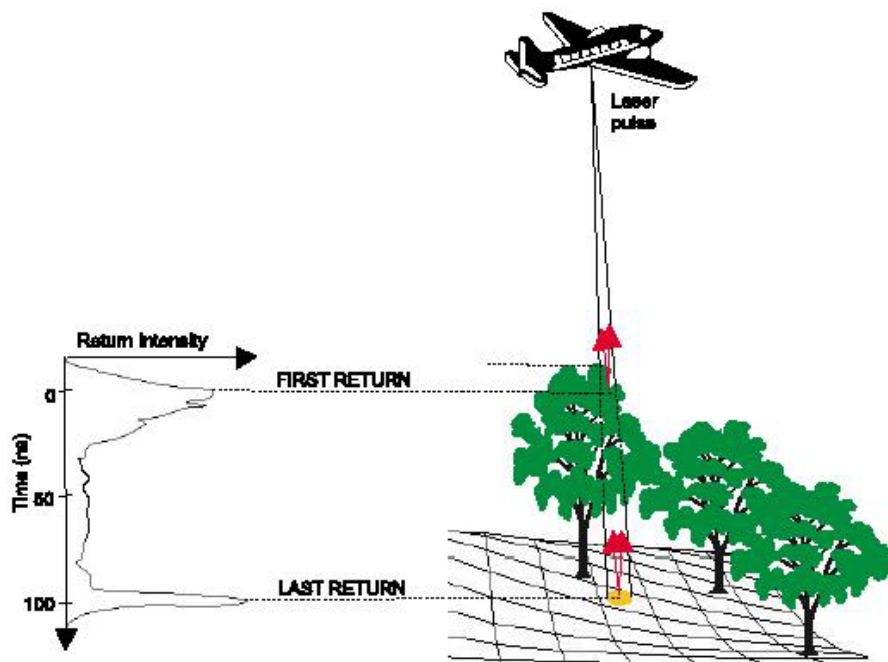


Figure 4-1 Lidar returns from vegetation are dispersed. Airborne laser scanners detect returns above a threshold. (Image reproduced from Gaveau and Hill, 2003).

Currently, only ALS systems are in commercial operation. Advances in digitiser technology have made it possible for some newer systems to record waveform data for a subset of output pulses. However these instruments still employ small beam divergence and are not yet available in Australia.

ALS systems employ a scanning or rotating mirror to produce a pattern of laser pulses along the ground track. An example of this is illustrated in Figure 4-2. In this case the scanning mirror produces a zig-zag pattern. A rotating mirror, by contrast would produce points in a set of parallel scan lines. Factors that affect the distribution of the points include: aircraft height, flight speed, half scan angle, pulse frequency and scan frequency and topographic variation. Pulse frequency is normally fixed for a given instrument (current-technology instruments have pulse frequencies of at least 25 kHz). Scan frequency can be varied and, in practice, is adjusted to equalize the in-flight and across-flight point spacing.

The spatial density of the lidar points can be varied in two ways: first, by reducing the half scan angle and/or the flying speed and second, by acquiring data in multiple flights over the same area. While both of these methods will vary the spatial density of the lidar points, they result in different ground footprint spatial patterns and the interaction of these with a regular plantation can influence the results. For single flight line data, the spatial coverage is less near the edges of the swath and this affects the retrieval accuracy.

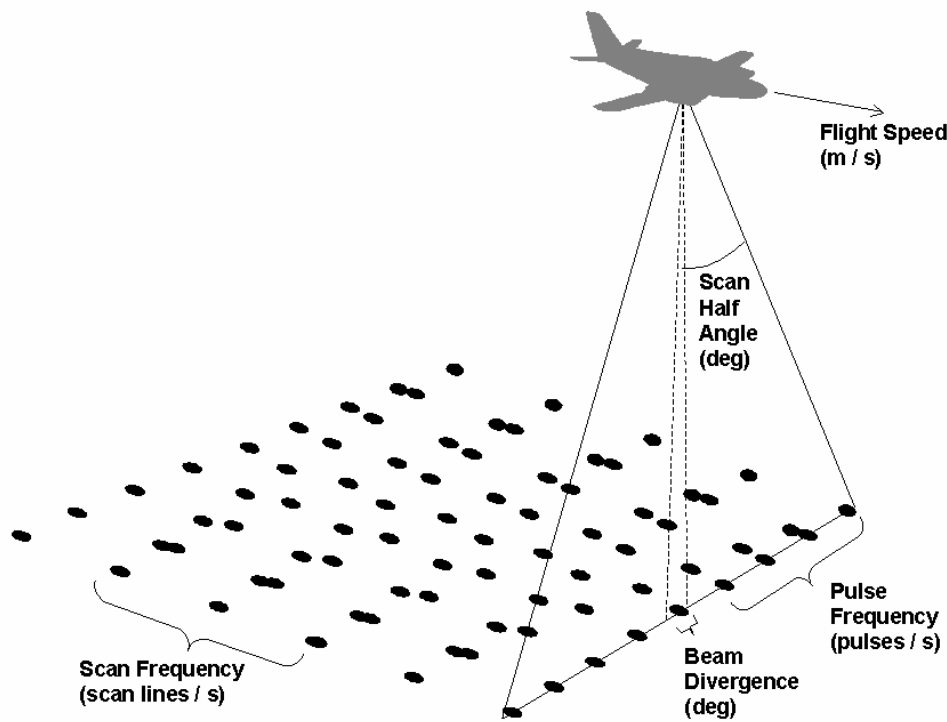


Figure 4-2. Example of an airborne laser scanner.

### 4.3 Analysis of Discrete Point Data

The primary use of airborne laser scanning (ALS) technology is to measure ground elevation to produce digital elevation models (DEM). Recording multiple returns from each laser pulse provides important information about the vegetation canopy above the ground. Lidar returns from the canopy (canopy hits) can be assigned a height above the ground on the basis of the difference in their elevation relative to an interpolated ground surface (DEM).

Many researchers have achieved good agreement between lidar-derived parameters and a variety of height measures (Næsset and Økland 2002, Persson *et al.*, 2002, Magnussen *et al.*, 1999), however these are often site and species dependent and may only apply to a particular instrument. Since lidar is a sampling technology, the operational parameters of the instrument affect the accuracy of retrieval of measured parameters as well as the cost of acquisition. The interaction of sampling characteristics with forest structure, particularly regular arrangements such as those found in plantations, can lead to bias and high uncertainty in the results (Lovell *et al.*, 2005). It is critical to understand the nature of such bias and uncertainty in order to specify suitable scan parameters to obtain both useful and cost-effective results.

### 4.3.1 Digital Elevation Model

Retrieval of vegetation canopy structural information from ALS data depends on an accurate model of the underlying ground surface. The detection of lidar returns from the ground surface through a canopy is affected by the density of the canopy, the angle of incidence, beam size and the level of detection thresholds. Operational parameters such as scan angles, flying height and possibly beam divergence can be adjusted to maximise the probability of sufficient ground returns while minimising the number of flight lines required. The first step in generation of a DEM from lidar data is to classify each return as either ground or non-ground (e.g. vegetation, buildings). Once the points have been classified, the ground returns can be interpolated to form a regular grid.

In multiple return systems DEM generation is usually done using only the last returns. There are many methods of classification applied to lidar data due to the necessary trade-off between accuracy and computational efficiency. The simplest method is to find the minimum height of returns within each cell of a grid, however, this is likely to retain many non-ground returns unless the grid cells are large, in which case the spatial resolution of the resulting DEM will be poor. The most common classification methods are iterative, where an initial rough surface is determined and points exceeding a threshold level above the surface are rejected. The surface model is then recalculated and the process iterates until a stable surface is achieved. Other techniques involve geometric or model constraints over regions of data, for example, testing convexity and removing upward spikes.

After classification, the interpolation of ground returns may be performed by linear interpolation based on Delauney triangulation or more complex methods based on expectations of surface behaviour (such as hydrological flows or other catchment properties). Data used in this project were acquired with reduced scan angles to both increase the point density for vegetation analysis and to ensure accurate DEMs could be achieved. The data provider provided the classification of data into ground and non-ground hits and in most cases DEM interpolation was performed using ANUDEM (<http://cres.anu.edu.au/outputs/anudem.php>). For some smaller areas a simple minimum grid and linear interpolation method was used with the classified ground points.

### 4.3.2 Canopy Height

A key issue in the application of lidar data to estimate individual tree or stand height is the definition and measurement of “height”. While the height of an individual tree is well defined, an appropriate measure of height for a plot or overall forest stand height is more problematic with forestry organizations using a wide variety of measurement methodologies and definitions. In each case it is likely that the allometry based on “height” will also be different.

The spatial separation of ALS samples relative to the size, shape and openness of tree crowns affects the probability of obtaining a height measurement using Lidar “hits” from near the top of a tree. High spatial density of sampling reduces the impact of this

effect, but also increases the cost of acquisition due to the requirement for lower flying altitudes, reduced flying speed, smaller scan angles (resulting in smaller swath widths), multiple overflights, or combinations of these. Different analysis methods account for this problem in a variety of ways, such as by modelling or using a statistical measure of height.

#### **1.1.1.1 Canopy Elevation Model**

The non-ground hits from ALS data may be interpolated to produce a canopy elevation model (e.g. Leckie *et al.*, 2003). This represents the upper envelope of the forest canopy and can be used to identify individual trees, their heights and crown dimensions. Popescu and Wynne (2004) and Popescu *et al.* (2003) present probably the most advanced analysis of this kind. They use a variable window local maximum filter to identify tree centres and then fit polynomial functions to two perpendicular transects across each crown to identify the interpolated crown centre and the edges. This provides an alternative estimate of the tree height that may overcome the statistical chance of lidar hits being at the top of the tree and also allows crown diameter to be estimated. However, the trees identified will generally be the emergent or taller trees and it is not clear how the heights determined in this way correspond with other measures of stand “height”.

#### **1.1.1.2 Plot-based Height Measures**

Conventional plot-based inventories employ a variety of height measures, many of which can be replicated with lidar data. Most strategies are based on the average height of a number of trees within a given area (plot), sometimes with spatial stratification within the plot or weighted according to DBH or another structural parameter. The digital nature of ALS data means that a variety of sampling methodologies can be implemented from the same dataset.

In a recent paper (Lovell *et al.*, 2005) ‘predominant height’ (Lewis, 1971) was selected as the primary field measure for comparison with retrieved heights from several simulated lidar datasets. Predominant height can be defined in a number of ways but generally involves sampling the largest trees in a plot or a number of plots. In defining an equivalent lidar-based definition for stand height, it is clear that the mean height of lidar hits (which may come from within crowns as well as from the tops of trees) has a complex relationship with the tree heights (Harding *et al.*, 2001, Ni-Meister *et al.*, 2001). Foresters prefer to use predominant height as it is not affected as much by thinning operations. In both cases there are good reasons to derive measures based on the hits near the top of the canopy. Magnussen and Boudewyn (1998) explored the use of upper percentiles of the hits in a specified lidar data ‘plot’ and found good relationships with mean height of the emergent layer. In previous research (Lovell *et al.*, 2003) it was similarly concluded that the mean of a specified number of highest hits (separated enough so as not to be from the same crown) provides a good match to any of the various predominant height definitions used by foresters.

The shape of tree crowns affects the likelihood of a lidar beam hitting near the top of a tree. It has been shown (Nelson, 1997) that knowledge of crown shape is important in

the interpretation of lidar data for single trees. It is also a consideration when designing the parameters for lidar data acquisition. In our simulations, cones were used to simulate the trees of a pine plantation, and these were compared with simulations using ellipsoidal crowns (e.g. eucalypt plantation) for the same tree locations, heights and crown radii. The predominant heights derived for simulated ellipsoidal crowns were found to be much closer to the true predominant height than for conical crown simulations. The key factor is the rate at which canopy height decreases with distance from the centre of the tree. Clearly in the case of conical crowns this is more significant than for ellipsoids. Thus the required density of lidar points needed to achieve accurate heights for ellipsoidal trees can theoretically be lower than for conical trees. However, in the case of a eucalypt plantation, the leaves tend to hang almost vertically, thus presenting only a small surface area to the near-vertical sampling of an airborne lidar. This may counteract the positive effect of ellipsoidal crown shape.

The simulation study concluded that although it is well known that airborne lidar can be used to measure forest inventory parameters such as height, the absolute accuracy of these measurements depends on the operational characteristics of the instrument that determine the spatial density of the sampling and the growth form of the trees (or crown size, shape and openness) being measured. The separation of lidar sample points and the tree grid spacing in a regular plantation also interact in a significant way to affect the accuracy of height measurement.

In a scanning lidar system, the spacing of the lidar points is less even near the edge of the swath. Overlapping swaths help alleviate this problem by producing a more random pattern of point locations. Therefore, it may be operationally more advantageous to increase point density by using multiple overlapping flight lines, rather than by reducing the scan angle. However, reducing scan angle does have the added advantage of improving ground detection under dense foliage, which is often an important consideration. If individual flight lines are being used, it is important to consider not only the average point spacing, but the distribution of point spacing in comparison with tree spacing and crown size.

#### **4.4 Foliage Analysis**

When a lidar beam is used to sense a canopy, it may be partly reflected by a number of surfaces, thus providing a distributed return. The amount of light penetrating to lower levels is determined by the occlusion effects of foliage in the upper layers. That is, the probability of penetration is related to the amount and distribution of foliage elements. This is the basis for extraction of canopy structure from airborne lidar data. For canopy lidars with their larger spot size, a vertical profile of canopy structure can be obtained from each shot since the full waveform is recorded. ALS data can be used to simulate waveform data by considering statistics of the penetration of individual shots within a specified averaging area and building a probability distribution from them. In this case, the averaging area is the equivalent of the spot size of the canopy lidar. However, due to the fact that generally only one or two returns are recorded the averaging area will generally be larger than the equivalent canopy lidar spot size to obtain an equally stable profile.

The use of ALS in this way to study forest canopies is described in detail in Lovell *et al.* (2003). It is shown that multiple (e.g. first and last) returns can be used together to minimise the bias induced by the interaction between the size of the lidar footprint and the thresholding used to identify targets. Intensity can also be used providing the instrument response is known or assumed linear. Analysis of data over a range of spatial scales can provide information about the size of the objects (i.e. tree crowns) present. The use of models in combination with ALS data can provide greater stability in analysis.

#### **4.4.1 Canopy Cover**

Total canopy cover is the vertically projected fraction of area that is covered by any part of the canopy. Terrain lidar interacts with the canopy cover in a complex way and in the past the use of single-hit data has led to biased estimates and variable outcomes. The ALS data used in this project provides first and last hit information that can improve the capacity of the system to map foliage cover and profiles. We devised a method to use information from both first and last ALS returns in the cover. Each lidar shot was allocated to one of three categories according to the classification (vegetation or ground) of the first and last returns from each shot;

1. veg-veg;
2. veg-ground, and
3. ground-ground.

An estimate of cover is made by weighting shots in category (1) with weight 1.0 and those in category (2) with weight 0.5 and summing them as a proportion of the total shots within an area. In effect, when the first hit is foliage and the last is ground, it is assumed that half the beam hit the foliage and half hit the ground. It is possible to obtain ALS data with the intensity of the return beam included and this can improve the estimate.

Cover measures of this kind from airborne instruments provide an estimate of the fraction of the ground covered by vertically projected tree elements, because the foliage area is sensed from a vertical view. Foliage angle information derived from multi-angular scanning is necessary to convert these measures into actual foliage amounts due to the complex variations in the angles at which canopy elements occur in trees with different growth forms and at different stages of their growth.

#### **4.4.2 Vertical structure**

The vertical distribution of canopy components provides information on vegetation stratification and understorey. It is also a valuable input to light microclimate and rainfall interception models that can be used to model forest growth. Lidar data can be used to probe the vertical distribution of canopy components by considering the penetration of all laser shots within a given area. Specifically, the laser power reflected from different levels within the canopy is compared to the total power incident on a given region and the probability of a laser pulse reaching a given height in the canopy computed.

Terrain lidars such as the ALS provide a limited but useful sample of this returned power. The effectiveness depends on shot density and could be improved if more than first and last hits were recorded – such as multiple hits and returned intensity. Nevertheless, by effective processing, there is a great deal of useful information to be obtained from standard ALS data.

### 1.1.1.3 Foliage Profiles

The foliage profile is the vertical distribution of phytoelement (leaf, stem, twig etc.) density above the ground. Foliage profiles have been derived from large footprint Lidars as described in Lefsky *et al.* (1999b) and Harding *et al.* (2001) and extended to the case of discrete canopies as described in Ni-Meister *et al.* (2001).

ALS data can also provide estimates for the foliage profile by considering all shots within an averaging area. The smoothness and stability of the profile depends on the size of the averaging area. However, if the averaging area is too big the profile may include too much variation. Because the averaged data are often still quite variable, it is useful to fit a model to the resulting profile, both to provide a stable distribution for further processing, and to provide spatial representations of profile properties through the model coefficients.

Figure 4-3 shows an example of an apparent foliage profile and a fitted model. The left-hand panel is the estimated cumulative projected foliage area per unit area. The value at zero (i.e. the ground) is the estimated total projected foliage cover. The middle panel shows the derivative of the model, which is the relative foliage density at different heights through the canopy. The right-hand panel of Figure 4-3 is a comparison of modelled foliage profiles at three *P.radiata* plots of differing site quality. The contrast in foliage density and distribution between these sites is immediately apparent.

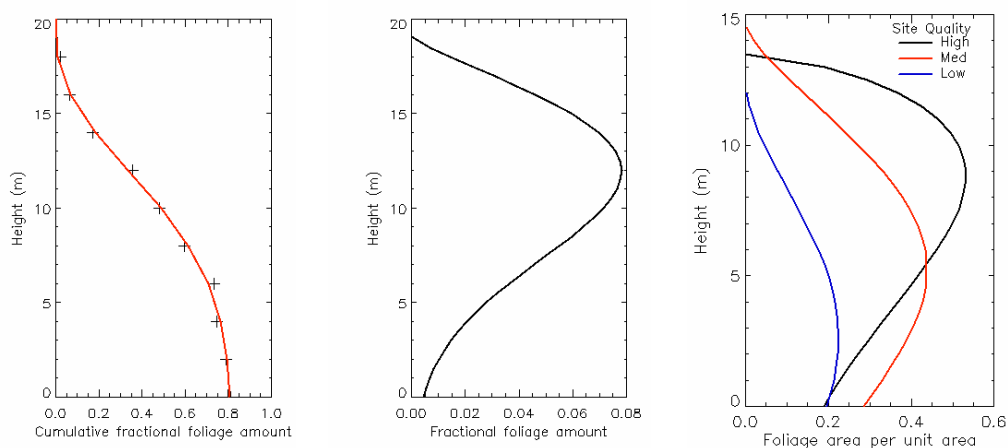


Figure 4-3. Example foliage profiles from *P.radiata*. The cumulative profile (left) is modelled providing an analytical derivative (middle) to define the foliage profile. Contrasting sites have differing profiles (right).

The methods described above have all been based on the principle of the distance to the first ‘hit’ and its use to estimate gap probability as a function of range by ranging Lidars. However, most currently used terrain Lidars also provide the intensity of the Lidar return. It is possible to use this information to provide alternative estimates for gap probabilities and cover.

The intensity calibration of the Lidar may not be known, but that is not necessary as long as some information about relative plant and ground reflectivity is known and the instrument intensity response is linear. An approximate Lidar ‘waveform’ (or returned energy as a function of range) can be simulated for a spatial averaging area by binning data from returns within that area into regular height intervals and summing the intensities within each interval. The data in this case are separated into vegetation and ground hits using the initial classification and include both first and last returns.

#### **1.1.1.4 Percentile Heights**

Another method to study the vertical structure of a canopy using lidar data is to calculate the heights of a range of percentile points in the distribution of target returns. This includes returns from both canopy and ground and can provide simple measures that account for both the height and the density of the canopy. For example, heights of median energy return derived from airborne canopy lidar have been found to correlate well with aboveground biomass (Drake *et al.*, 2002). This measure is sensitive to changes in both the vertical arrangement of the canopy and the openness. Areas of high density drive the level up, due to lack of penetration to lower levels, while in more open canopies, the level is reduced due to the large return from the ground. Other examples using ALS data include correlations of height percentiles with mean tree height (Naesset, 1997a), Lorey’s mean height, basal area and volume (Naesset, 2004) and the use of low percentiles to infer crown length (Naesset and Okland, 2002).

## **4.5 Scaling up ground-based measurements**

Airborne lidar cannot make direct measurements of some parameters essential for forest inventory e.g. DBH, basal area, bole height. Therefore it is common to seek other measures that can be correlated with these and thereby use the airborne data to map their properties over large areas. The principle of allometry is common in forest inventory and allows parameters that are easy to measure (e.g. DBH) to be used to infer those that are more difficult (e.g. height). The reliability of such practices relies on correlations between different aspects of tree size and structure and relationships are species- and possibly management-dependent.

Airborne lidar has been shown to provide stable measures of height and various canopy properties such as cover and foliage profiles. When combined with ground-based information, correlations can be found with other structural properties. Suitable ground-based measurements may be standard inventory data from plots within the area surveyed by the lidar. Alternatively, a ground-based lidar instrument such as ECHIDNA® can directly measure inventory parameters (e.g. basal area) as well as

measuring foliage profiles that provide a direct link to ALS data. In this way, the richer, ground-based lidar data is used to calibrate the airborne data which in turn provides wide area coverage.

Another example of ground-based calibration and scaling-up is the use of field data to refine the tree height estimate from airborne lidar. Heights derived from ALS data are usually underestimates of the true height, but the extent of this depends on properties of the canopy (e.g. tree shape) and the data acquisition. Therefore ground data can be used to calibrate the ALS-derived tree heights and provide more accurate maps.

## 5 RESEARCH OUTCOMES

### 5.1 Introduction

This section of the report discusses results from validation work completed for the ECHIDNA® Validation Instrument (EVI), airborne lidar, and the integration of EVI and airborne data.

Field validation of these technologies was undertaken for a range of forest attributes. Where possible, validation was performed relative to established best practice measurement techniques or innovative variations on established techniques where traditional methods did not permit direct comparisons.

Sections 5.2, 5.3 and Appendix 1 describe the field sites and field inventory methods used to collect validation data. EVI-derived estimates of forest structure are discussed in Section 5.4 followed by a comparison of forest measurements from EVI and alternative approaches. The role of airborne lidar is also presented as a potential means of directly assessing canopy structure and as a tool for scaling-up structural estimates from the EVI over broader areas.

Table 5-1 shows the key forest structural attributes of interest in the current EVI validation, including the field assessment techniques used to collect validation data.

**Table 5-1: Key forest structural attributes for EVI validation and field measurement techniques.**

<b>Attribute</b>	<b>Description</b>	<b>Field assessment approach(es)</b>
stem diameter	mean stem diameter at breast height (DBH)	diameter tape measurement of selected trees*
stem number density	tree locations	range and bearing to stems of selected trees*
canopy height	mean or predominant tree height at plot scale	tree height measurement using Vertex hypsometer*
bole height	mean bole height at plot scale	bole height measurement using Vertex hypsometer*
leaf area index (LAI)	one sided leaf area per unit ground area or projected needle area per unit ground area	hemispherical photography, LICOR LAI meter
foliage profile	vertical distribution of foliage within the canopy	hemispherical photography and telescopic mast
* Note that trees were selected for measurement using both fixed and variable sized plots. Details of the Angle Count sampling technique are given in Appendix 2.		

## 5.2 Field sites

Field validation of lidar technology was undertaken at four field sites in South-eastern Australia. These were:

1. ‘Westfield’ plantation, about 20 km North of Maydena in South-central Tasmania. The plantation is owned by Norske Skog and was established with *E. nitens* in October/November 1992. The plantation has been used as a long term nutrition study site by CSIRO Forestry & Forest Products and Norske Skog (e.g. Smethurst *et al.* 1997).
2. ‘Wedding Bells’ State Forest near Coffs Harbour on the North coast of NSW. Five separate study sites were identified within the State Forest relating primarily to hardwood plantation (*E. pilularis* and *E. grandis*) although two mixed species, uneven-aged sites were also assessed. Wedding Bells State Forest is managed by Forests NSW.
3. ‘Penola’, ‘Springs Rd’ and ‘Patchells’ *P. radiata* softwood plantations near Mt Gambier, South Australia. All managed by ForestrySA, the Penola and Patchells sites were assessed at age 9 years, the age at which site quality assessment is typically performed. The Springs Rd plantation was established in 1982 and is used as a long term nutrition response study site by CSIRO Forestry & Forest Products Mt Gambier office.
4. Bago-Maragle State Forest near Tumbarumba, NSW. Four diverse study sites were established in an area that has seen intensive research over the past decade. The sites were selected within the following mature forest types:
  - a) *E. delegatensis* (Alpine Ash)
  - b) *E. pauciflora* (Snow Gum)
  - c) *E. globulus* (Blue Gum)
  - d) *P. ponderosa* (Ponderosa Pine)

Across all field sites, the assistance and support of the forest management agencies ForestrySA and Forests NSW has been an essential and greatly valued component of the field work.

Field work as part of terrestrial and airborne lidar investigation spanned three years, from December 2001 to December 2004. During this time the project naturally progressed through various iterations of research and development. Consequently, some differences exist between sites in terms of field techniques, equipment used and types of data collected (including airborne data).

For the purpose of this report some key field sites and dates were selected for detailed analysis. Site selection was performed on the basis of forest type and age class (to ensure a broad spectrum of types are represented), and data consistency (including the types of available data and collection method).

Appendix 1 contains further details of the field sites. Figure 5-1 shows the location of the study areas in South-east Australia.

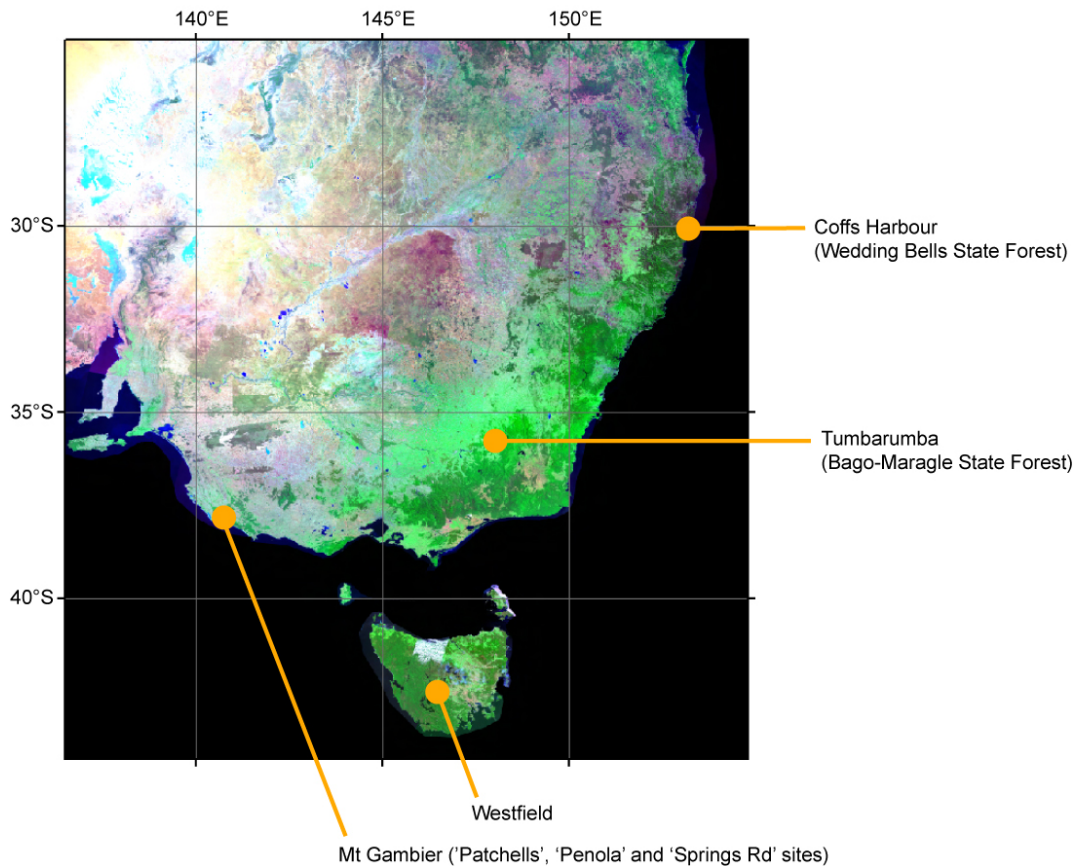


Figure 5-1: Location of study areas.

## 5.3 Hemispherical photography

### 5.3.1 Principles and applications

The analysis of hemispherical photographs is a well-established technique used to study the light environment under forest canopies and to infer characteristics of the canopy architecture. Specifically, such techniques can be used to determine the foliage area index and mean projection angle, which both contribute to the proportion and distribution of gaps in the image.

Gaps are defined by setting a threshold value to partition the image into plant and visible sky. Given the subjective nature of this thresholding, at least two operators performed the process and results were compared to ensure agreement. To increase separability between foliage and sky, images can only be recorded under uniform incident light field conditions. This restricts image capture times to a short time window at dawn and dusk or to times when the sky is uniformly overcast. Photographs were recorded using a Nikon 900 digital camera with a Nikon fisheye lens attachment. A Delta-T self-levelling platform was also used to ensure control over the relationship between image coordinates and zenith angle.

Photographs were analysed using the Delta-T HemiView© software program, which uses the Campbell (1986) model to determine the projection angle of foliage as a function of zenith angle. It also uses an integral relationship called Millers equation (Miller, 1964; 1967) to determine a total or “unprojected” foliage area index.

### 5.3.2 Mast system

In order to validate the EVI and airborne lidar as a means of deriving foliage profiles, the established hemispherical photography technique was converted into a profiling system using an extendable mast to enable photographs to be taken at varying heights within the canopy. The ‘mast’ technique involves a digital camera with fisheye lens mounted on a 15 m extendable mast.

The mast used was a Clark QT15M telescopic unit with seven sections and a separate support tripod. The mast has a minimum extendable height of 2.8 m and maximum height of 15 m. Using a manually operated pneumatic pump it can be extended and secured at any height within this range.

The Nikon camera and fisheye lens was mounted on the top of the mast. Due to maximum head load limitations the Delta-T self-levelling platform could not be used. Instead, a dual-axis post level was used to secure the mast in a precise vertical position.

A wireless shutter release system was custom designed and built for the Nikon 900 camera. Because the Nikon 900 does not have an electronic shutter release port, the system used a UHF-controlled solenoid switch to manually depress the shutter button. A series of fibre optic cables redirected the (upward-pointing) camera flash to a downward-pointing diffuse lens to alert the operator when a photograph had been successfully captured. Figure 5-2 shows the system built for wireless camera operation and the mast being extended.



(a)



(b)

Figure 5-2: System for remote camera operation (a) and mast partially extended with camera (b)

During operation a long tape measure is attached to the top of the mast so that the height of extension is accurately known at any time. Early tests found it was easier to fully extend the mast to 15 m and then take photographs as pressure is released and

the mast gradually retracts under its own weight. A locking bolt attached to the mast tube secures the mast at the desired height before a hemispherical photograph is taken. At all field sites where the mast was deployed, photographs were taken at 1 m height intervals, including the maximum and minimum height range. An additional photograph was also taken at the same location with the tripod-mounted Delta-T system to provide a near-ground image.

### 5.3.3 Photograph processing and modelling

The product of image analysis using the hemispherical camera and mast system is a vertical profile of cumulative foliage area index values  $F(z)$ . Typically this profile will show a low foliage area at the top of the mast, which slowly increases as the mast is lowered and greater amounts of foliage can be seen in the images. Some example thresholded images from the South Patchells site are shown in Figure 5-3.

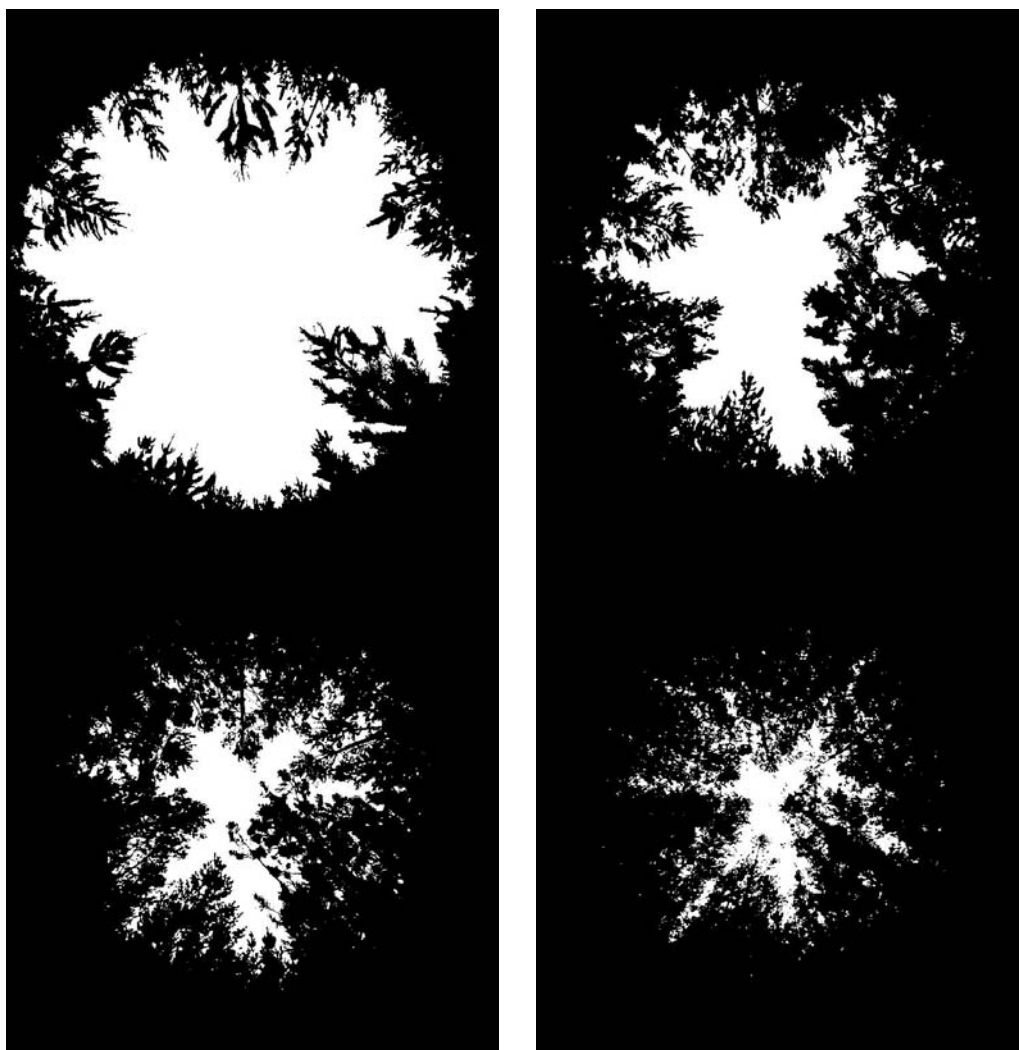


Figure 5-3: Example thresholded hemispherical photographs from South Patchells plot 3. Heights of the images are 14 m, 10 m, 8 m and 3 m.

Foliage area density  $f(z)$  can be a more useful parameter than  $F(z)$ , since it describes the actual amount of foliage within a given height layer or region. This can be computed from  $F(z)$  simply by taking the derivative with respect to the vertical coordinate ( $z$ ). However, limitations of the data and thresholding subjectivity can lead

to spurious computed foliage area densities. This can be overcome by fitting a smooth function to  $F(z)$ , such as the Weibull distribution used by Yang *et al.*(1999),

$$F(z) = a(1 - e^{-b(1-z/H)^c}).$$

The derivative of this function is then computed analytically as,

$$f(z) = \frac{abc}{H}(1 - z/H)^{c-1} e^{-b(1-z/H)^c}.$$

Interpretation of  $f(z)$  not only describes the foliage density profile and overall foliage area index, but can also show other structural parameters such as bole height / height to green and canopy height.

Modelled  $F(z)$  and  $f(z)$  profiles for the South Patchells and Springs Road sites, estimated by fitting the Weibull function to the hemispherical photo derived values of foliage area index are shown in Figure 5-4.

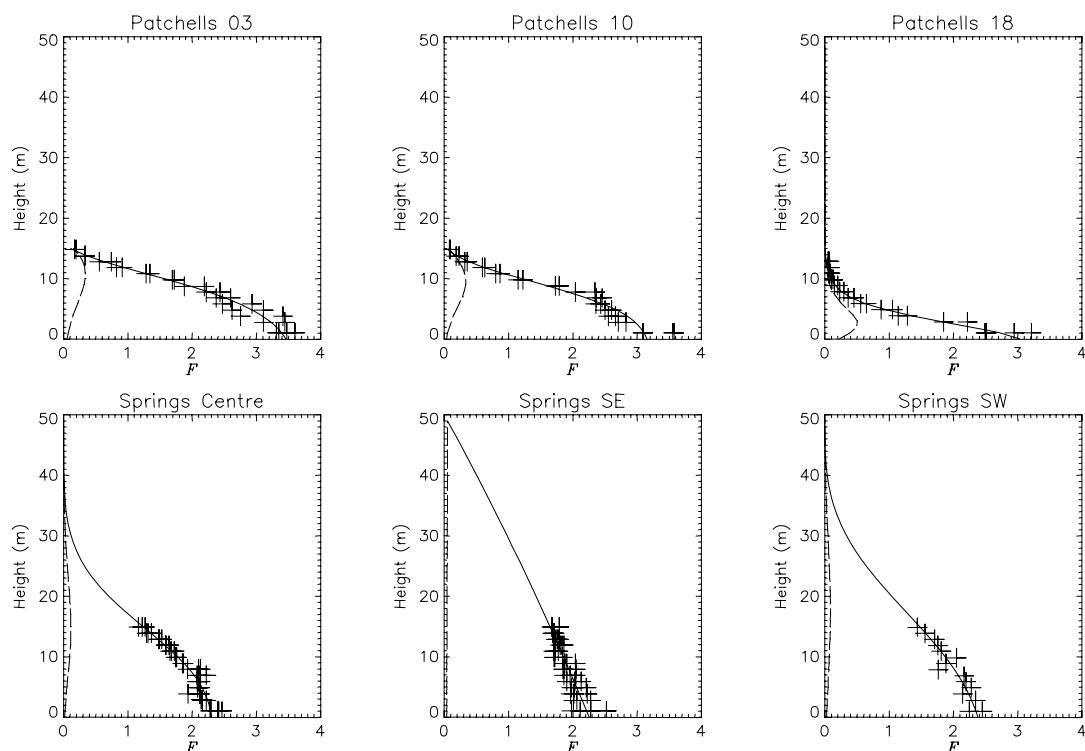


Figure 5-4: Vertical distributions of  $F$  as measured using hemispherical photography (+) and modelled using the Weibull distribution (—). The foliage density profile computed using the derivative of the fitted Weibull distribution is also shown (- - -).

A significant limitation of the system is the limited height to which the camera can be elevated by the mast. In tall canopies such as at Springs Road site in Mt Gambier, the data does not extend high enough to constrain the model and show the true shape of the  $f(z)$  distribution.

## 5.4 ECHIDNA® processing results

Two-dimensional representations of the ECHIDNA™ data from all sites showed good agreement with the various field records. These included panoramic photos derived from conventional digital photography acquired at each site which can be compared with Andrieu projections of the ECHIDNA™ data as shown in Figure 5-5. This showed good agreement for tree directions and angular diameters in mature and pruned forests. However, in areas of dense understorey, although images correspond well, quantitative comparisons of stem characteristics become more difficult.



Figure 5-5: Andrieu projection of the ECHIDNA™ data (top) and panoramic photo (bottom) for the Springs Rd site in Mt Gambier

Visual comparisons with hemispherical photography and hemispherical projections of the ECHIDNA™ data showed similar agreement as illustrated in Figure 5-6. These images highlighted some of the benefits of lidar data over passive optical techniques since it is not subject to penumbral effects which increase the apparent gaps in areas of bright sunlight. The data is also more conducive to the separation of foliage and woody components based on the intensity distribution of the return beam.

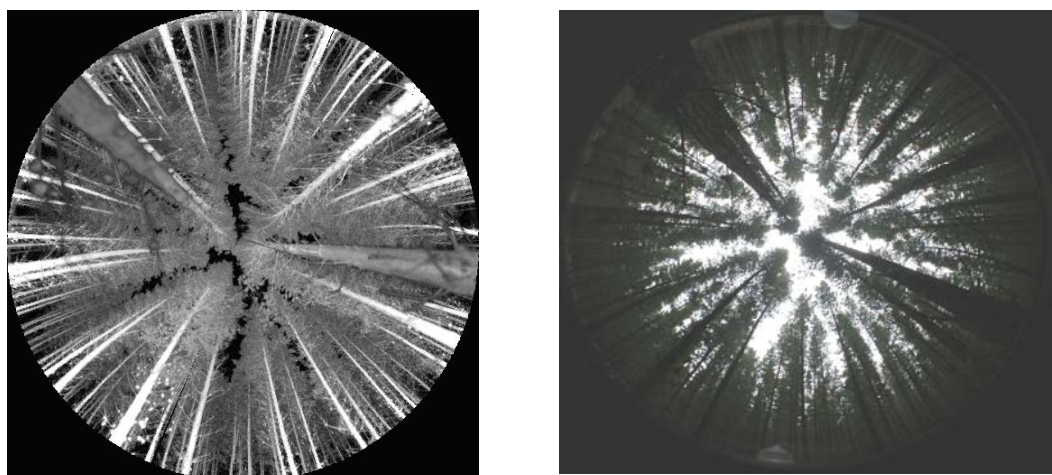


Figure 5-6. Hemispherical projection of the ECHIDNA® data (left) and corresponding hemispherical photograph (right) for the Springs Rd site at Mt Gambier

### 5.4.1 Pgap Method

As described in Section 3.3.3, mean gap probability profiles within zenith angle ranges can be computed from the ECHIDNA® data, as shown in Figure 5-7. These can be used to infer structural characteristics of the canopy such as leaf area index and canopy height. At the instrument (range = 0) the gap probability will be close to unity and will fall as a function of the amount of plant material that is encountered.

In an ideal situation, the mean gap probability profile ( $P_{gap}$ ) closest to the zenith (e.g. 10 to 20 deg in Figure 5-7) decreases to its minimum rapidly due to the small distance travelled by the beam before it reaches the crowns of the trees above. With increasing zenith angles, the beam must travel a greater distance before reaching tree crown but then travels further through the overstorey layer, leading to a decrease in the total gap. This is reflected in the mean  $P_{gap}$  profiles for site 2 at Wedding Bells and the Westfield site shown in Figure 5-7, where the mean  $P_{gap}$  curves for larger zenith angles decrease slowly but eventually reach a lower minimum  $P_{gap}$  value than the near-vertical ones.

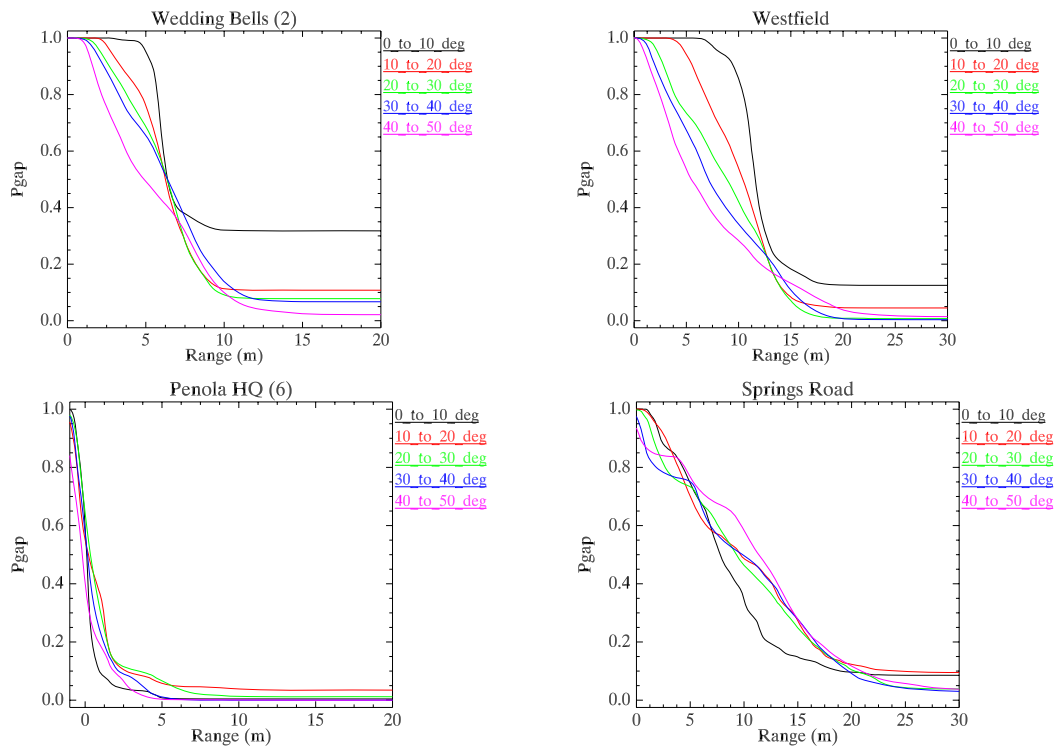


Figure 5-7. Mean gap probability ( $P_{gap}$ ) curves for each of the primary research sites.

The mean  $P_{gap}$  profiles for Penola HQ are more difficult to interpret due to the extremely high foliage density in the young stand. These reach their minimum value within a very short range from the instrument, partly due to the thresholding method employed. In the case of the Springs Road site, the  $P_{gap}$  profiles appear more random due to the smaller tree number density and the resulting variability of the waveforms within a given zenith angle range. In such cases it appears that averaging data from scans recorded at multiple locations within the stand may be preferable.

In general, the inversion of the Pgap profiles produced poor estimates of LAI. This was particularly true for the Westfield site, where field records showed unusually high LAI values that were not replicated in the ECHIDNA® data. This may be due to the way the field data and other measurements have been calibrated. Removal of the Westfield data did improve the estimation accuracy to some extent and this is presented in Figure 5-8.

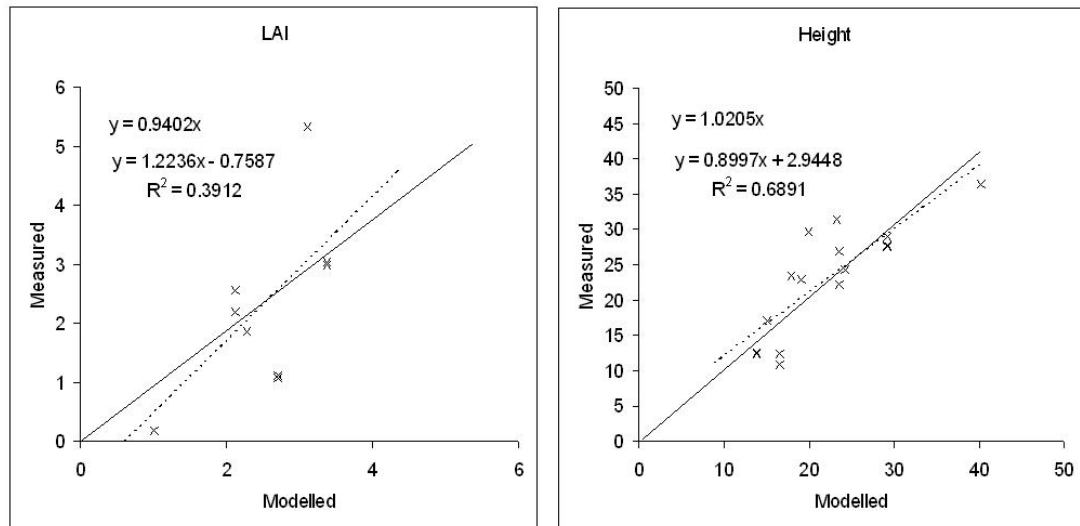


Figure 5-8: Relationship between LAI and canopy height measured in the field and those derived from inversion of Pgap profiles from ECHIDNA™. The Westfield LAI field data have been excluded due to their unusually high values.

The inherent errors and variations in the methods used for validation will have a large influence on these results. The measurement of LAI is very difficult and at most sites the method chosen is calibrated from cutting experiments or from cross-comparisons between different techniques. Almost every method will respond to the “clumping” of leaves into modules and crowns. The greater flexibility of the EVI data provides a base for future investigations of the effects of such clumping effects on LAI estimation.

Height proved to be more reliably estimated using the technique and showed very little bias and high correlation between Pgap inversion and standard inventory measurements. This is also influenced by the relative standardisation and repeatability of height measurements recorded in the field.

#### 5.4.2 Waveform Modelling Method

Mean waveforms derived from the ECHIDNA® data (post baseline removal and saturation fixing) for ten degree zenith angle ranges show a decreasing foliage response and an increasing trunk response with increasing beam zenith angle, as described in Section 3.3.3. Due to the fact that foliage within the tree crowns and the trunks below are the dominant plant components interacting with the beam, there are generally two distinct sets of peaks seen in the data. The peak due to trunks occurs at close range and becomes more intense with increasing zenith angle. The peak due to foliage occurs at a greater range from the instrument and becomes less intense with

increasing zenith angle. A typical example is shown in Figure 5-9 using the best fit parameters for the Westfield site.

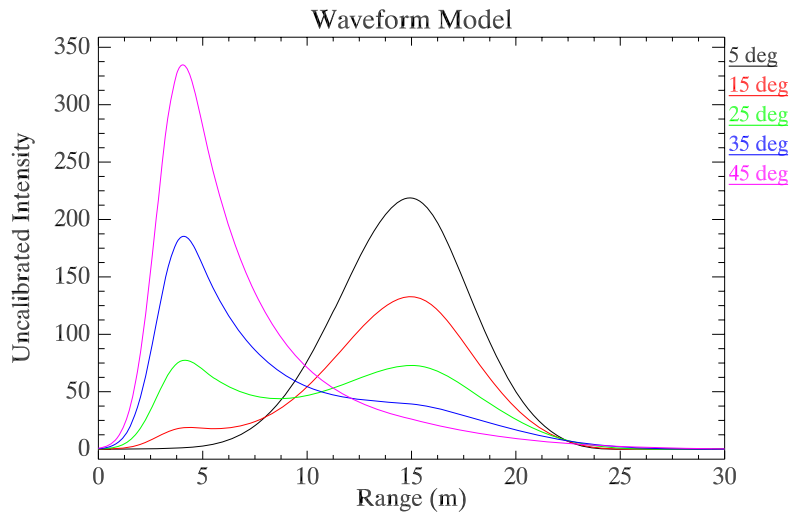


Figure 5-9: Best fit waveform model for the Westfield site in Tasmania.

As with the Pgap profiles discussed previously, the mean waveform data (see Figure 5-10) conformed well to the model in cases of medium density forests such as the young plantation at site 2 in the Wedding Bells state forest and at Westfield in Tasmania.

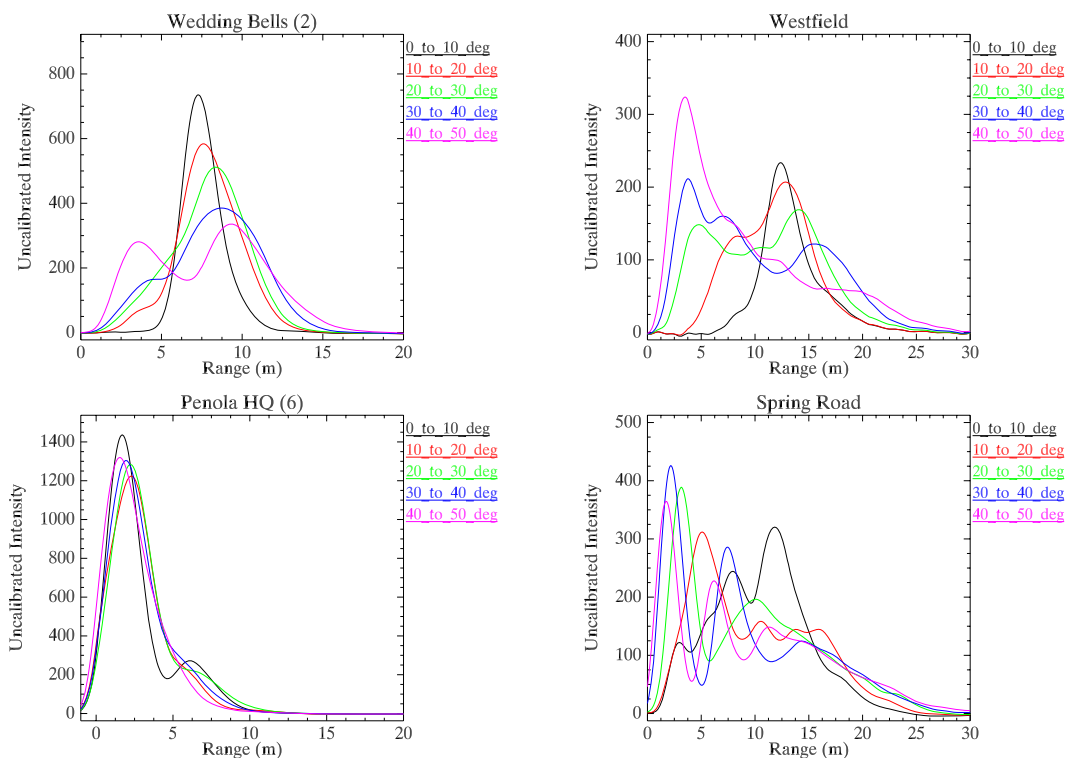


Figure 5-10. Mean waveforms derived from the EVI data recorded at the primary research sites.

In areas where there is dense understorey, such as at Penola HQ in Mt Gambier, the separation of foliage and trunk responses in the waveform are difficult to distinguish

and the waveform approaches that of a more homogeneous “turbid” medium. Once again, at the mature plantation at Springs Road in Mt Gambier, the low tree number density resulted in a less predictable series of mean waveforms that may indicate the need to average data from multiple ECHIDNA™ setup locations.

LAI values were retrieved for all sites through inversion of the mean waveform model. Once again these showed a strong relationship with field measurements (see Figure 5-11) except (as before) at Westfield, where there were very high field measured values that need some investigation. Height estimates from the model inversion also conformed well to field measured values - even for the Penola and Springs Road sites where the model was not an ideal representation of the data.

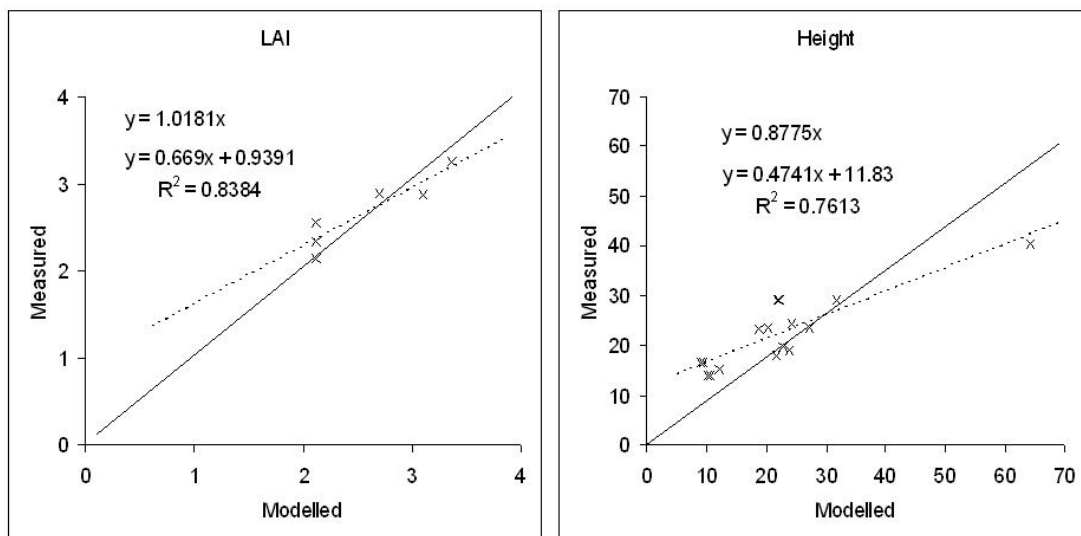


Figure 5-11: Relationship between LAI and canopy height derived from inversion of the waveform model and those measured in the field.

The Pgap inversion showed low estimation accuracy for LAI and a slight over estimation of height, while the waveform model inversion showed a greatly increased LAI estimation accuracy with some bias introduced in the estimation of height. The more predictable relationship between measured and estimated values of LAI produced using the waveform model ( $R^2$  of 0.84) supports the notion that full waveform recording lidar instruments provides advantages in characterising soft targets like foliage over single return instruments. Both techniques have the potential to be developed further for accurate retrieval of other parameters such as the angle distribution of foliage and parameters related to basal area. However, the stability of the inversion method will play a large part in dictating the accuracy with which these parameters can be estimated.

## 5.5 Comparisons between ground and airborne data

### 5.5.1 ALS Canopy height

The first canopy height comparison is between field data and airborne lidar (ALS). The comparisons presented here used predominant height. The exact definition of predominant height depends on the field protocols employed at each site but in all cases the same sampling strategy was replicated in the ALS data.

Table 5-2: Comparison of predominant heights from field measurements and ALS data.

Site	Plot*	Field height	ALS height	% discrepancy
Westfield, Tasmania	1	26.2 ± 0.35	26.4 ± 0.15	0.8
	2	25.4 ± 1.0	25.7 ± 0.30	1.0
	3	23.2 ± 1.4	22.3 ± 0.83	-3.9
	4	25.7 ± 0.26	26.8 ± 0.53	4.3
	5	25.0 ± 0.84	24.9 ± 0.3	-0.4
Wedding Bells, Coffs Harbour	1	44.1 ± 5.6	52.1 ± 1.1	18.1
	2	16.0 ± 0.17	15.8 ± 0.2	-1.3
	3	39.5 ± 5.5	38.9 ± 2.1	-1.5
	4	33.8 ± 3.0	33.9 ± 0.3	0.3
	5	37.4 ± 2.0	37.0 ± 1.5	-1.1
South Patchells, Penola	3	19.2 ± 0.29	18.3 ± 0.62	-4.7
	10	17.6 ± 0.42	16.0 ± 0.61	-9.1
	18	13.5 ± 0.95	11.5 ± 1.1	-15.0
Springs Rd, Mount Gambier	9	29.1 ± 0.69	27.8 ± 0.47	-4.5
Bago-Maragle, Tumbarumba	Ponderosa Pine	30.0 ± 1.1	29.1 ± 4.7	-3.0
	Snow Gum	30.5 ± 2.2	31.0 ± 3.2	1.6
	Alpine Ash	44.3 ± 5.9	36.0 ± 2.7	-18.7
	Blue Gum	29.3 ± 7.4	31.6 ± 8.5	7.8
* Plot numbers at South Patchells are ForestrySA permanent plot numbers. The Springs Rd plot number is a CSIRO FFP fertilizer trial plot number. Plot numbers at other sites were assigned according to data collection order during field work.				

Table 5-2 presents the comparison of predominant heights from field and airborne lidar data. The study sites cover a wide range of forest types (see Appendix 1) and in some cases multiple plots within the same type of forest (e.g. different site quality indices at South Patchells). Therefore we can study the effect of different canopy structure including different site quality or fertiliser treatment within even-aged plantations. The uncertainties quoted in the table are the standard deviation of the height measurements used in the predominant height average. These do not account for measurement-based uncertainties and therefore should be regarded as underestimates of the real uncertainty.

The data shown in Table 5-2 can be used in linear regression and compared with the EVI results shown in the previous section. Fig shows this result for the same forest types as used in Figure 5-8 and Figure 5-11. In this case, two linear fits have been made to the datasets, first with the intercept fixed to zero and second with both parameters free. It can be seen that the fit with the non-zero intercept is better, indicating a bias in the height comparisons. This is an expected result for the ALS data, and is not surprising in the EVI data since the instrument is located below the canopy and the results shown are based on the first-hit gap probabilities.

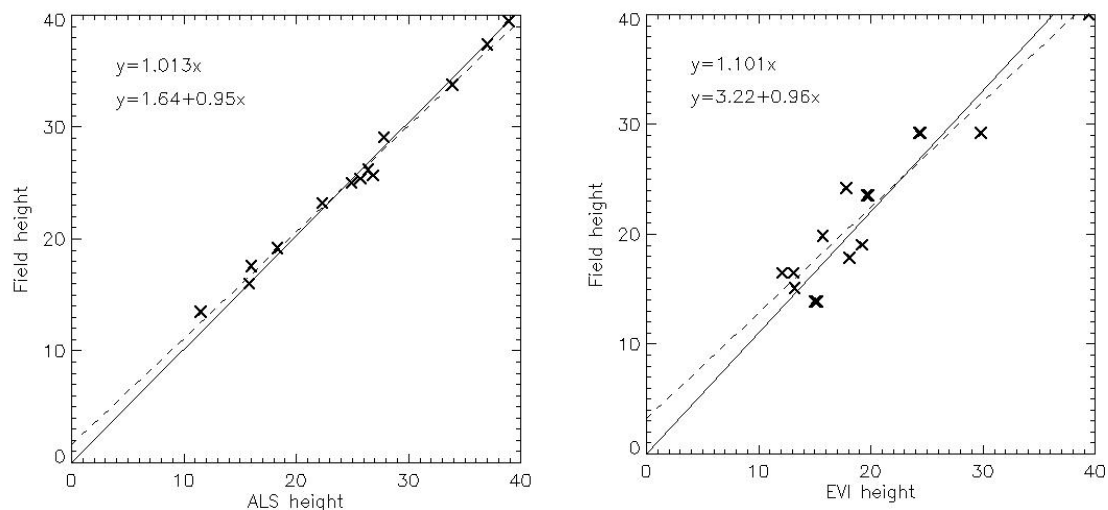


Figure 5-12 Linear regression between ALS and field canopy heights (left) and EVI and field canopy heights (right).

In most cases, the ALS predominant heights are lower than the field heights. This is an expected result due to the probability of discretely sampled airborne data coinciding with the peaks of tree canopies. The use of an average measure such as predominant height helps to reduce the significance of this effect. There are a few examples in the table where the ALS data gives higher results than the field data. In most of these cases the sites are in steep terrain (e.g. Bago-Maragle Blue Gum, Wedding Bells station 1). This increases the likelihood of inaccurate ground-based height measurement and also increases the uncertainty in the ALS heights if the DEM is inaccurate or poorly interpolated. Other large discrepancies may be due to uncertainties in the location of the ground data. The Bago-Maragle and Westfield plot locations were recorded with hand-held GPS which performs poorly under dense canopy. This is likely to be a contributing factor to the large discrepancy found at the Alpine Ash site where the canopy structure was highly variable and accurate plot location is critical to making a proper comparison.

The effect of canopy density on ALS-derived heights is clearly illustrated in the South Patchells results. The three plots are listed in the table in order of increasing site quality index i.e. decreasing productivity and hence canopy density. The underestimation of the predominant height by the ALS method increases as the canopy becomes sparser.

Both the South Patchells and Westfield sites provide a number of samples within an even-aged plantation. Structural variation between locations within these plantations is due to different growing conditions which are enhanced at the Westfield site by the application of different fertiliser amounts in a trial. For these sites, it is interesting to look at the way the canopy cover and height vary. The plots in Figure 5-13 show projected fractional cover plotted against canopy height. The Mount Gambier example shows the South Patchells data in green and the sample plots are indicated. It is clear that the structural differences represented by the range of site qualities can be separated to a certain degree by these two simple variables. The data shown for the Westfield site are colour-coded by relative fertiliser amount and illustrate differences in structure and growth due to the different fertiliser applications.

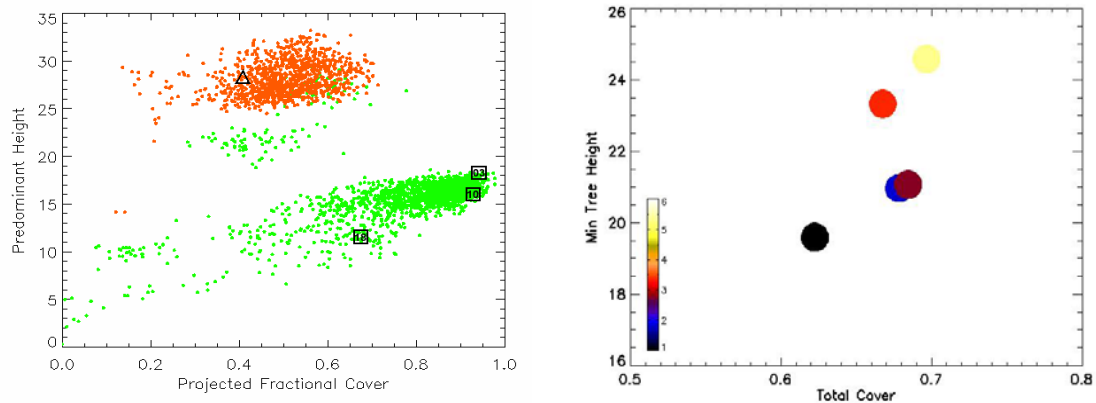


Figure 5-13. Canopy structure illustrated by fractional cover and canopy height. Mount Gambier data (left) are shown for 20 m grids at South Patchells (green) and Springs Rd. Westfield data (right) are colour coded according to levels of fertiliser applied.

The measurement of canopy structure at the Mount Gambier sites is described further in the report to ForestrySA (Lovell *et al.*, 2003a). The use of ground-based data to calibrate the ALS-derived measure would lead to enhanced products of greater use in an operational inventory protocol such as site quality assessment.

### 5.5.2 Foliage profiles from ALS, EVI and field data

A direct comparison between ALS data, hemispherical photography profiles and EVI data is possible by using first-hit gap probabilities to calculate apparent foliage profiles. EVI waveforms representing near-vertical sounding of the canopy are used for this comparison. The foliage profiles are calculated from the lidar data (both EVI and ALS) by calculating gap probability as a function of height. Occlusion effects of canopy elements by those at closer range are taken into account and the result is a profile of vertically projected foliage amount. The resulting foliage profiles have been modelled with a Weibull distribution. This model describes the cumulative foliage distribution as a function of height i.e. the final value is an estimate for the total foliage amount throughout the canopy – a vertically projected foliage area index. The hemispherical photographs are processed as described in Section 5.3.3 with each photograph providing a foliage area index for the part of the canopy above the camera. Thus, when combined, these results also provide a cumulative distribution. The hemispherical photograph analysis method also attempts to calculate the mean leaf angle, so these data should incorporate angular effects rather than being a vertically projected sample. However, the presence of trunks and branches influences this calculation, so the angle determination tends to be unstable.

The methods used for calculation of the foliage profiles presented here are all based on thresholding of data to find the first foliage element in a given direction or the lack of it. This method often over-estimates the amount of foliage present as the combination of the threshold level with a finite sized spatial sample (lidar beam or photograph pixel) leads to bias. EVI data has much more information than this since the full waveform of returns from each direction is available. However, its information has been restricted to provide results that are directly comparable with the other methods available. Comparison of these results with the ALS data profiles

provides us with the opportunity to build up relationships between the two datasets and thus enhance the broad-area coverage of the ALS data with other information available from the EVI data and correlated with the vertical profile and horizontal variation in the profiles.

The plots in Figure 5-14 show a comparison of the ALS and hemispherical photograph results at the Mount Gambier field sites. EVI data were not acquired coincident with the other data collections at these sites. The foliage profiles at the three Patchells sites (plot 3, black; plot 10, red; plot 18, blue) display a trend in foliage density with site quality. The ALS profiles for the two more productive plots (3 and 10) show a skewness of foliage towards the top of the canopy. This may be partially due to the fact that with only the first lidar returns recorded, in a dense canopy the lower parts of the canopy are almost always obscured. However it is also true that foliage is more prevalent in the upper levels of these canopies. The hemispherical photograph profiles provide good agreement with the ALS data at plots 3 and 10 however the agreement is poor at plot 18. The analysis of the hemispherical photographs is based on the presence of visible sky through the canopy. Since the locally sparse canopy of plot 18 was surrounded by plantation of variable density, there may have been fewer or smaller gaps near the horizon than would be present in a homogeneous area of consistently sparse canopy. The ALS data provide a vertical sounding of the canopy averaged over an area of 20m x 20m and are not affected by the surrounding areas.

The profiles for Springs Rd shown in Figure 5-14 (right) are a single ALS profile from a 20m x 20m plot and three hemispherical photography profiles from within approximately the same area. There is poor agreement between the ALS and hemispherical photograph profiles. The canopy at this site is much taller than the highest extent of the mast used to raise the camera, therefore the profiles shown are extrapolated based on the fitted Weibull distribution for LAI values below 15m. The mature trees at this site result in clumped foliage which is not well handled by the algorithms used to analyse the photographs. This may have caused the bias to much higher LAI values from the low-level photographs and the extrapolation of the model has exacerbated the effect. Analysis of the ALS data for regions surrounding the plot location display considerable spatial variation with some areas resulting in foliage area indices of up to 1.9 (compared with ~1.3 for the profile shown). Therefore, any inaccuracy in the location of the ground plot within the ALS data could also contribute to the poor agreement between the profiles.

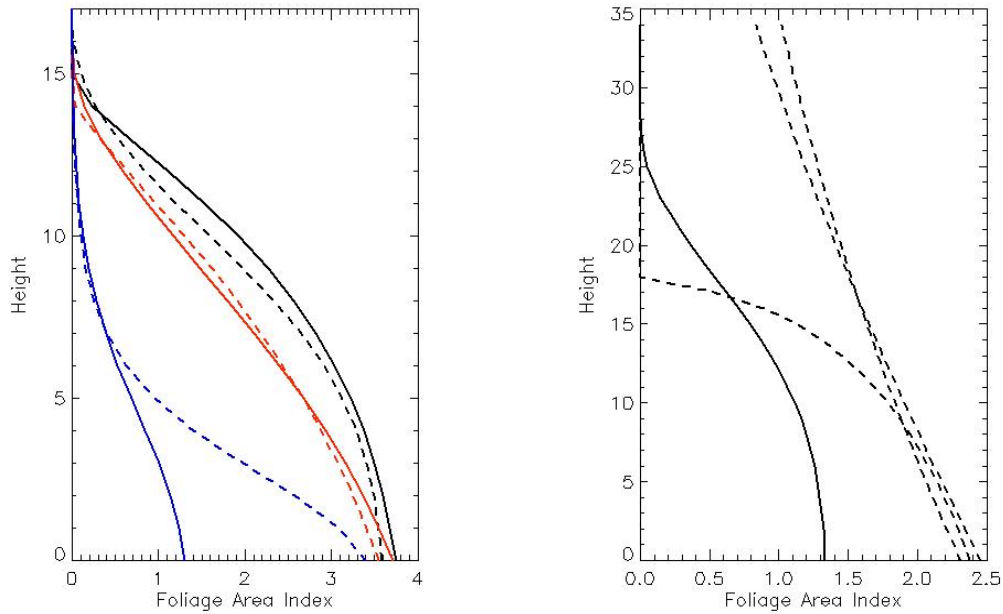
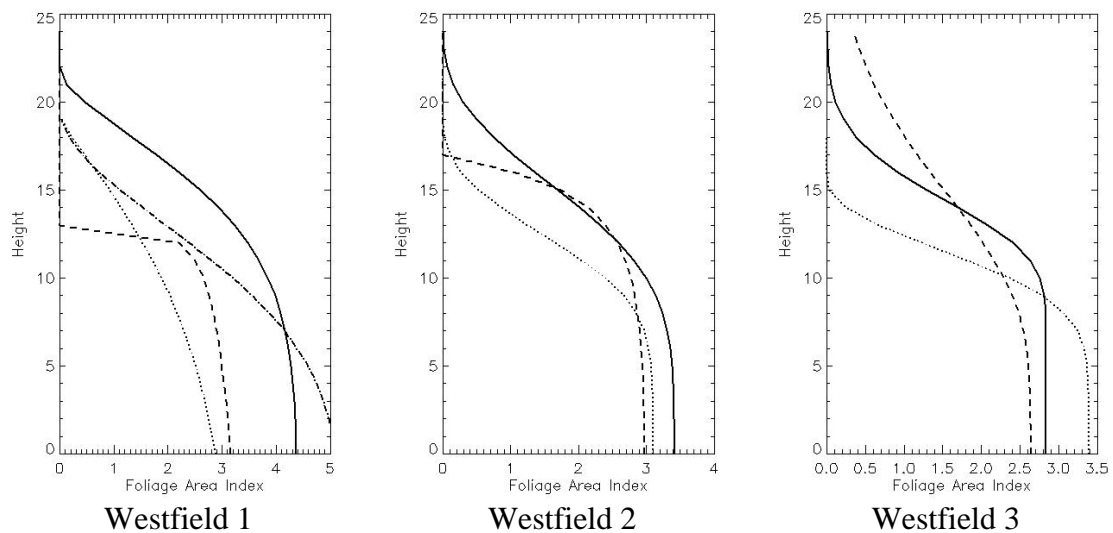


Figure 5-14 Examples of comparison of cumulative foliage profiles from ALS and hemispherical photographs for Mount Gambier sites. The Patchells plots (left) show results for three different site quality plots while the Springs Rd plot (right) shows a single result from ALS data compared with three hemispherical photograph profiles.

Figure 5-15 presents a comparison of cumulative foliage profiles for sites where coincident ALS, EVI and hemispherical photograph data were collected. In each plot, the solid line is ALS, dashed is photography and dotted is EVI data. In the Westfield 1 case there is an additional dataset shown as a dot-dash line which is also EVI data but acquired with a different beam divergence.



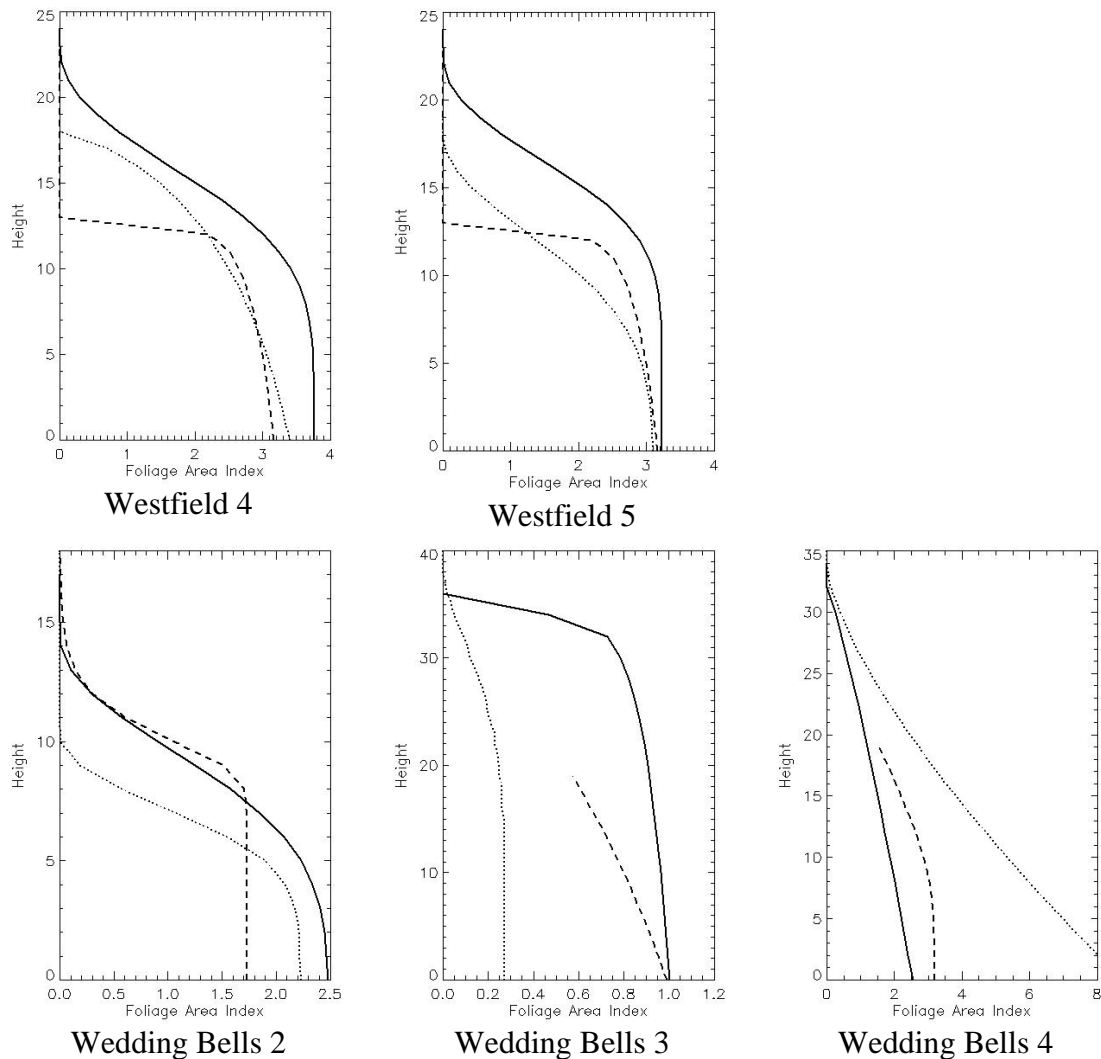


Figure 5-15 Examples of comparison of cumulative foliage profiles from ALS, hemispherical photographs and EVI for Westfield and Wedding Bells sites (as labelled). ALS profiles are shown as solid lines, hemispherical photograph profiles are dashed and EVI data are dotted. Westfield 1 has an additional profile (dot-dash) which is from EVI data with smaller beam divergence.

The profiles from the Westfield site show a concentration of foliage at the top of the canopy and display similar shapes across the five test plots with some variation in magnitude. In general, the canopy height shown in the EVI and hemispherical photography profiles is lower than that in the ALS profiles. This is due to the difference between bottom-up and top-down sensing. The data used here have been processed simply to find the first target in a given direction, so when a canopy volume contains gaps smaller than the spot size of the sensing instrument, a top-down sensor will detect the top of the volume while a bottom-up sensor will detect the lower envelope.

Westfield station 3 is worthy of further comment, as the comparison between ALS and EVI profiles is different to that at the other stations. While the terrain in the immediate vicinity of the EVI was flat, there was a steep downward slope to the west of the station. Since terrain variation is not taken into account in the EVI processing, it

is likely that the EVI is sensing more foliage apparently close to the ground in this case.

Comparison of the two EVI profiles at Westfield station 1 provides information on the effects of beam divergence and threshold level. The dotted line was calculated from 5 mrad EVI data with a neutral density filter of 2, while the dot-dash line is 2 mrad EVI data with no neutral density filter in place. The size of the 2 mrad beam changes from approximately 0.2 cm at 1 metre range to 4 cm at 20 metres (roughly the top of the canopy) while the 5 mrad beam changes from approximately 0.5cm at 1 metre range to 10 cm in diameter at 20 metres range. By comparison, the ALS beam is approximately 20 cm diameter throughout the canopy. For systems with the same detection thresholds, a larger spot size will generally result in greater over-estimation of foliage amount, with the exact behaviour depending on the size distribution of foliage elements and gaps. However, in the example shown here, the system detection thresholds are not the same. The threshold for the ALS data is not known, but is likely to be relatively high since the instruments are designed for detection of the ground in preference to aboveground vegetation. A high threshold reduces the effect of large spot size in the presence of small canopy elements. The two EVI datasets have been processed in the same way, but because of the differences in neutral density filter placed in the beam, the effective detection threshold is much higher in the unfiltered (3 mrad) data. A qualitative comparison of this effect can also be seen by comparing the relative magnitude of the 5 mrad EVI profile with those from the other Westfield sites which all used neutral density filters of 1.

The Wedding Bells 2 station is in a plantation of a similar structure to the Westfield site and the behaviour of the ALS and EVI profiles are also similar. Differences are again explained by the position of the sensors above and below the canopy and the combination of spot size with detection threshold.

The remaining Wedding Bells stations shown do not exhibit as good agreement between the ALS and EVI profiles. Station 3 is a mature plantation located on a steep (~15%) site. The EVI was located in an open part of the plantation; therefore trees on the down-slope side of the instrument are likely to make only a very small contribution to the near-vertical data included in this analysis. The terrain effect is removed from ALS data before analysis and the profile shown here is an average over a 40m x 40m area. In this case, the EVI profile records a greater canopy height than the ALS data. This may again be related to the slope as returns from the tops of trees further up the hill will make the canopy appear to be a taller. However, it also illustrates that in an open site such as this, the effect of foliage occlusion is less.

Wedding Bells station 4 was located within mixed native eucalypt forest. The shape of the foliage profiles is consistent with such a forest type with contributions from all levels within the canopy rather than a single dominant layer. There is a significant magnitude discrepancy between the three profiles shown here. This may be due to the specific location of the EVI which was in an enclosed part of the site, while the ALS profile is an average over an area that includes both this dense area and other more open areas. It is expected that the domination of dense foliage close to the EVI will be less when the full waveform information is taken into account.

EVI data were collected at Mount Gambier more than a year after the ALS data. The plantations at Penola HQ were about the same age (site quality assessment age, SQA) as the previously studied site at South Patchells. The Springs Rd site was revisited, but the exact plot centre may differ from the previous visit. The forest structure would not have changed substantially. Comparisons with the ALS profiles from the first field experiment are shown in Figure 5-16. There is reasonable agreement between the lowest productivity sites (blue curves) in the SQA age plantations, however, the EVI profile for the more productive site (red, dotted curve) is a different shape to those from similar site quality in the ALS data (black and red curves). These stands are extremely dense and the first-hit distances from under the canopy are extremely small meaning that very little information about the upper parts of the canopy is present in the EVI profiles. The agreement between the two profiles at the Springs Rd site is much better. The EVI underestimates the canopy height relative to the ALS, as expected. The larger foliage area index seen in the EVI profile may be due to uncertainty in the location of the plot as the ALS profiles varied by similar amounts over the local area.

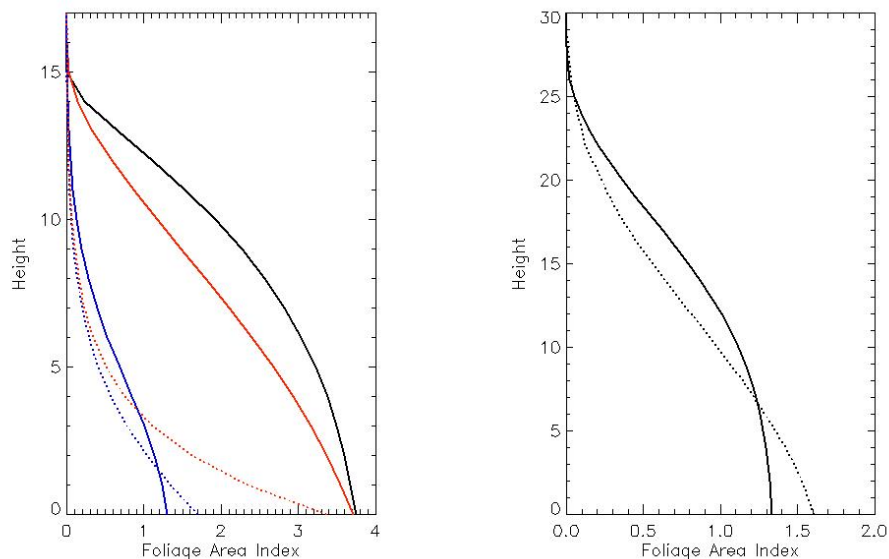


Figure 5-16 Comparison of EVI and ALS foliage profiles at Mount Gambier. The profiles shown on the left are from two different site quality assessment age plantations while those on the right are from the Springs Rd site. ALS profiles are shown as solid lines while EVI profiles are dotted.

By using the fitted Weibull model we can calculate analytical derivatives of these profiles and thus present the results as apparent foliage density profiles where the value at each level within the canopy represents the vertically projected foliage amount at that height. Examples of these are shown in Figure 5-17. These examples again show the bias of top-down compared with bottom-up sensing in that the concentration of foliage is found to be at lower heights in the EVI profiles. The apparent foliage profiles illustrate more clearly some of the structural aspects of the canopy. For example, the Westfield profile clearly shows the concentration of foliage at the top of the canopy and thus an estimate of bole height or height to green can be made. These and other structural parameters are discussed in more detail for modelling of the multi-angular EVI data.

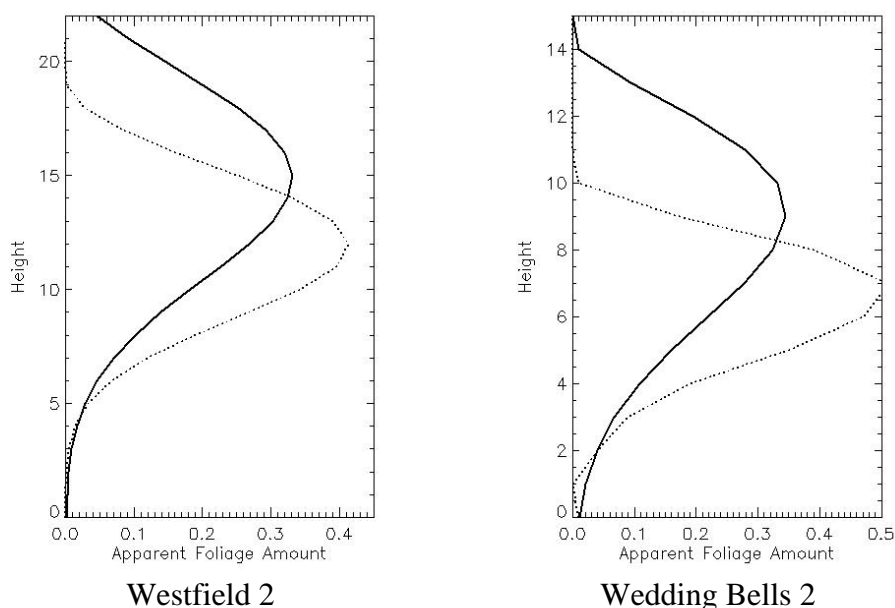


Figure 5-17 Vertically projected (apparent) foliage profiles at selected sites. Solid lines are from ALS data and dotted lines are from EVI.

In summary, these results show generally good agreement in the shape of foliage profiles derived from ALS and EVI gap probability data but magnitudes often differ. This variation can largely be explained by the effects of different beam sizes and averaging footprints (the scale of the different methods) and the different ways in which threshold levels are selected between the methods. However, there are a number of improvements to the EVI results that will be gained from more sophisticated processing of the data. The effect of terrain appears to be significant. The EVI scans  $\sim 18^\circ$  below horizontal, so provides information about the terrain around the instrument. This information could be interpolated to provide a ground surface model and used to adjust the heights of canopy returns. The situation would improve further if the airborne derived digital elevation model (DEM) can be used as a base for this interpolation. Another significant difference between the ALS and EVI profiles relates to the obvious limitations on the placement of the EVI in the field. For example, it cannot be located where there is a tree trunk. Therefore, it is likely that the region directly above the EVI will contain less foliage than other parts of the canopy. This will often produce vertical foliage profiles that underestimate the foliage amount relative to the canopy as a whole. Analysis methods which incorporate all the multi-angular EVI data should provide more consistent plot-scale averages.

## 5.6 Trunks and Counting methods

As explained previously and in detail in Appendix 4, an instrument that can recognise the (visible) trunks and measure range, bearing and angular span of each trunk allows angle count methods to be used from a fixed station to estimate size distributions, BA and other parameters. There are as many issues with trees being hidden or obscured as there are with “relaskop” surveys but we will show how the EVI data provides the potential to understand these effects and current developments underway in

measurement may provide a complete means to overcome what has previously been a serious limitation to angle count methods.

### 5.6.1 EVI Data Processing

The EVI data were processed using Cylindrical projections as described in Section 3.3. Figure 5-18 shows EVI data projected in what we term an Andrieu projection:

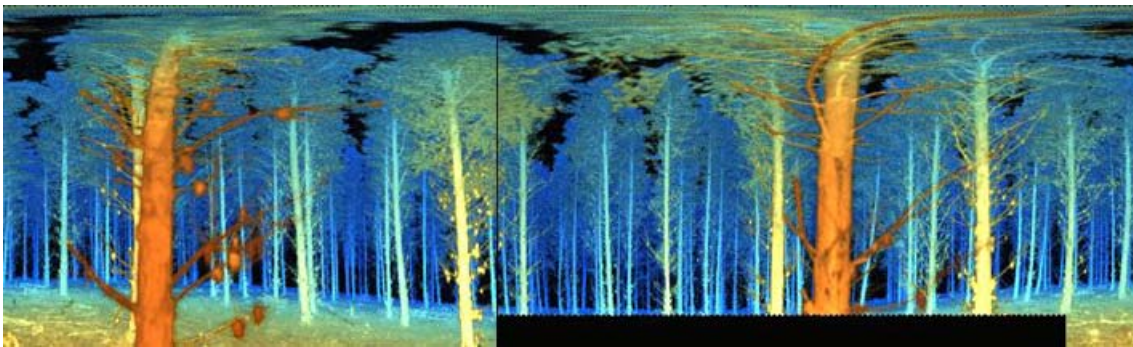


Figure 5-18: Projection to zenith (Y) and bearing (X) averaged over range

Figure 5-19 shows the result of creating a horizontal “slice” through the data to display the trunks:

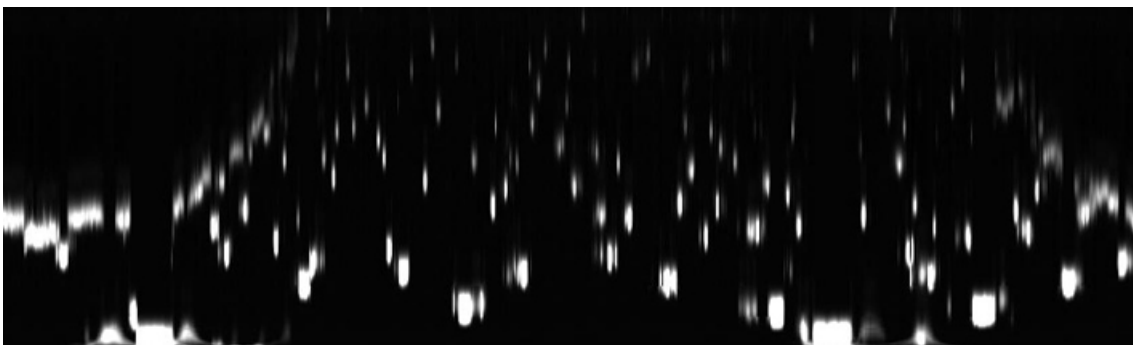


Figure 5-19: Slice across data at a constant height the same as the EVI. Dimensions are bearing (X) and range (Y).

Trunks are spread in the radial direction by the EVI Laser pulse width. Because tree trunks are “hard” targets the peak of the smeared pulses form the outline of the returns from the trunks.

The processing algorithm needs to recognise the trees, their location and extent and then apply a measuring tool to estimate width. There are some limitations to the current implementation of this method which is under active development as a key processing and interpretation tool, but the results presented here show generally good agreement with the field data and will be improved further by enhanced processing methods and changes to the instrument being undertaken in the near future.

The processing was applied at five sites that are indicated by a code in the tables and graphs to follow. These are:

Site	State	Code
Westfield 1	Tasmania	WF1
Westfield 3	Tasmania	WF3
Wedding Bells 2	Northern NSW	Coffs2
Wedding Bells 3	Northern NSW	Coffs3
Springs Rd 1	South Australia	SR1

The output from the software for each site is a list of trees recognised together with the range to the front of the tree, the bearing from the EVI and the angular width of the main stem or trunk at the chosen height. For the purposes of this Report it is assumed (not always correctly) that the terrain is flat so that this is also the height above the ground. The main comparisons we will make for this Report are for tree counting as a function of range and the use of the EVI as an advanced “Relaskop”.

### 5.6.2 Tree Counting by range

In the same way as with a stem plot, the number of trees within a distance “r” from the EVI can be plotted and modelled. This was done for each site but the main purpose of this section is to describe the kind of output we get and its use.

The following Figure 5-20 shows a plot of the number of trees within a given range at the Westfield 3 site (WF3) using all trees found by the EVI processing. It also shows the un-occluded and occluded models explained previously and in Appendix 2. The “occluded” model allows for the tree hiding by the trunks. The un-occluded model is what you would expect if there was no tree hiding.

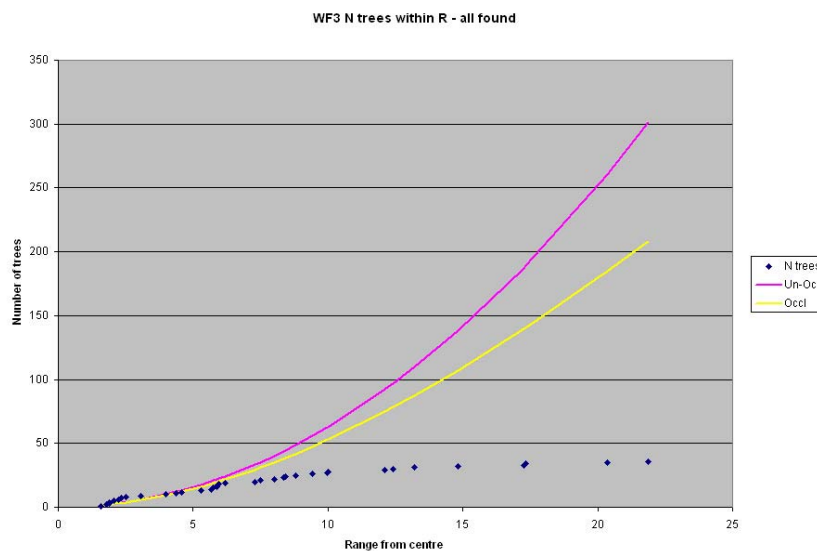


Figure 5-20: Number of trees within “r” as a function of “r”. All trees found.

The number of trees found falls away from the models (which use the stem density and mean diameter found by the processing – as described below) and seems to indicate considerable extra “tree hiding”. This is to be expected as the models do not allow for foliage and branches in this case.

In the following Figure, Figure 5-21 (a) shows the result of plotting the same function restricted to the number of EVI trees tagged as “in” for a “Relaskop” wedge of 1°. A similar divergence from the models can be seen indicating the tree hiding, to some extent, will also affect the Relaskop estimates. Figure 5-21 (b) shows the same plot for the true Relaskop data collected in the field and the similar behaviour tells us that this behaviour is a combined effect of the sampling method and inherent forest properties rather than a limitation unique to the EVI data.

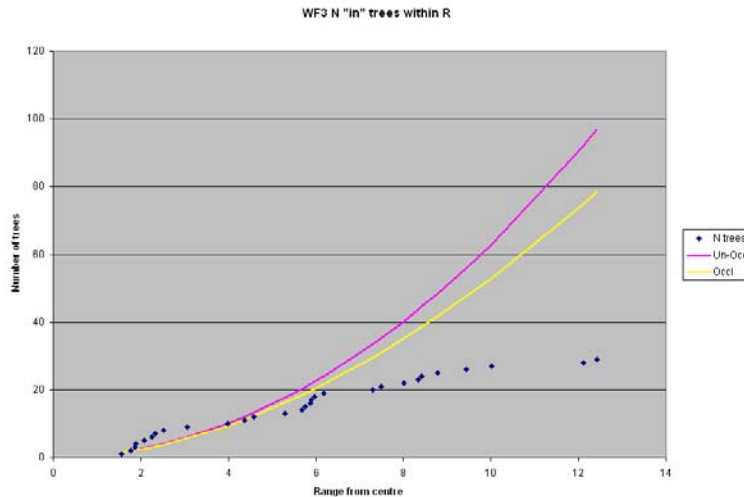


Figure 5-21 (a) Number of trees within “r” for a simulated 1 degree “Relaskop” wedge

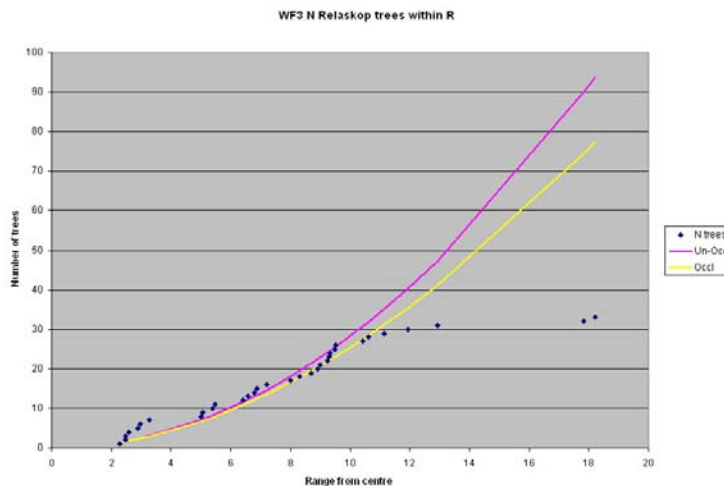


Figure 5-21 (b) Number of trees within “r” for field Relaskop data.

Inventory data taken at the Springs Road site (SR1) were not plotless but measurements of every tree within 20 metres of the EVI. They do not show the tree hiding effect – even for simulated Relaskop data.

The final Figure 5-22 shows the effect of allowing the effective diameter of the trees as “occluding agents” to increase. It shows that we can model the tree hiding effect and using methods outlined in Appendix 2 there is also the potential to develop ways to allow for the effect in the EVI data outputs. That is future work but the type of data collected by the EVI allows it to be considered.

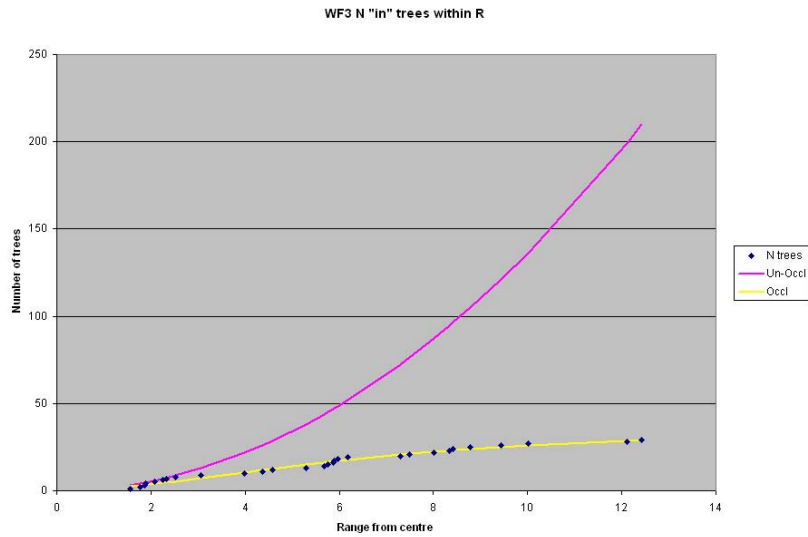


Figure 5-22: Number of trees within “r” as a function of “r”. All trees found.

The fitted “occlusion” model is effectively twice the density of hiding objects with 66 cm linear size.

### 5.6.3 Using EVI as a “Relaskop”

The other approach we can take is to select trees that are greater than a given angular width and simulate an angle count method as described in both Appendix 2 and Appendix 3.

The EVI-derived data for the five sites and comparative field data (in four cases obtained by using a real Relaskop with the wedge angle in degrees indicated) are presented in Table 5-3 and Table 5-4 respectively. The base data are basal area (BA), mean stem diameter (D, cm) and the coefficient of variation of stem diameters (Cd, %) and the number of “in” trees (N). Two additional lines of data provide the mean diameter (Hist D) and number density (Hist N) calculated from histograms of the measured diameters. The field results shown for Springs Rd (SR1) are simulated Relaskop results from the complete field survey.

Table 5-3: Stem parameters from automated EVI processing.

	WF1	WF3	Coffs2	Coffs3	SR1
Wedge	1.5	1.25	1.25	1.25	1.25
BA	34.3	27.4	15.5	11.8 (5.9)	26.2
D	16.2	12.7	16.4	36.1	37.0
Cd	13.1	21.6	12.7	11.0	18.9
N	20	23	13	10 (5)	22
Hist D	19.8	19.9	19.9	42.3	34.7
Hist N	25	29	14	7	36

The field diameters were measured at breast height, however the height at which the stem diameters were measured in the EVI data varied somewhat due to the necessity to find a clear view of the stem without branching and the effect of sloping terrain. The sloping terrain at Coffs3 resulted in identification of trees in only half the EVI azimuthal sweep, therefore the quoted BA and N values shown are double those found in the data with the actual figures indicated in parenthesis.

Table 5-4: Stem parameters from field data

	WF1	WF3	Coffs2	Coffs3	SR1*
Wedge	1.5	1.25	1.25	1.25	1.25
BA	39.4	28.6	11.9	10.7	36.9
D	20.03	17.8	15.6	39.7	32.7
Cd	10.6	9.1	5.7	11.2	8.3
N	23	24	10	9	31
Hist D	22.8	20.3	17.3	41.6	34.32
Hist N	30	31	15	14	50

The basal area results show generally good agreement between the EVI data and the field data, but there is greater discrepancy among the diameters. There is also a greater variation (as indicated by the coefficient of variation) in the EVI based estimates. Some of this is due to the way the Relaskop data are processed. To untangle results that are likely due to the forest and its variability as well as those due to field procedures we will look more closely at the histograms of the diameter data. These are summarised as “Hist D” and “Hist N” in Table 5-3 and Table 5-4 and show good agreement in the mean at all sites except one. The main differences will be shown to be in the CV. The larger differences that occur with the “Relaskop” processing are due to the way we compensate for the selection for large trees. If the sample numbers are small a few small trees can significantly influence the results. This is a well-known issue for angle count methods with larger wedge sizes. When the EVI processing has “matured” to the level covered in the theoretical development in Appendix 4 we will be able to use both small and large wedge sizes, locate potential problem trees and edit them easily from the original EVI data. The present study is an initial set of findings to demonstrate the capacity rather than the final product.

The following collection of graphs (Figure 5-23 (a) to (e)) shows the diameter histograms of the “in” trees for EVI and the equivalent Relaskop data at each of the selected sites:

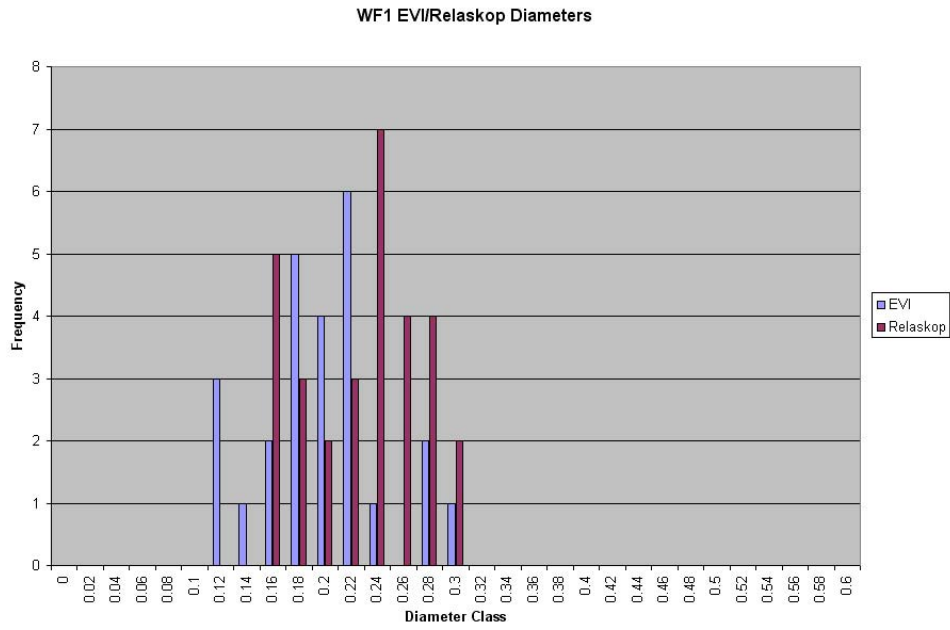


Figure 5-23(a): Westfield Site 1 EVI & Relaskop diameter comparison

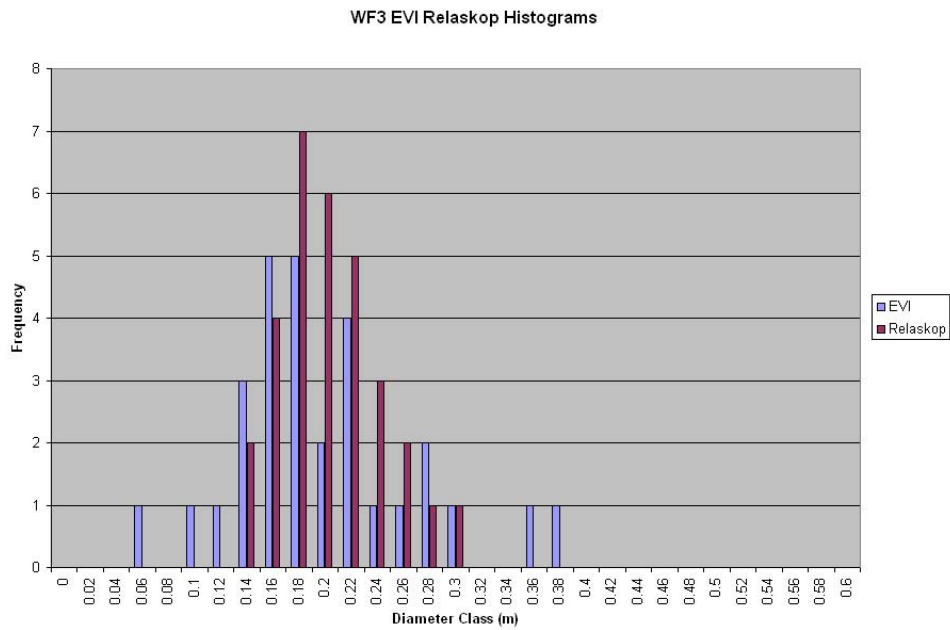


Figure 5-23(b): Westfield Site 3 EVI & Relaskop diameter comparison

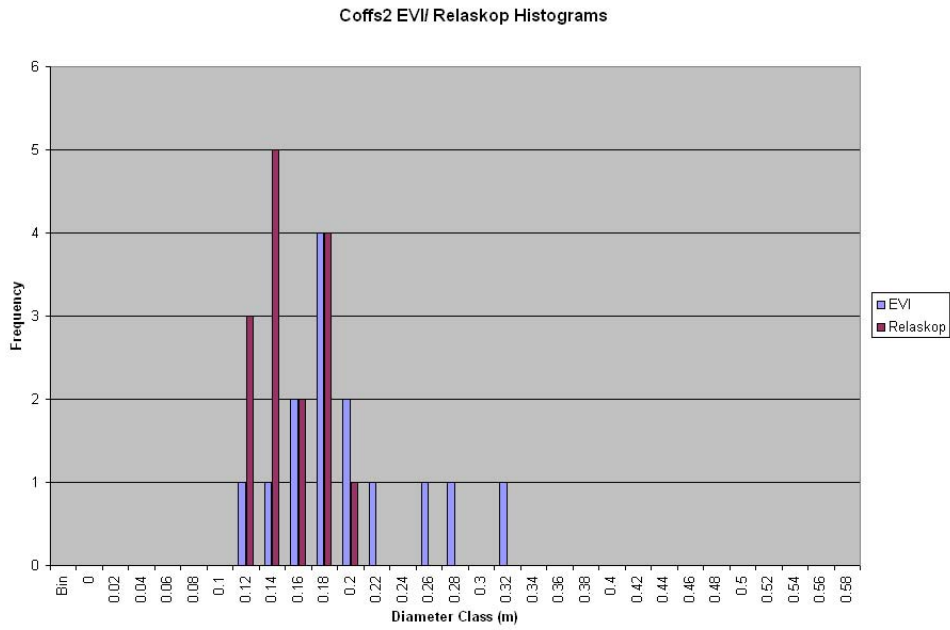


Figure 5-23(c): Coffs Harbour Site 2 EVI & Relaskop diameter comparison

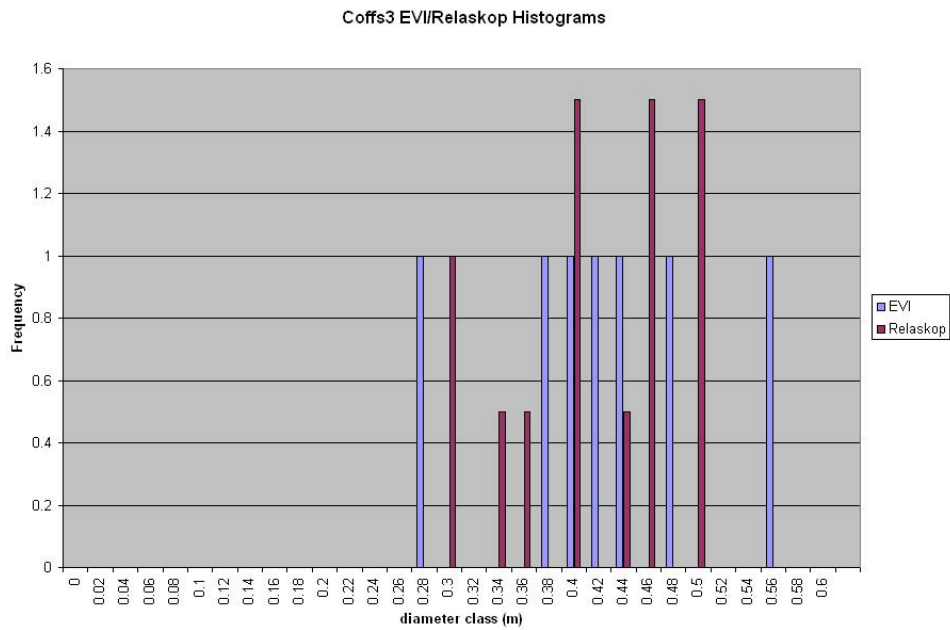


Figure 5-23(d): Coffs Harbour Site 3 EVI & Relaskop diameter comparison

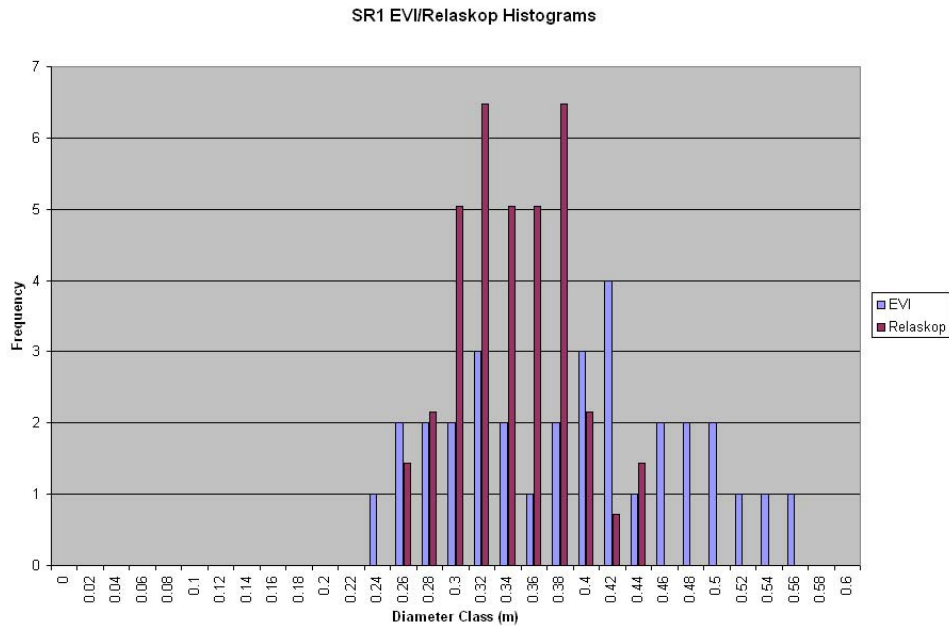


Figure 5-23(e): Spring Road EVI Site 1 EVI & Relaskop diameter comparison

Among these plots, there is a similar story of agreement in the mean with more variation in the EVI based results. The Springs Road case is different from the rest in that the field data are not actually from a Relaskop survey but are simulated from data where all trees were measured. Some of the differences are a function of the differences between total plot and angle count techniques rather than between EVI and the field data. But generally, despite all of the variation in the different forests they support the same findings as above.

The trunk finding method used with the EVI data to date has not taken topography into account. Therefore for sloping sites the height at which stem widths are measured will vary and in severe cases, the EVI slice may include some areas of ground that obscure any trees in that direction. This is most severe at Wedding Bells 3 where the slope was approximately 15%. A refinement of the procedure is straight forward and will enable the extraction of non-horizontal planes, or topographically adjust the data using terrain information present in the EVI scans. It is an important addition and is very high on the priority for current program and processing development.

The limited number of results presented here show that under conditions where stems are not obscured by large amounts of foliage, the EVI data can be used to provide reasonable estimates of basal area and mean diameter and stem diameter distributions. These are inputs to volume by size class depending on the allometry used. Further enhancement of the processing will seek to overcome terrain effects and reduce the impact of minor obscuration by small targets in the foreground (foliage, twigs etc.). Modelling of obscuration effects in regular plantations will also provide more stability to the results.

## 6 POTENTIAL COMMERCIAL APPLICATIONS

### 6.1 Commercial opportunities in forest measurement

The CSIRO Canopy Lidar Initiative (CLI) has been developing on the basis of market survey and analysis showing that there is a large world-wide market in the provision of forest measurement for inventory and planning both by forest owners and independent forest information providers. As part of the market research for commercial development, it has been estimated that 8.4m ha in Australia and NZ and 281m ha of forests in the rest of the world are likely to be measured each year and that there is about \$A 5b (assuming a cost of \$20 per ha out of a range of \$10-\$30 per ha) being spent performing such measurements. Nevertheless, the common story and claim from all of the market research was that the accuracy of the surveys is generally unsatisfactory, due primarily to limitations imposed by the high costs of current survey methods.

Implementation of forest inventories depends on factors such as management scale – spatial and temporal, and the sensitivity of product value to the timing and quality of management decisions. Measurements taken in managed plantations tend to be more extensive, detailed and costly (per ha) than in native forests and woodlands. However, the basic requirements of such measurement strategies are common and include provision of:

1. Timber volume by size class for forest blocks.
2. Quality and grade including defect and product type.
3. Logistical data such as need to prune and access.
4. Forest “health” and performance monitoring.
5. Spatial estimates of performance to plan management actions.

To obtain this or other information for forest plots and stands, ground based forest measurements are essentially governed by statistical controls, where the accuracy depends on sampling density and stratification. In practice, the accuracy achieved is ultimately determined by the point where the measurement costs outweigh the (present) value of the added information. The market for measurement is therefore cost and price driven and accuracy can suffer.

The CLI developed in this situation from two basic principles:

- (i) Remote sensing has the potential to make cost-effective measurements

Remote sensing from an airborne or space platform can cover large areas as a “census” and deliver information in a cost effective manner due to its “platform advantage”. For example, there is potential for airborne data based products to be delivered at less than \$5 per ha (a figure based on hyperspectral products).

The major problem is that remote sensing cannot, at this time, deliver the range of products required for forest survey (such as timber volume and size classes) at a competitive level of accuracy. Indeed, it is unlikely that airborne or spaceborne

remote sensing alone can ever deliver these requirements. At this time, the use of ground-based data to augment traditional remote sensing is possible, but the links between the different data types are difficult to establish and a significant amount of added ground work is needed. The total cost is generally not competitive with current methods. This leads to the second principle that:

(ii) Integration of airborne and ground based Lidar may provide the required information in a cost-effective manner.

CLI business planning and financial modelling has been based on a model business that uses airborne Lidar to measure forests at the broader scale plus ground based Lidar to undertake in-forest measurements and provide “calibration” for the airborne data. This is based on the ideas that:

- Airborne canopy Lidar provide products more in tune with forest measurement needs than other remote sensing technologies but still retains the “platform advantage”;
- Ground based Lidar provides information compatible with airborne sensors, as well as key in-forest data required for forest survey;
- The combination of these two approaches can deliver the information required for forest surveys, covering large forested areas at an accuracy as high as or higher than current ground based techniques at a competitive overall cost and price structure.

The information and arguments on which these statements are based have been developed from previous CSIRO business planning. They provided the basis for financial modelling and resulted in impressive IRR and NPV values for business activities in Australia, New Zealand and (eventually) worldwide. The CLI commercial plan has also considered a range of business models including the development of a partnership or company to take up the opportunities.

Out of discussions with the forest industry, it also became clear that there was great interest in the ECHIDNA® as a forest measurement technology. Its stand-alone potential is to increase the quantity and value of information available to forest managers from a given site. Thus, its use enables fewer sites to be measured to achieve the current accuracy levels at lower cost or greater accuracy to be achieved at current cost levels. ECHIDNA® is fully owned CSIRO IP and the subject of patent applications in a number of countries<sup>4</sup>. The work undertaken through the FWPRDC project and the decision to build a prototype of the ECHIDNA® have also been strongly supported by a number of forestry industry groups.

A critical need for the project has been to locate the ideal position in the market and to promote the uptake of the type of technology that has been developed at CSIRO and the uptake of the associated technologies and management opportunities the new technology supports. The location of the CSIRO activity and its opportunities can be illustrated by the following diagram showing the measurement activity and its supporting users and suppliers:

---

<sup>4</sup> US patent No 7,187,452, Australian Patent No. 2002227768, New Zealand Patent No 527547 with Priority Date Feb 9 2001. Others pending.

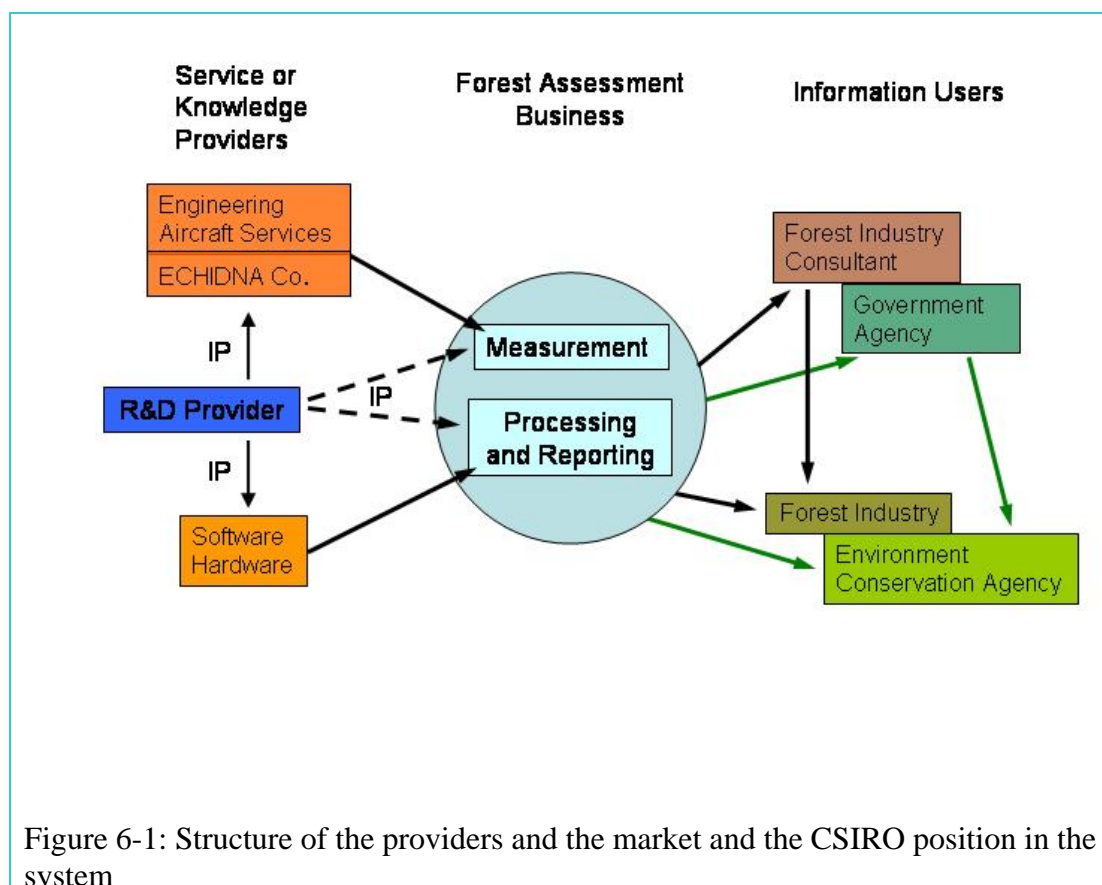


Figure 6-1: Structure of the providers and the market and the CSIRO position in the system

There is certainly a large market activity to be served by the technology – provided it solves the problems it faces and is cost-effective. Our planning can therefore be summarised as having three basic premises:

1. Waveform generating ground based Lidar, as demonstrated by the innovative CSIRO ECHIDNA® instrument, can provide key in-forest data required for forest survey at high accuracy and competitive cost at the scale of small forest plots;
2. Airborne canopy Lidar, especially more recent waveform generating instruments that are emerging into the commercial market, can be used with effective (CSIRO) software to provide broad scale information products that by themselves are useful but unable to provide key in-forest data;
3. The combination of ECHIDNA™ based information with airborne Lidar can provide more detailed forest survey maps that deliver the information required for forest surveys, covering large forested areas at an accuracy as high as or higher than current ground based techniques and at a highly competitive overall cost and price structure.

## 6.2 Industry uptake arising from the FWPRDC Project

A key objective of the FWPRDC Project was to “Develop strategies for the widespread adoption of the technology and the methods for Australian and international forest inventory”. The combined results arising from the CSIRO build of a prototype research instrument (the EVI), and this project with FWPRDC which has validated the ideas and principles embodied in CSIRO patents and patent applications have been to significantly enhance the potential for successful commercialisation and to meet this goal.

Technology based projects have a significant problem in that it is hard to find investment for R&D from non-government sources at the stage where the risks are still high. While investment at this stage promises the highest returns, the IRR demanded by risk-averse investors is generally much greater than a conservative estimate of future IRR from the project. For successful technology transfer and industry uptake to occur it is therefore necessary for the technology risk to be reduced by pilot projects or validation trials. It is also often the case in Australia that this stage needs to have support from government.

With regard to the outcomes of most relevance to technology transfer in the short-term, this Final Report has shown that:

- The ECHIDNA® ideas can be realised in current hardware and supplied by Australian engineers;
- The instrument provides data of high quality that allows forest information of direct value to timber volume estimation by size class;
- The data can be matched conformably in the vertical dimension with airborne Lidar and provides a basis for combined allometry;
- The data also provides a wide range of forest industry and other environmental information;
- This information can be provided in an acceptable timeframe with levels of mapping accuracy similar to current intensive site survey.

As well as providing an excellent response to the goals of the project and evidence of its successful conclusion, these outcomes provide the basis for significant risk reduction and evidence that the business planning had a sound basis.

However, since the CSIRO EVI was developed as a research instrument, the scientific validation work that was done for this project does not provide all of the information required to reliably estimate the expected savings that deployment of the commercial instrument will achieve through reductions in survey costs. Demonstrating this is the next operational step towards commercialisation. However, the EVI has provided a fund of information on which the engineering basis of commercial instruments can be planned and proposed in the next stage of commercialisation.

The next stages of commercialisation, with the sound base of the evidence arising from the CSIRO EVI instrument and the FWPRDC validation project are planned to include the following:

### **6.2.1 Increased Industry Adoption**

It is planned to re-visit industry leaders and provide them with the outcomes of the Project. We see the position of the FWPRDC as an industry forum to be very important for the success of this activity.

It is also planned to work with a small group of key industry contacts who have shown great interest in technology development and to undertake pilot projects. The projects are planned primarily to test the upgraded EVI system in an operational setting and in situations where the most significant information can be provided – such as timber volume from harvesting operations carried out after, and close to, the EVI measurements. The outcomes of this Report provide the entry point to this activity.

Outcomes from the airborne surveys undertaken during the project have demonstrated to industry partners the relevance of simple variables available from ALS data that correlate well with inventory or site quality parameters. Barriers to uptake have included both the cost of data acquisition and difficulties with processing. We have provided a beta-version of CSIRO processing software to the partners involved in this project and are pursuing a commercial version. This will reduce the processing barrier and if sufficient demand is generated, the price of data acquisition will be reduced. We therefore plan to also promote and develop the airborne opportunities and the links possible between the ground-based Lidar and airborne data.

### **6.2.2 Commercialisation of ECHIDNA®**

The success of this work will depend on a combination of two factors. One is the uptake (or the desire for uptake) of the technology and its associated opportunities by the industry in Australia and New Zealand and (eventually) the rest of the world. The other is access to the technology and instruments that can achieve its benefits that are available at an affordable cost. Making good use of the forum and exchange provided by the FWPRDC will enhance the uptake and access to the technology will be developed through commercialisation.

CSIRO has an active plan for commercialisation that involves:

- Taking the outcomes of the FWPRDC project on (re-)visits to FWPRDC partners and the wider industry;
- Engaging in pilot projects in parallel with market development;
- Establishing specifications for future commercial instruments based on this Project and the pilot projects;
- Finding industry partners and sufficient investment/support to develop a commercial prototype; and
- Establishing a business model to develop the market and provide access for users to the technology through a commercial framework.

This activity has been recently enhanced and its major added impetus has come from the findings of the current project.

### **6.3 Future R&D**

We believe that the activity that now exists world-wide in which Airborne Lidar is increasingly being used or investigated for forest inventory and the future developments of the airborne instruments as the forestry market increases all point to a very active environment for the CLI. The capacity of the ECHIDNA® to provide key forest information and to link conformably with the airborne information places it in a good position for commercial success.

The outcomes of the FWPRDC project can also be seen as pointing to the vast and yet un-developed potential that the innovative ECHIDNA® idea and instrument provide. The potential to develop multi-frequency Lidar hardware to separate living and dead vegetation components and to develop processing methods and algorithms to uncover structural information of wide environmental and scientific application from the improved system are just some of the likely directions.

The EVI is a prototype of an instrument that has not existed before and its data have entered new areas that will be explored in many ways in the future. Its applications to the forest industry are only beginning. R&D is the basis for the future development of the CLI as well as for it to hold its place in the market as the world develops new ideas and competition in the future. It is to be hoped that the commercialisation does not detract from investment and funding for the R&D but rather that it can feed back support to build the future applications.

It will be clear from reading the report that the R&D and the software developments associated with the Project are not complete but are moving ahead very fast. Many of the aspects not covered in the examples we chose are already being resolved as the FWPRDC Project moves on to the pilot projects. These include the more complete establishing of the obscuring in forests, the extensions to the software to measure Form Factors, the handling of local slope and aspect as well as increased stability in the models and inclusion of regular and semi-regular stem layouts in the available analysis. The future will also see an expansion of opportunities and uses in native forests for environmental and forestry purposes. These forests are more complex but we feel that the EVI and the future ECHIDNA® instruments provide the best tools there have been to cope with that additional complexity.

## **7 CONCLUSIONS**

This project has addressed a set of objectives and made a number of advances in the application of Lidar Technology for forest assessment. The decision to design and build the EVI was critical and the instrument has proven to be an essential component in the validation of Lidar based inventory methods, as described in the supporting documentation of the initial project application. Despite being a prototype the EVI has shown significant advantages over current commercially available ground based lidar instruments in forestry applications. It has also shown the synergy of ground based and airborne Lidar instruments as an integrated forest mapping system.

### **7.1 Modelling and Measuring Canopy Structure**

The Report outlines the way in which data from airborne Lidar and the ground-based EVI can be processed to provide forest information of value to both the Forest Industry and environmental assessment. These include cover, foliage profiles, leaf area index (LAI) and canopy height.

Both airborne Lidar and EVI data have shown themselves capable of mapping these components in a consistent way over our study sites (Section 5.5). Variations exist due to differences in the field of view for the two techniques and the “viewpoint” from which they are recorded but these differences do not necessarily indicate inaccuracies in measurement or processing but as complementary perspectives that can be used to provide even greater detail of forest structure.

The EVI data have provided the first opportunity we know to investigate forest structure as well as measure the aggregate statistics such as LAI and foliage profile (Section 5.4). This can be done at both the individual tree and stand scale. The issue of field data “truth” has been shown to be a significant factor in the variations observed (e.g. Section 5.4).

The effects of canopy structure on something as basic as the measurement of LAI are well-known and among these the effect of leaf “clumping” is very significant. In most cases where LAI has been successfully measured and monitored it has been done through local “calibration” of instrument readings or observations for the types of vegetation present. With EVI, these same procedures can be followed – or the source of the differences between forests can be used to overcome the need for local calibration. However, this is the subject of our ongoing investigations. At this time the EVI has been shown to measure precisely in the way an ECHIDNA® type instrument was designed to measure, both as a stand-alone instrument and through integration with appropriately processed airborne Lidar data for structural mapping at local and regional scales.

### **7.2 Tree Counting and Trunks**

The EVI has been shown to be an accurate tool for measuring range, bearing and angular spans (Section 5.6) and therefore provides the means to measure tree spacing

and sizes at different heights within the canopy. Provided the software is developed to a point where it can recognise trees in the presence of branches, leaves and topography, the instrument provides a tool for assessing individual tree form as well as stand basal area and form factor by size class. This is the basis for a very valuable timber inventory system.

We have shown that our initial analysis based on the first EVI model has provided credible estimates at the stand level (Section 5.6.3) and are now preparing for detailed forest trials where the measure of accuracy will be the result of actual harvest. Building on the system and methods demonstrated in this report through destructive field trials is the logical next stage of technology validation.

In our work we have also addressed the issue of tree occlusion that has been an issue for angle count (e.g. Relaskop) methods for many years (Section 5.6.2). The EVI provides information that can be used to compensate for this effect. Again this needs to be resolved by research but the current project has produced a tool that measures the type of added information that can address these issues.

### **7.3 Accuracy and Value of the Data**

The report validates the techniques and tools from a scientific perspective and in terms of a range of field data. The outcomes are presented in detail in Section 5. However, the effects of leaf clumping on LAI measurements, of occlusion and statistical sampling on angle count estimates of BA and of variability in growth form and structure on the accuracy of any set of measurements is unquantified. It is only with the development of tools such as ECHIDNA® that improvements may come in this task. At this time, however, the measures of accuracy we must accept include the inaccuracies of current forest mensuration techniques and it is difficult to make fully definitive statements about true accuracy of Lidar-based parameter estimates.

The EVI has already provided data that will, with further research, allow many of these effects to be managed or overcome in an objective and quantitative manner. Its primary capacity is to provide a detailed three-dimensional record of forests in which range to objects, relative and absolute bearings and structural geometry are accurate and can be extracted. Its performance in these aspects can and has been validated in this Report. With such rich data, the task of extracting forest information can be addressed primarily through software development. We have shown by a small number of important examples just how valuable the information is. Nevertheless, with any further development of the software, every site can be re-visited in the EVI data without the need for costly travel to each field site.

The ultimate level of “accuracy” we need to address is the accuracy of measurements in an operational setting. That is, the relationship between pre-harvest assessment and final deliveries of timber products. A fair test must be relative to the accuracy of current practice as forests can be measured to any degree of accuracy with enough sampling. The current project has shown clearly that this operational testing is a worthwhile endeavour in our future work.

## 7.4 Commercialisation and Adoption

This FWPRDC project described in this report has enabled CSIRO to work with a range of industry leaders to examine airborne and ground based Lidar technology. The airborne data analysis has demonstrated clearly to the forest industry how airborne Lidar data can be used to map forest structural attributes over large areas. The cost effectiveness of current technology airborne Lidar for this task is still an open issue, but the value of the products is clear.

The EVI has also been well received and supported by various industry groups. However, we believe on the basis of this report that there is a need to extend the industry interaction through pilot studies investigating the way an operational ECHIDNA® instrument may integrate with standard field operations and the level of operational accuracy required. This will also include realistic cost benefits analysis of ECHIDNA® based inventory methods relative to conventional assessment techniques.

Ultimately, adoption of Lidar technology by the forestry industry will be based on its cost and its ability to integrate with current forest measurement and management systems. However, in the case of the ECHIDNA® it will also depend on the future development of the concept. This is being pursued through commercialisation. The validation provided by this project has significantly reduced the technology risk that had been limiting ECHIDNA® commercialisation and uptake. The reticence to invest created by the technology risk can be seen as a major hurdle for the Australian forestry industry as well as potential instrument providers. The FWPRDC has now provided the means for it to be overcome.

## 8 ACKNOWLEDGEMENTS

The CLI has had the input and support of many people. The FWPRDC, CSIRO and the forestry industry partners ForestrySA and Forests NSW have been the source of funding as well as interest, support in many other ways and people. As well it is important to mention people involved in the design and build of the RPE and EVI instruments. These include David Parkin, George Poropat, Phil Connor and Stuart Young of CSIRO for work on the ECHIDNA® design and specifications and the RPE instrument, Ian Wilson and his staff of OEAPL and Werner Fabian of LITE for their wonderful work to build the EVI. Their inputs have been crucial to the position we are now in. As well, Gary Cornelius of Leadenhall Pty Ltd developed the FWPRDC project from suggestions by Forest Industry partners and also provided the project with a firm base of market and business planning that is taking the work on the path to commercialisation. During field work we had the benefit of the hard work of many people including Edward King from CSIRO EOC and Petr Otahal (CRC for SPF) in Tasmania, Steve Rann (Forests NSW), Nick Goodwin (UNSW/CSIRO), and Russell Turner (Forests NSW) at Coffs Harbour and Colleen Schultz (CSIRO FFP) and David Gritton (CSIRO FFP) at Mount Gambier. Barrie May and Maria Ottenschlaeger (CSIRO FFP) provided important historical inventory data for the Spring Road and Westfield sites respectively and helped with the field trials in their areas.

## 9 REFERENCES

### 9.1 CLI Journal Papers

Lovell, J.L., Jupp, D.L.B., Culvenor, D.S. and Coops, N.C. (2003). Using airborne and ground-based ranging lidar to measure canopy structure in Australian forests. *Canadian Journal of Remote Sensing*, Vol. **29**, No. 5, pp. 1-16.

Lovell, J.L., Jupp, D.L.B., Newnham, G.J., Coops, N.C. & Culvenor, D.S. (2005). Simulation study for finding optimal lidar acquisition parameters for forest height retrieval, *Forest Ecology and Management*, in press.

### 9.2 CLI Conference Papers

Lovell, J.L., Culvenor, D.S, Newnham, G.J., Jupp, D.L.B. and Coops, N.C. (2003). *Efficient Lidar Data Processing Techniques for Forest Inventory*. Spatial Science 2003, Canberra, 23-25 Sept.

Newnham, G.J., Lovell, J.L., Jupp, D.L.B., Culvenor, D.S. and Coops, N.C. (2003). *Characterising Forest Structure Using Ground Based Lidar*. Spatial Science 2003, Canberra, 23-25 Sept.

Newnham, G.J., Jupp, D.L.B., Lovell, J.L., Culvenor, D.S. and Coops, N.C. (2004). Estimation of Foliage Density Profiles using Ground Based Multi-Angular Methods: Measurement and Modeling, International Geoscience and Remote Sensing Symposium (IGARSS'04), Alaska.

Lovell, J.L., Jupp, D.L.B., Newnham, G.J., Culvenor, D.S. and Coops, N.C. (2004). Airborne and Ground-based lidar to measure forest structure, International Geoscience and Remote Sensing Symposium (IGARSS'04), Alaska.

### 9.3 CLI Reports

Lovell, J.L., Newnham, G.J., Culvenor, D.S., Jupp, D.L.B. and Coops, N.C. (2003a). *CSIRO Canopy Lidar Initiative: Mount Gambier Field Trial*, EOC Technical Report 2003/02. [http://www.eoc.csiro.au/tech\\_reps/2003/tr2003\\_03.pdf](http://www.eoc.csiro.au/tech_reps/2003/tr2003_03.pdf)

Jupp, D.L.B. and Lovell, J.L. (2005). *Airborne and Ground-Based Lidar Systems for Forest measurement: Background and Principles*. EOC Technical Report 2005/....

### 9.4 CLI Patents and Applications

Petty Patent 23163/01 Lidar System and Method (Echidna)

Petty Patent 23164/01 Lidar System and Method (Echidna and VSIS)

Petty Patent 35196/01 Lidar System and Method (Products)

International Patent now in country phase: "Lidar System and Method (Echidna)"  
with Priority date Feb 2 2001:

US granted Patent No 7,187,452

Australia granted Patent No 2002227768

New Zealand granted Patent No 527547

(Pending in other jurisdictions)

## 9.5 General References

Aldred, A.H. and Bonnor, G.M. (1985). *Applications of airborne lasers to forest surveys*. Petawawa National Forestry Service, Canadian Forestry Service, Agriculture Canada, Information Report PI-X-51, 62p.

Andrieu, B., Sohbi, Y. & Ivanov, N. (1994). A direct method to measure bidirectional gap fraction in vegetation canopies. *Remote Sensing of Environment*, **50**,(1), 61-66.

Blair, J.B., Rabine, D.L., and Hofton, M.A. (1999). The laser vegetation imaging system; a medium-altitude digitisation-only, airborne laser altimeter for mapping vegetation and topography. *ISPRS Journal of Photogrammetry & Remote Sensing*, **54**, 115-122.

Brack, C. and Wood, G. (1998). *Forest Mensuration*.  
<http://sres.anu.edu.au/associated/mensuration/Brackandood1998>

Buften, J.L. (1989). Laser altimetry measurements from aircraft and spacecraft. *Proceedings of the IEEE*, **77**(3), 463-477.

Campbell, G. S. (1986). Extinction coefficients for radiation in plant canopies calculated using an ellipsoidal inclination angle distribution. *Agricultural & Forest Meteorology*, **36**, 317-321.

Drake, J.B., Dubayah, R.O., Clark, D.B., Knox, R.G., Blair, J.B., Hofton, M.A., Chazdon, R.L., Weishampel, J.F. and Prince, S.D. (2002). Estimation of tropical forest structural characteristics using large-footprint lidar. *Remote Sensing of Environment*, **79**, 305-319.

Fiocco, G. and Smullin, L.D. (1963). Detection of scattering layers in the upper atmosphere (60-140 km) by optical radar, *Nature*, **199**: 1275-1276.

- Gaveau, D.L. and Hill, R.A. (2003). Quantifying canopy height underestimation by laser pulse penetration in small-footprint airborne laser scanning data. *Canadian Journal of Remote Sensing*, **29**(5), 650-657.
- Harding, D.J., Blair, J.B., Rabine D.L., and Still, K.L. (2000). SLICER Airborne Laser Altimeter Characterization of Canopy Structure and Sub-canopy Topography for the BOREAS Northern and Southern Study Regions: Instrument and Data Product Description. NASA Technical Memorandum NASA/TM-2000-209891. Available from <http://www-eosdis.ornl.gov/BOREAS/guides/SLICER.html> [cited 1 October 2002].
- Harding, D.J., Lefsky, M.A., Parker G.G., and Blair, J.B. (2001). Laser altimeter canopy height profiles method and validation for closed-canopy, broadleaf forests. *Remote Sensing of Environment*, **76**, 283-297.
- Leckie, D., Gougeon, F., Hill, D., Quinn, R., Armstrong, L. and Shreenan, R., (2003). Combined high-density lidar and multispectral imagery for individual tree crown analysis. *Canadian Journal of Remote Sensing*, **29**(5), 633-649.
- Lefsky, M.A., Harding, D., Cohen, W.B., Parker, G., and Shugart, H.H. (1999a). Surface Lidar remote sensing of basal area and biomass in deciduous forests of eastern Maryland, USA. *Remote Sensing of Environment*, **67**, 83-98.
- Lefsky, M.A., Cohen, W.B., Acker, A., Parker, G.G., Spies, T.A., and Harding, D. (1999b). Lidar remote sensing of the canopy structure and biophysical properties of Douglas-Fir Western Hemlock forests. *Remote Sensing of Environment*, **70**, 339-361.
- Lewis, N.B., Keeves, A. and Leech, J.W. (1976). *Yield regulation in south Australia Pinus radiata plantations*. Bulletin 23. Woods and Forests Department – South Australia. A.B. James Government Printer, Adelaide, Australia, pp. 26-33.
- Maclean, G.A. and Krabill, W.B. (1986). Gross-merchantable timber volume estimation using an airborne Lidar system. *Canadian Journal of Remote Sensing*, **12**, 7-18.
- Magnussen, S., and Boudewyn, P. (1998). Derivations of stand heights from airborne laser scanner data with canopy-based quantile estimators. *Canadian Journal of Forest Research*, **28**, 1016-1031.
- Magnussen, S., Eggermont P., and LaRiccia, V. (1999). Recovering tree heights from airborne laser scanner data. *Forest Science*, **45**, 407-422.
- Measures, R.M. (1984) *Laser remote sensing: fundamentals and applications*. Krieger, Malabar, Florida. 510 pp.
- Miller, J.B. (1964). An integral equation from phytology. *Journal of the Australian Mathematical Society*, **4**, 397-402.

- Miller, J.B. (1967). A formula for average foliage density. *Australian Journal of Botany*, **15**, 141-144.
- Næsset, E. (1997a). Estimating timber volume of forest stands using airborne laser scanner data. *Remote Sensing of Environment*, **61**, 246-253.
- Næsset, E. (1997b). Determination of mean tree height of forest stands using airborne laser scanner data. *ISPRS Journal of Photogrammetry and Remote Sensing*, **52**, 49-56.
- Næsset, E. and Økland, T. (2002). Estimating tree height and tree crown properties using airborne scanning laser in a boreal nature reserve. *Remote Sensing of Environment*, **79**, 105-115.
- Næsset, E. (2004). Effects of different flying altitudes on biophysical stand properties estimated from canopy height and density measured with a small-footprint airborne scanning laser. *Remote Sensing of Environment*, **91**, 243-255.
- Nelson, R. (1997). Modeling forest canopy heights: The effects of canopy shape. *Remote Sensing of Environment*, **60**, 327-334.
- Nelson, R.L., Krabil, W.B. and MacLean, G.A. (1984). Determining forest canopy characteristics using airborne laser data. *Remote Sensing of Environment*, **15**, 210.
- Nilsson M. (1996). Estimation of tree heights and stand volume using an airborne lidar system. *Remote Sensing of Environment*, **56**, 1-7.
- Ni-Meister, W., Jupp, D.L.B., and Dubayah, R. (2001). Modeling Lidar waveforms in heterogeneous and discrete canopies. *IEEE Transactions on Geoscience and Remote Sensing*, **39**(9), 1943-1958.
- Parker, G.G., Harding, D.J. and Berger, M.L., (2004). A portable lidar system for rapid determination of forest canopy structure. *Journal of Applied Ecology*, **41**, 755-767.
- Persson, A., Holmgren, J. and Soderman, U. (2002). Detecting and measuring individual trees using an airborne laser scanner. *Photogrammetric Engineering and Remote Sensing*, **68**(9), 925-932.
- Popescu, S.C. and Wynne, R.H. (2004). Seeing the trees in the forest: Using lidar and multispectral data fusion with local filtering and variable window size for estimating tree height. *Photogrammetric Engineering and Remote Sensing*, **70**(5), 589-604.
- Popescu, S. C., Wynne, R. H. and Nelson, R. F. (2003). Measuring Individual Tree Crown Diameter With Lidar and Assessing Its Influence on Estimating Forest Volume and Biomass. *Canadian Journal of Remote Sensing*, **29**(5), 564-577.

- Ross, J. K. (1981). *The Radiation Regime and Architecture of Plant Stands*, Junk Publishers, The Hague, Netherlands.
- Smethurst, P.J., Herbert, A.M. and Ballard, L.M. (1997). A paste method for estimating concentrations of ammonium, nitrate, and phosphate in soil solution. *Australian Journal of Soil Research*, **35**: 209-225.
- Steers, J.A. (1962). *An introduction to the study of map projections*. University of London.
- Tanaka, T., Yamaguchi, J., and Takeda, Y. (1998). Measurement of forest canopy structure with a laser plane range-finding method - development of a measurement system and applications to real forests. *Agricultural and Forest Meteorology*, **91**: 149-160.
- Tanaka, T., Park, H. and Hattori, S. (2004). Measurement of forest canopy structure by a laser plane range-finding method. Improvement of radiative resolution and examples of its application. *Agricultural and Forest Meteorology*, **125**: 129-142.
- Witte, C., Norman, P., Denham, R., Turton, D., Jonas, D., and Tickle, P. (2000). *Airborne laser scanning – A tool for monitoring and assessing the forests and woodlands of Australia*. Forest Ecosystem Research and assessment Technical Papers, 00-10, Queensland Department of Natural Resources.
- Yang, X., Witcosky, J. J. & Miller, D. R. (1999). Vertical overstory canopy architecture of temperate deciduous hardwood forests in the eastern United States. *Forest Science*, **45**, 349-358.

## 10 APPENDIX 1: FIELD SITES AND DATA COLLECTED

### 10.1 Site Selection Criteria

An important objective of the study was to ensure that lidar based measurement strategies developed could be applied across a broad range of plantations types existing in Australia. Our objective in the selection of field sites was to include a range of forest types and management practices. The primary research sites detailed below include both softwood and hardwood plantation and native forests of differing age classes and subjected to vastly differing environmental conditions.

### 10.2 Tumbarumba

Bago Maragle study area is located near Tumbarumba in southern New South Wales. The current study was undertaken at four sites within Bago-Maragle. Three sites were located in native mixed age forest *E. pauciflora*, *E. delegatensis* and *E. globulus*, and the fourth site was established within a 40 year old plantation of *P. ponderosa*. Standard forest inventory data were recorded in 0.1 ha plots for all stems greater than 10cm at each field site and are shown in the table at the end of this appendix.

A prototype of the ECHIDNA™ instrument constructed from off the shelf components was also used to record measurements at each of the four sites and to assess the value of simple rangefinder technology in characterising forest structure at the plot scale.

Airborne lidar data were acquired on the 14<sup>th</sup> of December 2001 with an average point spacing of 0.8m over a 5km square area. Four 200m square study areas were overflown twice (on perpendicular flight lines) with reduced scan angle to achieve an average point spacing of 0.5m.

### 10.3 Mt Gambier

Airborne lidar data were collected in the Mt Gambier region on July 7 2002. This data includes coverage of the ForestrySA managed plantations at South Patchells and Springs Road. The Springs Road plantation is currently used by CSIRO Forestry and Forest Products as a fertiliser trial site. Ground based measurements were recoded during two periods; shortly after the airborne data capture at South Patchells and Springs road during the weeks of the 12<sup>th</sup> to the 16<sup>th</sup> of August 2002 and two years later at Penola HQ and Springs Road during the week of the 13<sup>th</sup> to the 17<sup>th</sup> of December 2004 after the fully functional ECHIDNA™ instrument became operational.

South Patchells and Penola HQ are intensively managed *P. radiata* plantations that were studied at site quality assessment age (approximately 9 years). The terrain in these regions is flat and is free from undergrowth. However, at the high quality sites, the understorey was dense, making measurements challenging. Measurement stations were selected to include a range of ForestrySA site quality classes. At Springs road, CSIRO FFP are conducting fertiliser trials in a 20 to 25 year old *P. radiata* plantation. The terrain slopes gently toward

the north with some debris remaining from thinning operations. Measurement stations were selected to fall within pre-existing CSIRO experimental plots.

The data collected during the 2002 field exercise included six hemispherical scans using the earlier prototype ECHIDNA™ instrument; one scan for each of the three South Patchells plots and three additional scans at Springs Road. Inventory measurements at South Patchells were recorded by ForestrySA and at Springs Road by Barrie May from CSIRO Forestry and Forest Products. These data are detailed in the table at the end of this appendix.

A large number of hemispherical photographs were also recorded at each location. In addition to standard photos recorded close to ground level at plot centres and plot corners, a 15m mast was used to record a series of images at different heights at each plot centre in order to build up a profile of LAI values.

The objective of the later field trip to Mt Gambier in 2004 was to test the new fully functional ECHIDNA™ instrument. This did not coincide with airborne lidar data measurements. Data were recorded at three site quality assessment plots at Penola Head Quarters and at two sites at Springs Road. A total of 25 ECHIDNA™ scans were recorded; five at each of these five stations along with standard inventory measurements as detailed in the table at the end of this section.

## **10.4 Florentine Valley**

The Westfield site is a 1992 *E. nitens* (Shining Gum) plantation located in Tasmania's Florentine Valley. The site is relatively flat with very little understorey and has been used by CSIRO FFP for various experiments including fertiliser trials.

Airborne lidar data were recorded over the site on the 2<sup>nd</sup> of March 2004, along with a number of other sites, commissioned by Forestry Tasmania. During the week of July 5 to 9, 2004, ground based measurements were recorded. At each location, a relaskop was used to establish basal area and to select "in trees", for which detailed inventory measurements were recorded (see table at the end of this appendix). 37 ECHIDNA™ scans were also recorded at the site.

Hemispherical photographs were again recorded at ground level at the centre of each measurement plot and at ten metres in the cardinal directions. A 15m mast was again used to measure multi-level hemispherical photographs at the plot centres in order to derive profiles of LAI.

## **10.5 Wedding Bells**

The Wedding Bells State Forest is located approximately 15 km northwest of Coffs Harbour and is a mix of native forest and eucalypt plantations. The site undulates significantly between a ridge running northwest-southeast and the valley floor to the southwest. Measurement stations were located both on the ridge, which is predominantly native forest, and within the valley in varying age plantations. All measurements were recorded during the week of August 23 to 27, 2004.

The five measurement sites were established as follows:

1. 1953 *E. grandis* (Flooded Gum)
2. 1999 *E. dunnii* (White Gum)
3. 1973 *E. pilularis* / *E. grandis* (Black Butt / Flooded Gum)
4. Native forest, *E. pilularis* (Black Butt) dominant
5. Native forest, *E. pilularis* (Black Butt) dominant

Relaskop sweeps were used to establish basal area at each site and standard inventory measurements were recorded for each “in tree” at each site by CSIRO and Forestry NSW staff. A summary of these measurements are detailed in the table at the end of this appendix.

A detailed set of hemispherical photographs were again recorded at both ground level and using the 15m mast. A total of 60 ECHIDNA™ scans were recorded over all 5 stations with varying neutral density filter strength, beam divergence and shot spacing.

## 10.6 Summary Tables

### 10.6.1 Details of Demonstration Sites

Table 10-1 Site Information

Site	Lat	Long	Elevation	Native / Plantation	Field Sampling	Airborne Sampling	Industrial Partner
Tumbarumba	35°45'	148°00'	700 m	Native / Plantation	Dec 01	Dec 01	SFNSW
Mt Gambier	37°49'	140°46'	50 m	Plantation	Aug 02 Dec 04	July 02	SAForest
Westfield	42°40'	146°26'	430 m	Plantation	July 04	Mar 04	CSIRO FFP / Forestry Tas
Coffs Harbour	30°05'	153°09'	200 m	Native / Plantation	Aug 04	Oct 04	SFNSW

## 10.6.2 Airborne LIDAR Data Specifications

Table 10-2 Airborne Data Properties

Parameter	Performance
Sensor	Optech ALTM 3025
Laser Pulse Frequency	25000 Hz
Mean Point Density	1.3 – 1.7 hits per sq meter.

Table 10-3 Site Airborne Data Mission Summary

Location	Site	Data Area	Acquisition Date	Data Format	Flying Height	Max scan angle
Tumbarumba	Bago Maragle	5km by 5km	14.12.2001	Classified and Time sequential	1000m	10 deg
Mt Gambier	South Patchells	~1400 ha	07.07.2002	Classified and Time sequential	1200m	15 deg
	Springs Road	~1200 ha	07.07.2002	Classified and Time sequential	1200m	15 deg
Tasmania	Westfield	Full Extent	02.03.2004	Time Sequential	1000m	10 deg 15 deg
Coffs Harbour	Wedding Bells	Full Extent (Box 1)	10.10.2004 11.10.2004	Classified and Time sequential	1000m 2000m 3000m	10 deg 15 deg
		Detailed (Box 2)	10-11/10/2004	Classified and Time sequential	1000m	10 deg
		Detailed (Box 3)	10-11/10/2004	Classified and Time sequential	1000m	10 deg

### 10.6.3 Summary of Ground Validation Measurements

Table 10-4 Tumbarumba and Mt Gambier Site Ground Data Summary

	Instrument Station	Species	DBH (m)	Stocking (m <sup>2</sup> )	Product of DBH and Stocking	Site Quality	Crown Diameter (m)	Crown Factor %	LAI	Height (m)	Bole Height (m)	Est.
Tumbarumba												
	1	<i>E. deligatensis</i>	0.512±0.228	0.020	0.010	N/A	7.89±5.35	44.00±12.73		33.96±12.37	18.81±7.03	Native
	2	<i>E. pauciflora</i>	0.259±0.123	0.033	0.854	N/A	5.10±4.41	38.03±10.68		20.58±8.45	11.55±5.93	Native
	3	<i>E. globulus</i>	0.372±0.317	0.022	0.008	N/A	7.48±5.86	47.50±12.13		20.99±9.74	9.97±3.86	Native
	4	<i>P. ponderosa</i>	0.442±0.045	0.036	0.016	N/A	4.76±1.13	75.00±0.0		29.85±1.27	17.52±2.13	1961
Mt Gambier												
	Patchells TP3	<i>P. radiata</i>	0.169	0.164	0.028	1	Not Measured	94	3.13	19.2	7.98±0.57	1992
	Patchells TP10	<i>P. radiata</i>	0.159	0.166	0.026	3	Not Measured	96	3.84	17.6	6.79±0.88	1992
	Patchells TP18	<i>P. radiata</i>	0.116	0.152	0.018	6	Not Measured	81	2.51	13.5	2.25±0.61	1992
	Penola HQ 1	<i>P. radiata</i>	0.163	0.148	0.024	3+	Not Measured	Not Measured	3.40±0.02	15.7	3.84±0.31	1996
	Penola HQ 2	<i>P. radiata</i>	0.148	0.182	0.027	3-	Not Measured	Not Measured	3.08±0.03	14.5	3.46±0.63	1996
	Penola HQ 3	<i>P. radiata</i>	0.151	0.174	0.026	3	Not Measured	Not Measured	3.36±0.06	15.4	3.16±0.30	1996
	Penola HQ 4	<i>P. radiata</i>	0.136	0.194	0.026	4-	Not Measured	Not Measured	2.70±0.05	13.9	1.90±0.47	1996
	Penola HQ 6	<i>P. radiata</i>	0.174	0.156	0.027	1-2	Not Measured	Not Measured	3.37±0.04	16.5	4.06±0.57	1996
	Springs Rd	<i>P. radiata</i>	0.349±0.054	0.035	0.012	N/A	3.60±1.45	57.29±19.87	2.12±0.09	29.23±1.49	12.31±4.62	1975

Table 10-5 Westfield and Coff's Harbour Site Ground Data Summary

	Instrument Station	Species	DBH (m)	Stocking (m <sup>2</sup> )	Product of DBH and Stocking	Site Quality	Crown Diameter (m)	Crown Factor %	LAI	Height (m)	Bole Height (m)	Est.
Westfield												
	1	<i>E. nitens</i>	0.208±0.045	0.117	0.024	N/A	3.66±0.88	36.16±14.57	5.39	23.56±9.32	14.54±1.10	1993
	2	<i>E. nitens</i>	0.175±0.054	0.108	0.019	N/A	2.65±1.10	22.82±13.68	6.27	19.06±4.26	12.05±2.11	1993
	3	<i>E. nitens</i>	0.178±0.036	0.112	0.020	N/A	3.83±0.74	45.27±14.30	5.25	19.87±2.07	12.26±1.22	1993
	4	<i>E. nitens</i>	0.198±0.028	0.162	0.032	N/A	3.25±0.60	35.82±13.00	5.98	24.24±0.97	14.96±0.62	1993
	5	<i>E. nitens</i>	0.149±0.038	0.162	0.024	N/A	2.85±0.73	15.80±10.32	6.05	17.87±2.79	11.04±1.82	1993
Coffs Harbour												
	1	<i>E. grandis</i>	0.292±0.106	0.027	0.008	N/A	3.13±1.82	46.73±26.29	2.77	33.3±12.76	22.31±12.42	1953
	2	<i>E. dunnii</i>	0.160±0.022	0.060	0.010	N/A	3.17±0.87	54.73±8.19	2.28	15.1±0.86	8.48±1.71	1999
	3	<i>E. pilularis</i> <i>E. grandis</i>	0.397±0.068	0.008	0.003	N/A	8.68±1.60	64.87±10.04	1.01	40.25±3.07	22.57±4.17	1973
	4	<i>E. pilularis</i> (dominant)	0.260±0.108	0.053	0.014	N/A	4.85±1.93	58.22±14.42	3.11	23.21±9.17	11.25±5.35	Native
	5	<i>E. pilularis</i> (dominant)	0.158±0.099	0.214	0.034	N/A	3.22±1.77	24.66±21.70	2.91	14.39±8.48	9.21±5.49	Native

## 11 APPENDIX 2: ANGLE COUNT METHODS USED AT FIELD SITES

### 11.1 Theory

The Angle Count (or Relaskop) method has been widely used by foresters and environmental scientists for inventory and forest measurement. There is a discussion that serves the needs of this document about the method in its general aspects in Jupp and Lovell (2005). That document also contains many references to the general theory and history of the method.

The capacity for a field procedure based on Relaskop methods to satisfy ecological measurement needs or those of EVI validation is not, however, quite the same as for the outcomes sought by foresters. Their objective is a reasonably accurate basal area (the cross sectional area of tree trunk per unit area of the forest) and some associated measurements (such as tree height) to make an estimate of timber volume at the stand scale. These can often be obtained with sufficient accuracy with low sampling density. However, the EVI validation (as will many environmental applications) needed much more detail on parameters such as tree trunk and crown sizes, green height and crown openness as well as stable estimates of their distribution functions. The plotless sampling involved in Relaskop measurements allows quite large tracts of forest to be sampled with a design that permits quite rigorous statistical analysis to be made. We will show how it is possible to allow for the sampling and arrive at estimates of parameter distributions. The main choice is one of sampling intensity and effective plot size and the Relaskop method has excellent options to keep control of these factors.

The theory of use for the Relaskop is relatively simple. Briefly, at a sample “plot” within the extent of the experimental “site”, an instrument (the “Relaskop” which is a brand name but will be used here to mean equipment that allows the Bitterlich method to be applied) is used to assess if tree trunks as viewed from a fixed point subtend a wider field of view than a wedge or sector angle that is selected before the assessment is made. If it does, the tree is an “in” tree for that wedge angle. Most Relaskops have a range of wedge angles between about 1.0 and 4.0 degrees. The number of “in” trees is then multiplied by a “Basal Area Factor” (BAF). The BAF is a constant for a given wedge angle. The result is an estimate for Basal Area (BA). In many forests, timber volume can be effectively estimated from allometric equations based either on BA alone or BA and a measure of height (such as tree height or bole height).

BA is defined as the cross sectional area (at breast height or 1.3m) of tree trunk per unit area of the forest. If the stem density is  $\lambda$  and the mean area of the trunk cross sections is  $\bar{A}$  then the BA can be expressed as:

$$BA = \lambda \bar{A}$$

This is sometimes written in terms of the mean RMS Diameter at Breast Height as:

$$BA = \lambda \pi D_{rms}^2 / 4$$

However, it needs to be kept in mind that the “mean RMS DBH” is the RMS DBH defined as (assuming an independent sample of N trees):

$$\bar{D}_{rms} = \left( \frac{1}{N} \sum_{j=1}^N d_j^2 \right)^{1/2}$$

It is straightforward to show that the mean RMS diameter and tree diameter mean and variance are related as:

$$D_{rms} = \bar{D}(1 + C_d^2)^{1/2}$$

where,  $C_d$  is the coefficient of variation of the diameters:

$$C_d = \frac{\sigma_d}{\bar{D}}$$

where  $\bar{D}$  is the mean tree diameter (DBH) and  $\sigma_d$  is the standard deviation of the tree diameters.

The “in” trees are not an independent sample and the way in which this may be estimated if the DBH values of the “in” trees are measured is discussed later.

At this stage, we will assume all of the “units” are compatible and that BA is unitless in that the unit for trunk cross-sectional area is square DBH units and the density is the number of trees per the *same* area unit as the tree cross-sectional areas. The practical use of different units for different components is discussed later.

Now suppose that the angle subtended by the wedge is denoted  $\alpha$ . In the field work protocol described below, the distance from the plot centre to the tree is measured to the centre of one side of the tree. Suppose that for tree j the distance is  $z_j$ . In this case, if the tree trunk just fills the field of view (so that the viewer is at the “limiting” distance from the tree) it can be shown that the distance to the tree (in the same units as the DBH) is:

$$Z_j = \frac{D_j/2}{\sin(\alpha/2)}$$

Basically, for any tree, if the plot centre is within a circle (disk) of this radius then the tree is an “in” tree. Moreover, if the trees are replaced by disks of radius  $Z_j$  then the number of “in” trees can be shown to be the number of disks overlapping the site centre point (see Jupp and

Lovell, 2005 for more details and references). For a Poisson distribution of tree locations<sup>5</sup>, the expected number of “in” trees is:

$$\bar{N} = \frac{BA}{\sin^2(\alpha/2)}$$

Hence, the (dimensionless) BA estimate will be:

$$BA = BAF \times \bar{N}$$

$$BAF = \sin^2(\alpha/2)$$

For the Poisson case, the number of “in” trees is also a Poisson variable. It will therefore vary naturally over a number of different plots in a forest stand with uniform BA. Over a number of Relaskop plots the sampling variance will tend to be equal to the mean and the ratio of variance to mean can be used as an indicator of “randomness” of the tree distribution.

The coefficient of variation is the ratio of the standard deviation to the mean. For the Relaskop, assuming the Poisson case the expected percent (%) coefficient of variation for the number of “in” trees observed between plots (due only to sampling variation and not to real change in underlying basal area) can be estimated by:

$$CV_{\bar{N}} = 100 \times \frac{\sin(\alpha/2)}{\sqrt{BA}} (1 + C_d^2)^{1/2} \quad (\%)$$

That is, the larger the wedge angle relative to the BA the higher the CV and vice versa. If the wedge angle is chosen so that there is an expectation that about 6 trees will be found the expected CV is 41% for a single plot if the tree sizes are not very variable. This may be sufficient for some inventory purposes but is a bit high for the EVI validation work given that many other factors will be present to increase variance. With an expectation of 12 trees the expected CV (assuming small variation in tree size) is less than 30% for a single plot (which is attractive) but each plot will take longer to complete as it is likely some trees will be well away from the plot centre. When the tree diameters vary a lot there is even greater need to sample more widely by decreasing the wedge angle.

However, for larger numbers of trees (smaller wedge angles for a given BA) other issues arise. Basically, the above theory assumes that the trees have a Poisson density *and* that all of the “in” trees are visible. As the number and range to the “in” trees becomes greater (for high BA and/or small BAF) the potential for trees to be hidden by others increases and decisions at the margins becomes harder. The best option is to keep the expected number per plot reasonable (perhaps 6-10) but not too great and have a number of plots spaced at about twice the effective radius of the plot. The “effective” radius can be taken as the “limiting” distance for a tree of average size. This can usually be estimated for the first plot taken at the site centre.

The “limiting” distance to a tree is  $Z_j$  above and if the measured distance is greater than this the tree is NOT truly an “in” tree. The distance can also be expressed in the form:

---

<sup>5</sup> Plantations will tend to be semi-regular and even in natural forests there will be departures from a random distribution. Hence, the effects of non-Poisson tree locations needs to be assessed (e.g. from previous studies!).

$$Z_c = \frac{D}{2\sqrt{BAF}}$$

In cases where there is uncertainty as to whether a tree is “in” or not it is therefore best to measure the distance to a tree and its DBH. In the case of an EVI validation site the distance and DBH are measured for all apparently “in” trees. The data can therefore be edited later.

The Relaskop method is a forest sampling method that tends to select trees of interest in forestry and for biomass studies. However, the form of its sampling is systematic and well defined and if other measurements (such as tree type and height, green height, crown openness, crown diameter etc) are made on the “in” trees it is possible to allow for the variable probability of sampling and obtain unbiased estimates for those other parameters over the forest stand and also provide estimates of their precision. This makes the technique complete as a design for forest measurement. How this allowance is made is described in the later section on site statistics.

## 11.2 Units

Units can be an issue. In the above, the units are assumed to be consistent in that DBH and limiting distance are the same units (such as *m*) and BA is unitless such as *m*<sup>2</sup> per *m*<sup>2</sup> etc. This is not the practical case where it is useful to use “normal” units for each component of the measurement and data ranges that are in “ordinary” numbers (such as 3.25 rather than 6.4571x10<sup>-7</sup>).

The Relaskop we used at the first site at Tumbarumba was North American and sought BA in units of sq ft per acre. The wedge angle settings (or, equivalently, the BAFs) are expressed as the BA per “in” tree at 5, 10, 20 and 40 sq ft per acre (per “in” tree). So, the number of “in” trees is multiplied by the setting to get the BA.

To distinguish these from the unitless BAF above we will call them *BAF<sub>u</sub>* factors (“u” for unit) and write the relationship as:

$$BAF_u = H_u \times BAF$$

where *H<sub>u</sub>* is the number of tree trunk cross-sectional area units in one base forest area unit. Typically, this would be sq ft per acre (43,560) for North America and sq m per ha (10<sup>4</sup>) for Australia and other metric countries. Units enter into the calculation of the limiting distance factor, which in unitless terminology can be written:

$$Z_c / D = \frac{1}{2\sqrt{BAF}}$$

For example, if the *BAF<sub>u</sub>* is in terms of sq ft per acre, the DBH in cm and the limiting distance wanted in metres the factor is:

$$Z_c(m) / D(cm) = \frac{1}{200} \sqrt{\frac{H_u}{BAF_u}}$$

In this case,  $H_u$  is 43,560 sq ft/acre. The following Table lists some of the factors for the set of  $BAF_u$  values used in the US Relaskop:

$BAF_u$ (ft <sup>2</sup> /acre)	BAF	$BAF_u$ (m <sup>2</sup> /ha)	$Z_c$ (ft)/D(in)	$Z_c$ (m)/D(cm)	$\alpha/2$ (deg)
5	1.1478E-04	1.1478	3.89	0.4667	0.614
10	2.2957E-04	2.2957	2.75	0.3300	0.868
20	4.5914E-04	4.5914	1.94	0.2333	1.228
40	9.1827E-04	9.1827	1.38	0.1650	1.737

Similar tables can be set up to convert between units and measurements made by Australian or European instruments for comparison with US data.

### 11.3 Site Protocols for EVI validation

The sites where the Relaskop were used for EVI validation used the following activities:

For each plot, the “in” trees are determined from the centre point using the Relaskop. If the decision is uncertain the distance to the tree and DBH can be measured to test it. “In” trees were marked with a number using a spray can starting from the north and working clockwise. Trees that were also “in” trees at one or more other plots were noted. The field notes could obviously also note species if relevant or any other information about the “in” trees. In our case, for “in” each tree in the plot, we measured:

1. Distance to the tree from the centre measured to the half point of the tree trunk at the side of the trunk and at breast height (1.3m);
2. DBH at the same height as the distance to the tree and perpendicular to the trunk axis;
3. Other people visit the “in” trees with a sonic range finder to measure tree height to top of the crown, height to base of crown (start of branching and foliage), crown diameter in two directions (major axis and its perpendicular) and crown factor or within-tree cover (fraction of sky covered when looking vertically up through the crown).

The use of a team of three people has worked well and is fast. If the sonic target is at the centre of the plot the distances can also be done from the tree side.

### 11.4 Output site statistics

The BA and its variation is known from the plots. If the mean (RMS) DBH is established then in principle the density and size can be separated. However, the mean over the “in” trees is a biased estimate for the DBH. To retrieve an unbiased estimate the effects of the sampling need to be taken into account.

Measurements taken for the “in” trees can be considered as samples from a variable probability scheme where the probability of selection is proportional to the contribution to the BA – or  $D^2$ .

The proof of this is quite straightforward since if the density of trees with diameter  $D$  is  $\lambda_D$  then the number of trees with this diameter among the “in” trees is:

$$\begin{aligned} N_D &= \pi Z_C^2(D) \lambda_D \\ &= \frac{\pi}{4BAF} D^2 \lambda_D \\ \lambda_D &= \frac{4BAF}{\pi} \frac{N_D}{D^2} \end{aligned}$$

That is, if  $p(D)$  is the proportion of trees with diameter  $D$  (the histogram of diameters) then it follows that in expectation:

$$\begin{aligned} \lambda_D &= p(D) \bar{\lambda} \\ p(D) &= \frac{4BAF}{\bar{\lambda} \pi} \frac{N_D}{D^2} \end{aligned}$$

An alternative way to express this is that if  $m_j$  is a data value at tree  $j$  for a plot of  $N$  “in” trees we have that the value for the tree in the (biased) sample contributes to the histogram of values in the underlying population in proportion to:

$$q_j = \frac{1/D_j^2}{\sum_{k=1}^N 1/D_k^2}$$

The mean and variance estimates are then:

$$\begin{aligned} \bar{m} &= \sum_{j=1}^N q_j m_j \\ \sigma_m^2 &= \frac{N}{N-1} \sum_{j=1}^N q_j (m_j - \bar{m})^2 \end{aligned}$$

That is, small trees have high weight in the estimate so it is important to ensure no small trees (in fact, *no* trees other than possibly those less than some very small minimum size (e.g. 3 cm DBH)) are missed in the field.

For the case of the mean RMS diameter estimate we have the interesting result that:

$$\begin{aligned}
 D_{rms}^2 &= \sum_{j=1}^N q_j D_j^2 \\
 &= \frac{N}{\sum_{j=1}^N 1/D_j^2}
 \end{aligned}$$

Hence, for each plot:

$$\bar{\lambda} = \frac{4 \times BA}{\pi D_{rms}^2}$$

It is also possible to consider the distribution of distances to the “in” trees or perhaps “all” trees to obtain ways to separate density and size.

If the mean and standard deviation or coefficient of variation as well as mean RMS DBH are known it is possible to model the distribution of diameters as (for example) a Lognormal distribution. Tree height is also often modelled as a Lognormal distribution and from this a confirmation of parameters such as “Predominant Height” can be made. However, as a note of caution, in most cases the relaskop wedge angle is kept large enough so that the number of “in” trees is about 10-15 at most. The statistics of these small plots are highly variable and it is possible for one or two very small trees to dominate the result. Smaller wedge angles create a lot of work but provide much better results.

## 12 APPENDIX 3: THE LIDAR EQUATION

To interpret the data from the EVI and the future ECHIDNA® instruments we will make use of its level of intensity recording and calibration. As discussed in the introduction (Section 2.3.1), the returned intensity that would be recorded for a hit from a wall perpendicular to the laser beam at range  $R$  from the instrument can be written:

$$I(t) = \Phi_0 \left( t - t_p - \frac{2R}{c} \right) \frac{\rho_t}{R^2}$$

where  $t_p$  is the time the peak of the outgoing laser pulse occurs,  $c$  is the speed of light and  $\rho_t$  is the (diffuse) target reflectance. That is, the return is a delayed copy of the outgoing pulse and the time difference between the peak of the pulse leaving and returning is:

$$t_{ret} - t_p = \frac{2R}{c}$$

$$R = \frac{c(t_{ret} - t_p)}{2}$$

For a general case where the beam may be intersected by a number of targets at varying angles the situation is more complex. First we usually express the return data in terms of apparent “range” ( $r$ ) where:

$$r = \frac{c}{2}(t - t_p)$$

When this is done, even the signal from a hard target appears to arrive from a dispersed interval of ranges, weighted by the pulse shape. But for a return from a wall we find:

$$I(r) = \Phi_0 (r - R) \frac{\rho_t}{R^2}$$

In this expression,  $\Phi_0$  has been re-expressed in the new range units. The expression for the general case can be written:

$$H(r) = \frac{K(r)}{r^2} p(g) \rho_t P_{Hit}(r)$$

$$I(r) = \int_0^\infty \Phi_0 (r - r') H(r') dr'$$

$$= \Phi_0 * H$$

The  $H$  function is the “unit response” for a very narrow unit pulse or an “ideal” return. The actual return is the  $H$  function convolved with the pulse. The function  $K(r)$  expresses a near range optical efficiency effect in which the return beam is not

focussed on the detector but overlaps or exceeds its collecting area. The optical efficiency reduces the measured return power and its functional form is established using modelling and vicarious calibration. The product  $p(g)\rho_t$  expresses the effective reflectivity of the scattering volume with  $g$  as an indication of the distribution of facets in the volume and  $\rho_t$  as the normal reflectivity of the elements.

The function  $P_{Hit}(r)$  is the probability of a clear path to range  $r$  but of a plant or other reflecting element being at range  $r$ . In a general canopy it can be related to the gap probability function ( $P_{gap}(r)$ ) that is the probability of there being a gap (or free path) from the instrument out to the range  $r$  in the given shot direction. The  $P_{gap}(r)$  is an important canopy property and is related to the probability of a “hit” at range  $r$  as:

$$P_{Hit}(r) = -\frac{\partial P_{gap}(r)}{\partial r}$$

The probability of a hit at the range is reduced by the presence of trees and foliage between the instrument and the target.

The EVI instrument was calibrated by using a range of trees at a range of sites from which the returns were assumed to be as from a “wall”. The inverse square relationship was validated in the data, the model for  $K(r)$  was validated and calibration coefficients expressing the equation in digital numbers were derived. For modelling, the calibration is applied to the pulse. Based on this work the data were analysed through modelling as described in the Report.

## 13 APPENDIX 4: TREE SIZE, BASAL AREA, FORM FACTOR & VOLUME

### 13.1 Basics and Summary

The EVI data – post cleaning and saturation repair – are in a form that can be used to measure tree stems for size, basal area at different levels (and therefore form factor) and (by implication) volume by size class. The data can be used in original spatial format or in projected formats of different kinds. The latter are certainly more convenient and directly applicable to compute form factors.

For example, Figure 13-1 shows the basic corrected EVI cube for a site near Mt Gambier (Springs Road EVI station 1). The geometry of the presentation is in the raw form and the EVI data are averaged over range to form the image shown in Figure 1. The central part of the image is the vertical view and each horizontal line is a scan of the upper hemisphere.

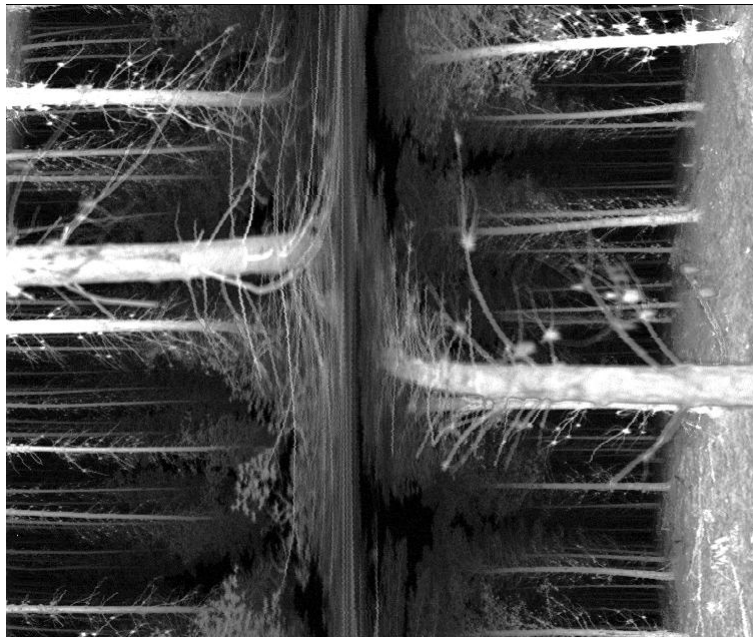


Figure 13-1: Raw data averaged over range

Figure 13-2 shows the same area in an “Andrieu” projection such that now the azimuth and zenith geometry has been enforced and many redundancies removed. The vertical dimension is zenith angle and the horizontal dimension is the azimuth.

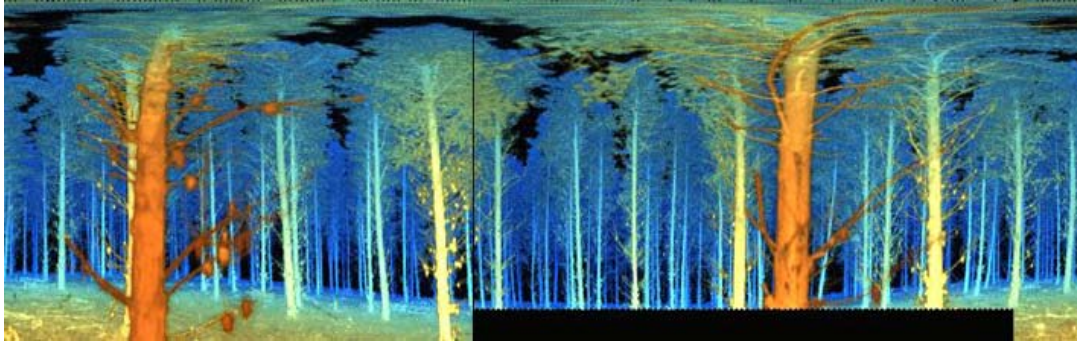


Figure 13-2: Projection to zenith (Y) and bearing (X) averaged over range

Figure 13-3 shows the same area in a “Cylindrical” projection where the vertical dimension is range and horizontal is azimuth. The slice shown is a horizontal slice at the height of the EVI and provides the basis for a “stem map” of range and bearing if the pulse traces can be reduced to trunks and intensities. The extension of trunk size in the range dimension is due to the width of the emitted laser pulse. The “bare” areas such as the one on the left side are where the data are blocked by topography. The value of the capacity to measure at different levels arises here, as trees will become apparent in this area for a higher elevation of data “slices”.

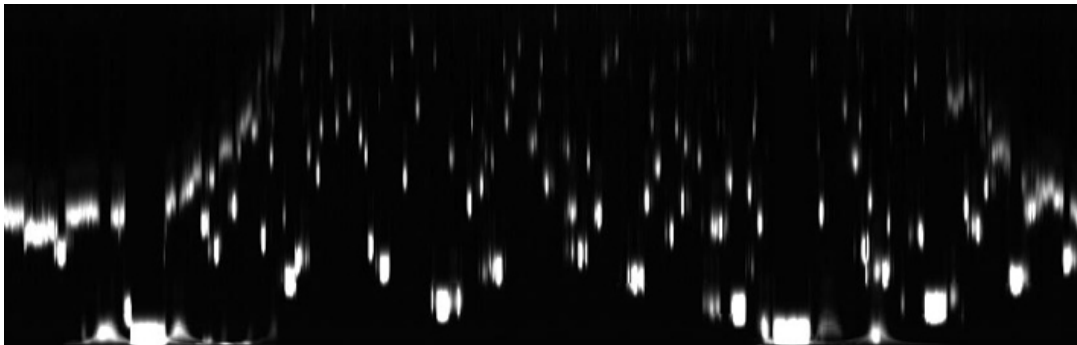


Figure 13-3: Slice across data at a constant height the same as the EVI.

The basic principles are the same whatever way the data are presented. A Lidar return from a tree trunk, when the beam is assumed to be fully within the angular span of the trunk from the EVI station, can be looked at as a reflection from a “wall” at a sloping angle to the beam and a specific range. We will describe the model for the image processing below and derive the “apparent reflectance”.

The objective is to identify the visible trees in the EVI scan. Since the EVI is usually at a fixed location not all of the trees will be visible (being obscured by other trees closer to the EVI) and some may be partly visible. We will therefore consider that there are three classes of partly visible tree. They are:

- (a) Fully visible tree. The full span of the trunk in a height range can be seen;
- (b) Partly obscured tree. Parts are obscured but the centre line of the trunk is visible. Note that this may occur from one or both sides;
- (c) Obscured trees. If the centre line is not visible the tree is ignored.

The basic image processing steps to find these trees, their ranges and their angular widths are as follows:

(i) Identify data points where the apparent reflectance is above a threshold (T1). It will be necessary to have an idea of the noise RMS and the ranges beyond the point where noise apparent reflectance is above some fraction of the threshold. This is an initial “sieve” and will most likely include a lot of “non-tree” material.

(ii) Identify “trees” as collections of such points. The most obvious criterion is vertical continuity. Other criteria for “tree” need to be intelligent and flexible. For example, significant returns at greater range in the same shot may exclude a point and rapid changes with height will indicate branch material rather than trunks. The full waveform in range/time space corresponding to each tree return should also be retained for further analysis. A classification mask for the peak positions on the waveforms is a useful output at this stage. Partly obscured trees may need to be accepted at this point but classified as such. Obviously, having an adjacent (abutting) “tree” at closer range indicates tree hiding.

(iii) The tree waveforms can be checked to see that the FWHM is within expected bounds. The FWHM is the integral over the waveform divided by the maximum value at the peak. A hard “tree” return should have a similar FWHM to the outgoing pulse. At this stage the “tree” can be replaced by the trace of the locations of the waveform peaks, the ranges and bearings to the peaks and the values at the peaks – and output as an image. The “central” return is hopefully the maximum and has a special value so that it needs to be identified specially. If a partly obscured tree has an identifiable maximum then that point may be taken as an identified “central” hit.

(iv) Using the modelling to be derived below, trees should be “clipped” at the edges to where the peak value falls below a given fraction of the value of the central return. It is important, however, that the clipping is not too severe. For each “tree” this defines an azimuthal span which is the span in central azimuths between the first and last “tree” pixels plus the width of the Instantaneous Field of View (IFOV, usually expressed in mrad). The IFOV is added to allow for the width of the beam. Alternatively, an interpolation can be used based on the models discussed later.

The geometry involved in this image processing is discussed below. For partly obscured trees the azimuthal span is not that of the tree but needs to be estimated at some stage based on the mean size or the smallest tree that fills the space if that is bigger. Useful but partly obscured trees are those such that the tree “centre” can be reasonably estimated. If it is not clear that the centre is being sensed then the tree is “obscured” rather than “partly obscured”.

For the trees identified the main things that may be useful to record are therefore:

- (1) Range and bearing to the central point of the trunk at the height being used;
- (2) The azimuthal span of the trunk (i.e. the span filled by the Lidar beam,  $\phi_{span}$ );
- (3) A classification of type (fully visible tree, partly obscured, obscured etc);
- (4) The apparent reflectance values (based on peak value or pulse integral or both estimates), and possibly ranges and bearings for the pixels across the span.

The equations behind the settings are to be derived below and then the main methods derived and described. As a quick summary they involve:

(a) Number of trees (tree “centres”) apparently within range “R” as a function of “R”. This may, by itself, provide estimates of basal area, mean diameter and stem density but possibly only some parameter combinations will be well resolved. It will be used for “consistency” checking in the final estimates;

(b) A number of “Relaskop” estimates of basal area based on the “in” trees defined by  $\phi_{span} > \alpha$  for various critical angles, or wedge angles,  $\alpha$ . Basal Area Factors (BAFs) which are modified for occlusion for the critical angles will be defined providing basal area estimates for each level in the canopy used for the analysis;

(c) Use of the diameters based on the azimuthal spans of the “in” trees to estimate mean and standard deviation of the diameters. The data can be corrected to estimates of site mean and Standard Deviation (SD) using generalisations of the normal Relaskop methods described elsewhere.

Tree heights are not usually estimated by individual tree, however, it can be imagined that if the data have been projected to radial distance and height coordinates then a “cylinder” centred on the corrected point of the tree centre (after tree diameter is known) and roughly an expected crown diameter wide can be used for a range corrected “profile” and height (possibly both tree height and bole height) estimated from percentage points above noise threshold. “In” trees will generally be better identified and not as likely to be wholly or partly obscured as some others so that may work quite well. Again, the bias from using “in” trees can be removed to obtain mean and variance of the tree heights for the stand or the mean can be used directly as a “Lorey” height. If needed in allometry, Predominant Height can also be estimated statistically from this information.

Assuming consistency between the different “Relaskop” results (for  $\lambda\bar{D}$ , BA, and mean and SD of diameter), assuming some form-factor (which may be estimated from EVI data as described later), assuming some height estimate is available (possibly just the site average) and that the diameters are lognormally distributed then it is possible to provide estimates for:

- Basal area by size class;
- Volume by size class; and
- Stem density by size class.

The rest of this document provides material to help with the thresholds and decisions involved in achieving this end and discussions of the materials needed to analyse the data to this level.

## 13.2 Identifying the angular spans of trees

### 13.2.1 Lidar return model

The projection shown in Figure 13-3 has the potential to provide tree sizes and basal area as a function of height – which can provide volume estimates or mean taper (form factors) at plot or stand level. The primary means to do this is to estimate the ranges to trees and the angular span as viewed from a position at or above the EVI station but in an effective “height slice” above the ground

We will initially assume the scan is horizontal and the tree is at range  $R$  and straight and vertical with diffuse (Lambertian) reflectance denoted  $\rho_t$ . In this case, the modelled lidar return ( $I_t$ ) may be described as a function of time by the equation:

$$\begin{aligned} I_t(t) &= \frac{K(R)}{R^2} \Phi\left(t - t_0 - \frac{2R}{c}\right) P_{\text{int}} \langle \cos \psi \rangle \rho_t \\ &= \frac{K(R)}{R^2} \Phi\left(t - t_0 - \frac{2R}{c}\right) \rho_{\text{app}} \\ \rho_{\text{app}} &= P_{\text{int}} \langle \cos \psi \rangle \rho_t \end{aligned}$$

In this equation:

- $R$  is the range to the target;
- $K(R)$  is the close range efficiency function;
- $\Phi(t)$  is the calibrated power of the pulse at time  $t$ ;
- $t_0$  is the time position of the peak of the outgoing pulse (zero range);
- $\rho_t$  is the normal tree reflectance (e.g. 0.45 to 0.55);
- $P_{\text{int}}$  is the normally projected proportion of the beam intercepted by the trunk;
- $\langle \cos \psi \rangle$  is the average cosine of the angle between the Lidar beam and the normal to the trunk over the intercepted beam;
- $c$  is the speed of light.

Within the trunk,  $P_{\text{int}} = 1$  and it is included to show that this return intensity will drop very fast at the edge of the trunk as the amount of the beam intercepted is reducing as well as the cosine continuing to decrease.

Time and range are assumed related according to:

$$r = \frac{c(t - t_0)}{2}$$

It is possible therefore to express the Lidar equation as a function of an “apparent” range as:

$$I_r(r) = \frac{K(R)}{R^2} \Phi_0 (r - R) \rho_{app}(R)$$

Because the EVI pulse is quite broad in time it therefore appears in the return data as being distributed in range – even for a target that is a solid “wall”. This is shown in Figure 13-3 by the vertical “smear” of the targets. By convention we have taken the time at the peak of the pulse as it leaves the EVI as zero EVI time and range. In the following it is assumed that the peak of a return from a hard object that contains the whole pulse can be associated with it the value of the peak return of the waveform at (true) range  $r = R$ ).

### 13.2.2 Measuring the angular span

A shot that is at one edge of the tree but still fully within the trunk is an important edge point to locate. It can be modelled as one in which the central azimuth is IFOV/2 back from the extreme edge azimuth. The objective is to identify the shots that are all “within” the trunk and to assume that those at either end of the set of “tree” returns are critically within the trunk in that the outer edge of the beam is just grazing the trunk tangent. The two end shots defined above will have centre azimuths and an azimuthal span between them. To get the true angular span of the tree (assuming the end shots are right out to the edges) you add the beam IFOV to this span. Estimating the full angular span is the image-processing task.

The geometry and notation being used is shown in Figure 13-4. The range to the central point will be denoted  $R$  and it is assumed that the tree has diameter  $D$ . The EVI scan is marked “EVI” and the outer tangents to the tree define the (true) full angular span of the tree from the EVI station.

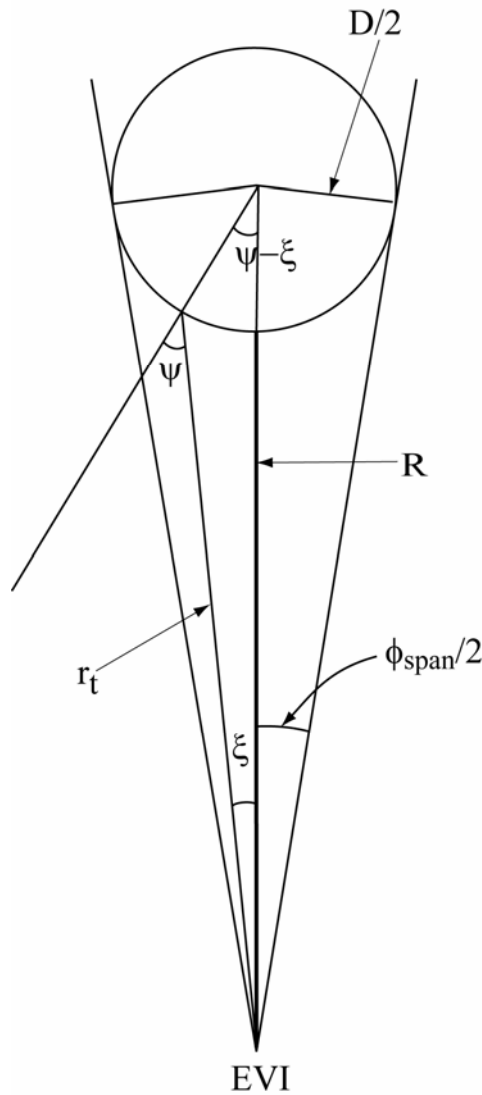


Figure 13-4: Geometry of EVI trunk returns

For a given shot, the angle between the normal to the tree and the shot is denoted  $\psi$  and the angle between the shot and the path to the central point on the trunk is denoted  $\xi$ . The complete angle between the tangent shots to the trunk is denoted  $\phi_{span}$ . At the “central” point the Lidar return and the apparent reflectance will be maximal. For a model tree of the kind shown in Figure 13-4 which is close enough to be resolved by a number of pixels<sup>6</sup> we would have for each shot, the ratio of apparent reflectance to that at the maximum (nearest front and central) point of the tree:

$$\frac{\rho_{app}}{\rho_{max}} = \frac{\langle \cos \psi \rangle}{\langle \cos \psi \rangle_{max}}$$

$$\langle \cos \psi \rangle_{max} \approx 1$$

<sup>6</sup> Trees spanned by fewer than three pixels are not going to be “in” trees for the resolutions we are working with.

For pixels away from the centre the average cosine could be taken as the cosine at the azimuth at the pixel centre. Taking the cosine at the centre of the range as an estimate of the average and assuming as in all of these cases that the scan is horizontal and as well that the “tree” is a nice vertical cylinder with constant diameter  $D$  we can derive a number of useful quantities.

The first thing to look at is the way the apparent reflectance ratio may change in an actual case. Using a 5 mrad EVI IFOV, then for a 40 cm DBH tree at 10 m range (to the front of the tree) we find that a plot of pixels that respond to the EVI may look something like Figure 13-5:

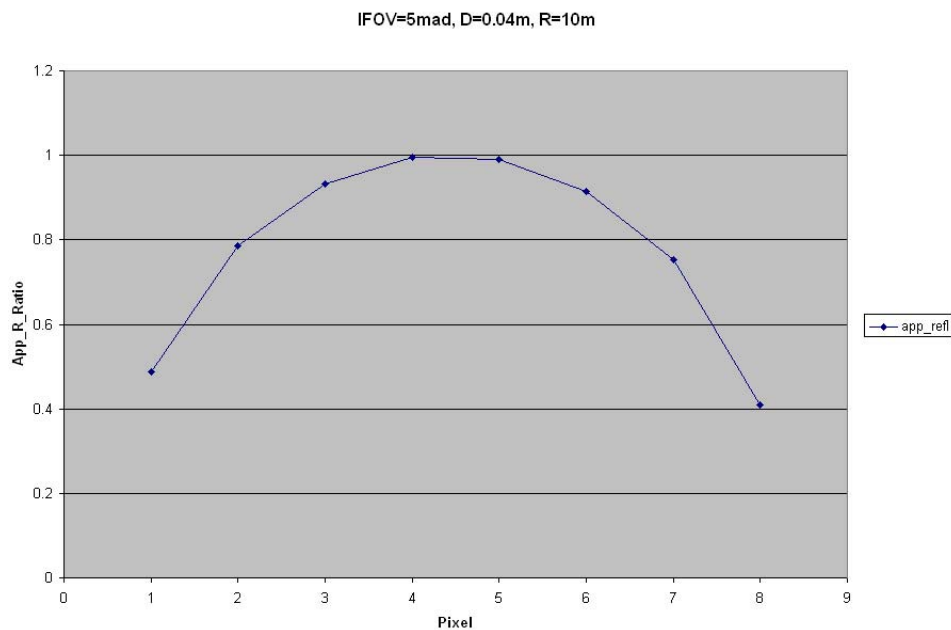


Figure 13-5: Plot of the apparent reflectance ratio across the EVI scan

Using the angle and distance definitions of Figure 13-4, this plot has been derived from the formulae:

$$t = \frac{D/2}{R + D/2} = \sin(\phi_{span}/2)$$

$$\sin \psi = \frac{\sin \xi}{t}$$

$$\cos \psi = \cos\left(\sin^{-1}\left(\frac{\sin \xi}{t}\right)\right)$$

The angle at the centre of the “pixel” is assumed to be appropriate for the estimate.

In addition to the change in intensity we can compute the variation in range across the scan as well. This is found from:

$$r_T = (R + D/2) \left( \frac{\sin(\psi - \xi)}{\sin \psi} \right)$$

$$= D/2 \left( \frac{\sin(\psi - \xi)}{\sin \xi} \right)$$

The corresponding trace of ranges is shown in Figure 13-6.

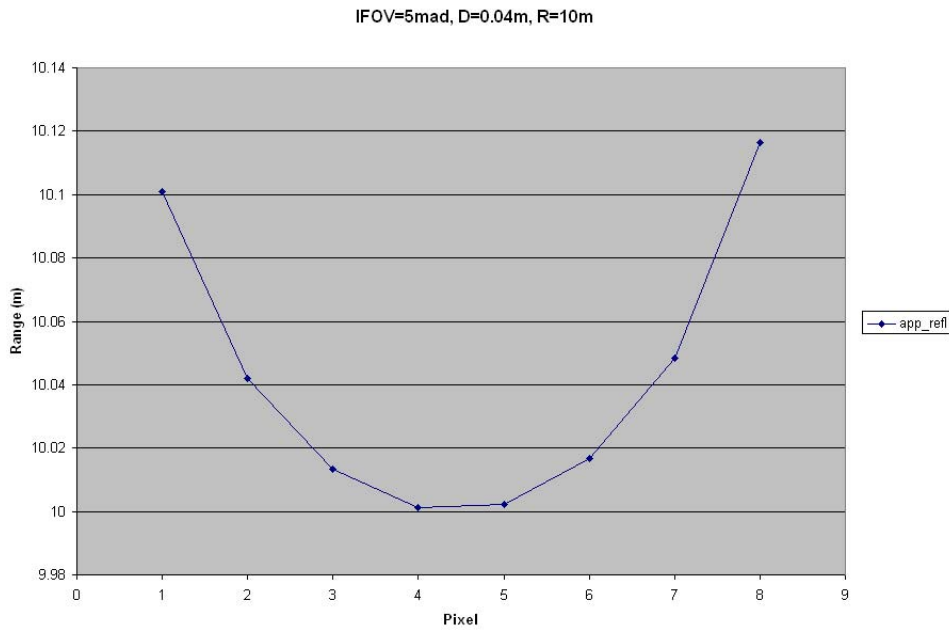


Figure 13-6: Plot of the range to the tree across the scan of the tree.

Obviously, at the resolution of EVI (about 7.5 cm precision) there is not much change in the range (in this case about 10 cm) – but there was quite a lot of variation in the intensity. It is best therefore to concentrate on using intensity to measure the span of the data and use the angular span for diameter determination and to determine “in” trees.

Assuming that the full angular span (span between the nominal bearings of the end shots plus the IFOV) is truly  $\phi_{span}$  as defined by the two tangent points across the tree, then it follows that if the range to the centre of the tree surface nearest the EVI is R and the tree diameter is D then the relationship between the three is:

$$t = \sin(\phi_{span} / 2) = \frac{D/2}{R + D/2}$$

$$D = 2R \left[ \frac{t}{1-t} \right]$$

We can use this to get diameters but in order to do it we need to determine the span precisely from the image data. One way to set the threshold is to note that at the centres of the two extreme and fully *within-trunk* intercepts we find that if IFOV

denotes the angular span of the EVI shot then the ratio of the value at the edge to the central value is given by:

$$\frac{\rho_{app,edge}}{\rho_{app,max}} = \cos \psi_{edge}$$

$$= \cos \left( \sin^{-1} \left( \cos(IFOV / 2) - \frac{(1-t^2)^{1/2}}{t} \sin(IFOV / 2) \right) \right)$$

This seems complicated but can be tabulated. It depends only on the ratio of D to R which obviously changes with the tree size and range. The thresholding will therefore need to be careful and adaptive.

To demonstrate the expected way the ratio changes at the edges, the following plot (Figure 13-7) shows the edge value for typical ranges up to 40 metres, an IFOV of 5 mrad and three tree diameters – 15cm, 30cm and 45cm. The smallest tree reaches the limit where there is only one pixel IFOV in the span of the tree at about 28m range and is therefore only plotted to that range.

Close trees fall off to much less in comparison with the central value than do far trees and larger trees show more fall-off than smaller trees – that is in each case as the ratio of D/R increases. But the fall away in signal is much sharper after the edge is reached as the proportion of the beam intercepted reduces, and as well, the mean cosine in the intercepted area heads more rapidly to zero. Because of the combination of these effects the edge should be quite distinctive. The SNR is also very high in the near range, which helps as the fall-off is greater in this region and more of the trees will be “in” trees.

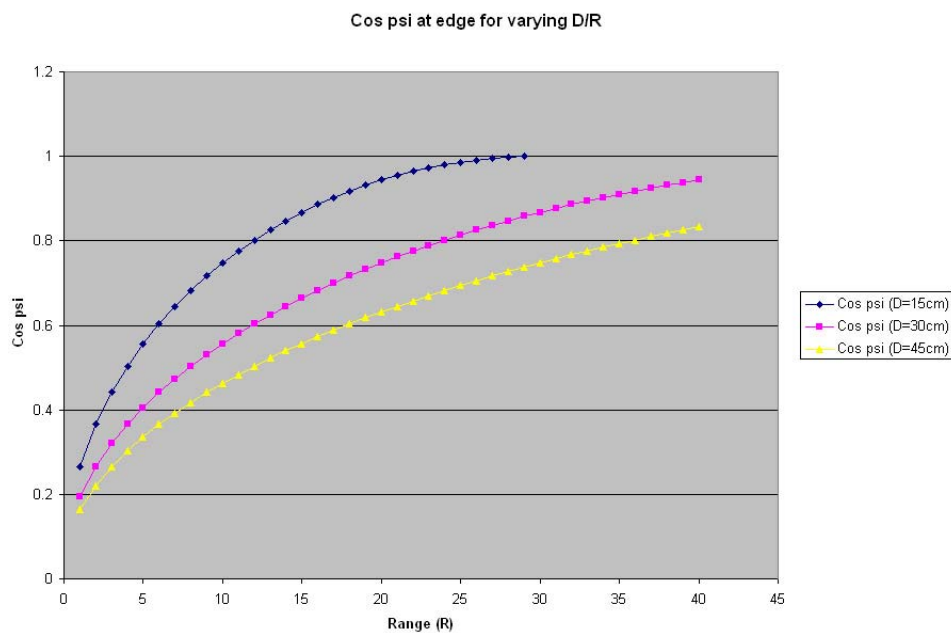


Figure 13-7: Plot of the reduction in central (maximum) value at the edge – greater reduction indicates the pixel is “off the tree”.

Since the threshold setting used to determine the edge will depend on the tree size it may be possible to use an initial threshold to estimate the span and hence an estimated diameter and iterate to obtain a better threshold. But this needs to be investigated.

### 13.2.3 EVI “Relaskop” methods

The formulae derived above can also be used to look at the angle span of trees as a function of range and size. This is shown in Figure 13-8 which has nothing particularly to do with EVI but only to normal Relaskop theory. It plots the angular span of trees of different size as a function of range and also shows wedge angles of 1 and 2 degrees to indicate the distances out to which the trees of a given size will be “in”.

As noted above, the tree sizes (diameters and possibly heights) for the “in” trees at possibly varying wedge angles can be used to obtain the site estimates without a bias due to selecting the “in” trees. It also allows us to base the information on trees that are better resolved in the EVI data.

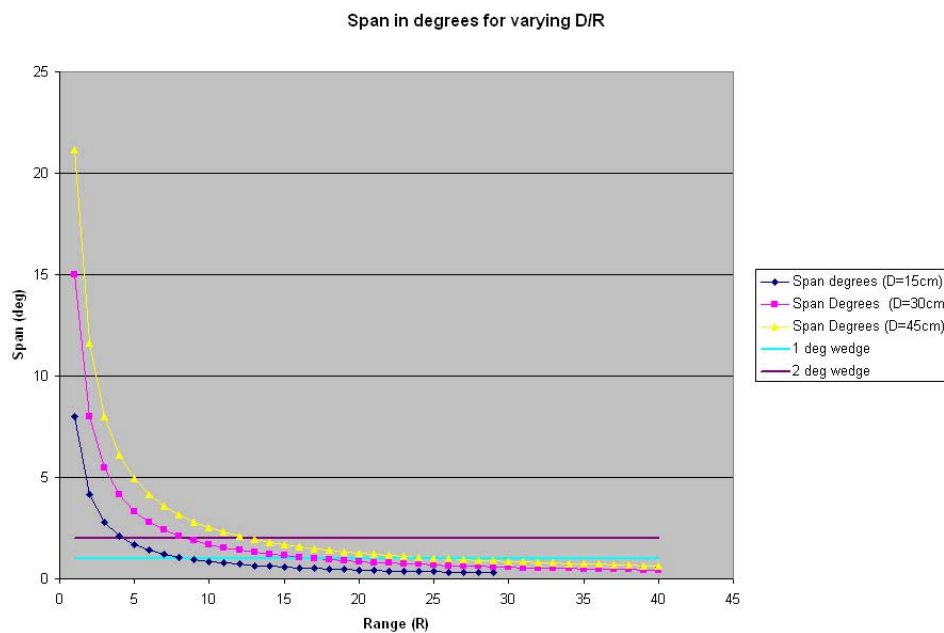


Figure 13-8: Plot of the angular span of trees as a function of size and range. The wedge values of 1 and 2 degrees show range to furthest potential “in” tree.

An alternative presentation for the same data is shown in Figure 13-9 where we have computed the number of EVI IFOVs (in this case 5 mrad IFOVs) in the span as a function of tree size and range.

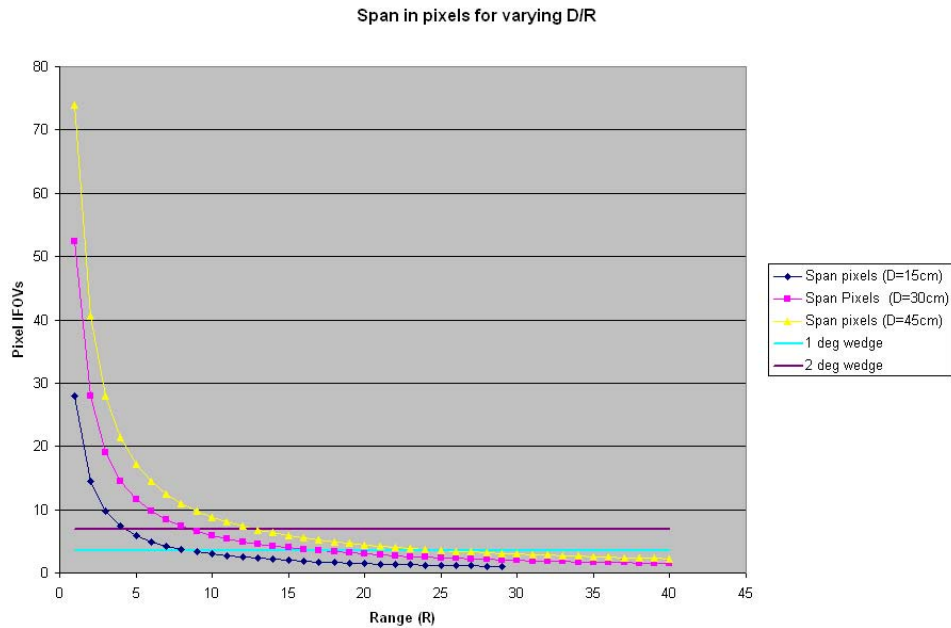


Figure 13-9: Plot of the angular span of trees as a function of size and range. The wedge values of 1 and 2 degrees show range to furthest potential “in” tree.

This presentation of the data indicates where there are many pixels to use and to locate and where the determination of width will therefore be more accurate. This seems to be the case if only the “in” trees are used – even at 5mrad resolution. At 3mrad resolution the results may be even more accurate – we need to determine by how much. Perhaps a “wedge angle” between 1 and 2 degrees will be quite useful for the EVI at 5mrad. The advantage of a larger angle is that the “in” trees will be closer to the EVI so that obscuring is less likely.

The key image processing issues are to estimate the “trees”, to classify them as visible, partly obscured or obscured, estimate the full angular span and identify and count the tree centres. None of these is easy but if they are done then the work described here can complete the task.

### 13.3 Computing the Basal Area estimates

#### 13.3.1 The standard “Relaskop” method

The “in” trees are those with angular span larger than a critical angle determined by the wedge size. In the standard relaskop method, Basal Area is derived as the number of “in” trees multiplied by the basal area factor (BAF) for the wedge size. The computation of the BAF values is simple to describe and will help to introduce the next section.

The geometry of Figure 13-4 is appropriate to this situation if the “EVI” point is taken as the point where the relaskop is located. If the half angle of the relaskop (or “wedge” angle) is denoted  $\alpha/2$  then for a given tree diameter  $D$  there is a distance

where the relaskop view just matches the angular span of the tree. This distance is the critical distance for a tree of a given size. It is best to compute this to the tree centre (rather than the front edge – which is more useful for EVI data) and so:

$$R_{crit} = \frac{D/2}{\sin(\alpha/2)}$$

For no obscuring (all trees can be seen), the expected number of trees for a given size that will be seen within this distance (see Appendix 2) is:

$$N_D = \lambda_D \pi R_{crit}^2$$

This is the total number of trees of the given size that will be “in” trees at the given wedge angle. Substituting the expression for the critical distance we have:

$$\begin{aligned} N_D(\alpha) &= \lambda_D \frac{\pi D^2 / 4}{\sin^2(\alpha/2)} \\ &= \frac{\lambda_D A_D}{\sin^2(\alpha/2)} \\ &= \frac{BA_D}{\sin^2(\alpha/2)} \end{aligned}$$

Taking this over all of the tree sizes weighted by the size distribution leads to:

$$\begin{aligned} \lambda_D &= p(D)\lambda \\ N(\alpha) &= \int_D \frac{\lambda_D A_D}{\sin^2(\alpha/2)} dD \\ &= \frac{\lambda}{\sin^2(\alpha/2)} \int_0^\infty A_D p(D) dD \\ &= \frac{\lambda \bar{A}}{\sin^2(\alpha/2)} \\ &= \frac{BA}{BAF} \\ BA &= N(\alpha) \times BAF \end{aligned}$$

This simple and convenient result provides a basal area estimate over the (arbitrary) size distribution of the tree sizes. The problem is that trees tend to obscure those behind them. In the field this leads to people moving around near the central site to locate “in” trees. This can lead to inaccuracies. Using a larger wedge size selects towards the larger and closer trees and they tend to be visible. However, the variance in the BA estimate will be higher. For the EVI it is not possible to move around to look behind trees – unless the whole EVI is moved and a new scan is taken. This is possible but it would be nice if the obscuring could be taken account of in the estimate.

## 13.3.2 Obscuring and a model for its effect

### 13.3.2.1 The number of trees apparently within a range “R”

The model we will use is an approximation but may be good enough to describe the situation and allow basal area estimation with obscuring. Its first step is to estimate the number of trees “apparently” within a distance R – where “within” means the tree centre is within R. As used above and for no obscuring this will simply be  $\lambda\pi R^2$ . This can be written:

$$N = 2\pi\lambda \int_0^R r dr$$

However, with obscuring, we can think of the effect as meaning that at range “r” there will be sections of the circle that are blocked and that these blank out the areas beyond. The unblocked areas are the “windows” through which more trees can be sensed. Since our model for the attenuation of view is that:

$$P_{gap}(r) = e^{-\lambda\bar{D}r}$$

it follows that we could estimate the number with allowance for this (and taking a sighting to mean the “centre line” of the tree can be sensed) as:

$$\begin{aligned} N(R) &= 2\pi\lambda \int_0^R r e^{-\lambda\bar{D}r} dr \\ &= \frac{2\pi}{\lambda\bar{D}^2} \left[ 1 - e^{-\lambda\bar{D}R} (1 + \lambda\bar{D}R) \right] \end{aligned}$$

This has the surprising implication that there would be a finite number of trees you can “see” even to infinite range (at least the centre lines if not the complete trunk width) and that the number is inversely proportional to the Basal Area.

$$N_{Total} = \frac{\pi^2 / 2}{BA}$$

It also suggests that if this number were computed from EVI data as a function of R and the model fitted then there would be a separation possible between  $\lambda$  and  $\bar{D}$ . It would not actually provide an estimate for Basal Area (BA) immediately since for an arbitrary tree size distribution:

$$\begin{aligned} BA &= \lambda \frac{\pi}{4} \int_0^\infty D^2 p(D) dD \\ &= \lambda \frac{\pi}{4} (\bar{D}^2 + \sigma_D^2) \\ &= \lambda \frac{\pi}{4} \bar{D}^2 (1 + C_D^2) \end{aligned}$$

where  $\sigma_D$  is the standard deviation and is the  $C_D$  coefficient of variation of the diameter distribution. Hence, some idea of the variation of the sizes will also be needed to obtain BA in addition to  $\bar{D}$ . This will come up again as we derive the Relaskop formulae.

### 13.3.2.2 Obscuring by trees of the same size

Suppose for the moment that all trees have the same diameter (D). In this case the above expressions do provide BA (since  $C_D^2 = 0$ ) and in the case of the Relaskop formula we simply need to find the number of visible trees within the critical range as derived above. In this case we find that:

$$\begin{aligned}
 N_D(\alpha) &= \frac{2\pi}{\lambda D^2} \left( 1 - e^{-\lambda D^2 / 2 \sin \alpha} \left[ 1 + \frac{\lambda D^2}{2 \sin(\alpha/2)} \right] \right) \\
 &= \frac{2\pi}{\lambda D^2} (1 - e^{-t} [1+t]) \\
 &= \frac{\pi}{\sin(\alpha/2)} \frac{1}{t} (1 - e^{-t} [1+t]) \\
 t &= \frac{\lambda D^2}{2 \sin(\alpha/2)} = \frac{2}{\pi} \frac{BA}{\sin(\alpha/2)}
 \end{aligned}$$

For a given size D and wedge angle, the number of “in” trees visible becomes proportional to the function:

$$F(t) = \frac{1}{t} (1 - e^{-t} [1+t])$$

The general plot of F against t in Figure 13-10 indicates how the number of “in” trees that are visible changes with BA:

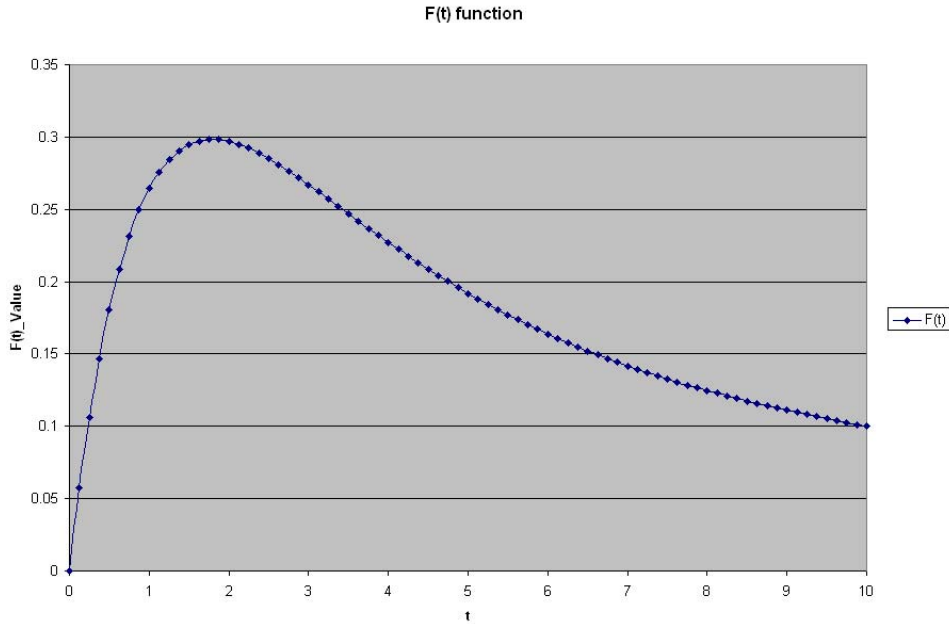


Figure 13-10: Obscuration function for trees of constant size

This plot shows how the number of “in” trees apparently reaches a maximum ( $t=1.792$ ) at some tree density (equivalently BA) and then decreases for higher densities. This implies that the solution of the angle count may have two values – one less than the peak and one above. However the solution above the peak is likely to correspond to an unrealistic BA e.g. a BA of  $50 \text{ m}^2$  per ha is quite high and using a wedge angle of  $2^\circ$  this situation would correspond to a  $t$  value of 0.182. The peak of the curve would, using the same wedge angle, correspond to a BA of more than  $480 \text{ m}^2$  per ha. This is not likely to be found in practice – in fact it may be very hard to get into or out of the forest in this case.

A more practical and encouraging plotting range would give the relationship in Figure 13-11 for the number of “in” trees against BA – compared with a traditional Relaskop (all trees assumed visible) plot. To scale the plots to these quantities requires setting the Relaskop wedge angle and an angle of 2 degrees has been used. The BA axis is in units of  $\text{m}^2$  per ha. Obscuring reduces the number of “in” trees but within the  $50 \text{ m}^2$  per ha range the difference in angle count is not huge. This plot still obviously goes to impractical densities.

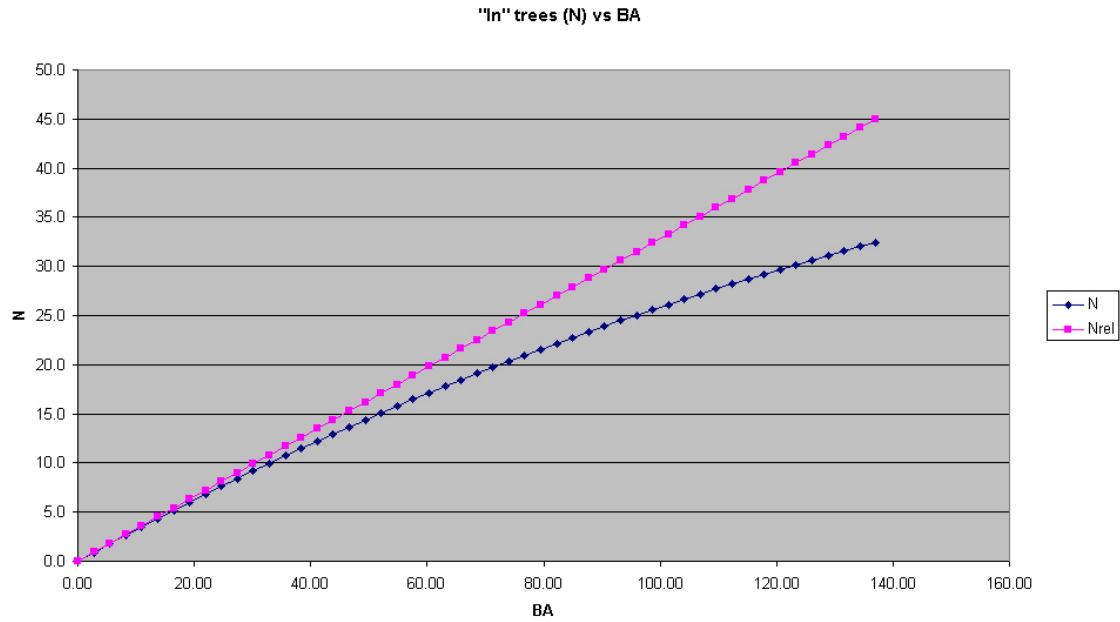


Figure 13-11: Number of “in” trees vs BA for 2 degree wedge and Obscured Model. Comparison with traditional Relaskop estimate added.

A polynomial approximation to the inverse function can be found with high accuracy over the practical range of the data ( $t \in [0,1]$ ) (using Horner’s scheme):

$$F^{-1}(y) = (a_0 + y(a_1 + y(a_2 + y(a_3 + y(a_4 + a_5 y))))))$$

- $a_0 = 0.000000$
- $a_1 = 2.157071$
- $a_2 = -3.884635$
- $a_3 = 93.745433$
- $a_4 = -477.251100$
- $a_5 = 1005.900655$

It follows that the new equation modified for obscuring and based on the practical range is:

$$BA = \frac{\pi}{2} \sin(\alpha / 2) F^{-1}\left(\frac{1}{\pi} \sin(\alpha / 2) N_D(\alpha)\right)$$

This suggests an approach in which, after all visible trees are measured the “in” trees are identified for a range of wedge angles, for each wedge diameter the diameters and the (bias corrected) mean and CV of the diameters are established. If the simple formula and the results of checking the number of trees apparently within a range as a function of range are all consistent then the above is used to get overall BA and density ( $\lambda$ ) for a variety of wedge angles and the result used to establish overall estimate for BA and tree size distribution. Finally these are used as described in the next section to obtain BA and by size class and (using the methods described

following that section) using estimates at different heights or allometry we can estimate timber volume by size class.

### 13.3.2.3 Obscuring in the general case

In the general case the approach needs to be a little different from the fixed size tree example. We will look at trees with the diameter  $D$  and note that the density associated with the trees of one size (class) is:

$$\lambda_D = p(D)\lambda$$

That is, the number of “in” trees in this size class will be the number of such trees with centres in the critical circle of radius  $R_{crit} = D/2 \sin \alpha$ . Within this circle there will be attenuation and we will assume that all of the trees contribute to the attenuation. That is, the number of “in” trees with diameter  $D$  that are expected to be visible will be (using the previous formula):

$$N_D = \frac{2\pi\lambda_D}{\lambda^2 \bar{D}^2} \left( 1 - e^{-\lambda \bar{D} D / 2 \sin(\alpha/2)} \left[ 1 + \frac{\lambda \bar{D} D}{2 \sin(\alpha/2)} \right] \right)$$

This number can then be summed (integrated) over all of the possible sizes of tree. The distribution has already been built in with the density. As a result we find for the total number of “in” trees:

$$\begin{aligned} N &= \frac{2\pi}{\lambda \bar{D}^2} \left( 1 - \int_0^\infty e^{-\lambda \bar{D} D / 2 \sin(\alpha/2)} \left[ 1 + \frac{\lambda \bar{D} D}{2 \sin(\alpha/2)} \right] p(D) dD \right) \\ &= \frac{2\pi}{\lambda \bar{D}^2} \left( 1 - \frac{2 \sin(\alpha/2)}{\lambda \bar{D}} \int_0^\infty e^{-t} [1+t] q(t) dt \right) \\ t &= \frac{\lambda \bar{D} D}{2 \sin(\alpha/2)} \\ q(t) &= p \left( \frac{2t \sin(\alpha/2)}{\lambda \bar{D}} \right) \end{aligned}$$

To go further we need some idea of the distribution function. Although we will make good use of the lognormal distribution later for now the next step will be based on assuming that the diameters have a *normal* distribution. In this case:

$$p(D) = \frac{1}{\sigma_D \sqrt{2\pi}} e^{-\frac{1}{2}(D-\bar{D})^2/\sigma_D^2}$$

$$q(t) = \frac{\lambda \bar{D}}{2 \sin(\alpha/2)} \frac{1}{\sigma_s \sqrt{2\pi}} e^{-\frac{1}{2}(t-\mu_s)^2/\sigma_s^2}$$

$$\mu_s = \frac{\lambda \bar{D}^2}{2 \sin(\alpha/2)}$$

$$\sigma_s = \frac{\lambda \bar{D}}{2 \sin(\alpha/2)} \sigma_D$$

Hence, developing the previous expression for N we get:

$$N = \frac{2\pi}{\lambda \bar{D}^2} \left( 1 - \frac{1}{\sigma_s \sqrt{2\pi}} \int_{-\infty}^{\infty} e^{-t} [1+t] e^{-\frac{1}{2}(t-\mu_s)^2/\sigma_s^2} dt \right)$$

From this we can derive the following expressions:

$$N = \frac{2\pi}{\lambda \bar{D}^2} \left( 1 - e^{-\frac{\lambda \bar{D}^2}{2 \sin(\alpha/2)} \left( 1 - \frac{1}{2} \frac{\lambda \sigma_D^2}{2 \sin(\alpha/2)} \right)} \left[ 1 + \frac{\lambda \bar{D}^2}{2 \sin(\alpha/2)} \left( 1 - \frac{\lambda \sigma_D^2}{2 \sin(\alpha/2)} \right) \right] \right)$$

$$= \frac{2\pi}{\lambda \bar{D}^2} \left( 1 - e^{-t \left( 1 - \frac{1}{2} t C_D^2 \right)} [1 + t(1 - t C_D^2)] \right)$$

$$t = \frac{\lambda \bar{D}^2}{2 \sin(\alpha/2)}$$

Finally, it should be noted that:

$$BA = \lambda \bar{A} = \lambda \frac{\pi}{4} \bar{D}^2 (1 + C_D^2)$$

$$\lambda \bar{D}^2 = \frac{4 BA}{\pi (1 + C_D^2)}$$

Hence:

$$N = \frac{\pi^2 (1 + C_D^2) / 2}{BA} \left( 1 - e^{-t \left( 1 - \frac{1}{2} t C_D^2 \right)} [1 + t(1 - t C_D^2)] \right)$$

$$= \frac{\pi}{\sin(\alpha/2)} \frac{1}{t} \left( 1 - e^{-t \left( 1 - \frac{1}{2} t C_D^2 \right)} [1 + t(1 - t C_D^2)] \right)$$

$$t = \frac{2 BA}{\pi \sin(\alpha/2) (1 + C_D^2)}$$

The above expression reduces to the previous one when  $C_D^2 = 0$ . However, the variation is not simply involved in other cases and so the expressions are rather messy.

If we compare the changes that occur in the relationship between the number of “in” trees and BA as there is variance added we find a situation illustrated in Figure 13-12:

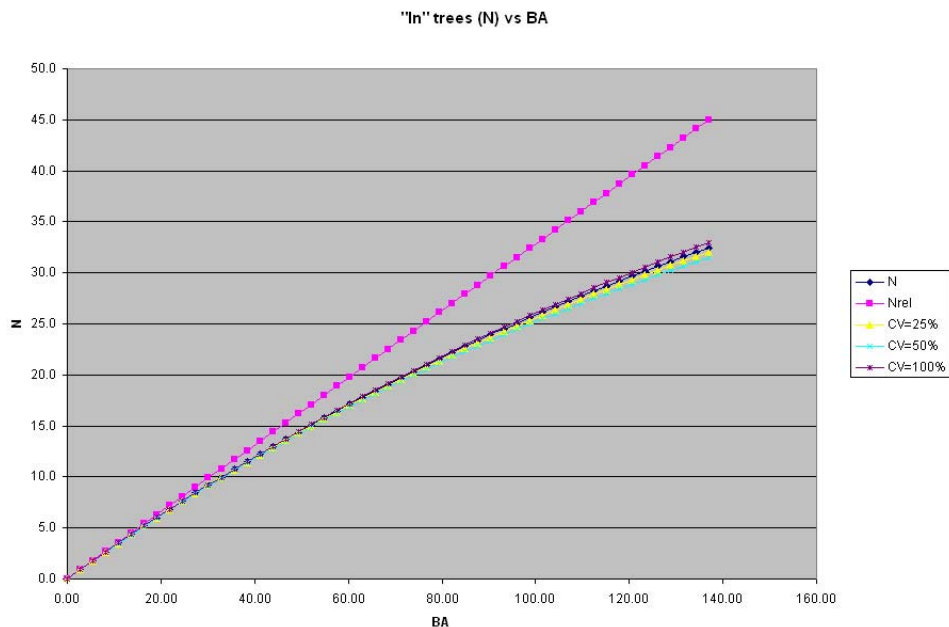


Figure 13-12: Number of “in” trees vs BA for 2 degree wedge and complete Obscured Model. Comparison with traditional Relaskop estimate and various values of CV.

It is clear from the Figure 13-12 in comparison with Figure 13-11 that the introduction of the CV has had only a small effect on the number of “in” trees and a negligible effect in the practical region up to BA of 50 m<sup>2</sup> per ha and little effect even at BA values of more than 100 m<sup>2</sup> per ha. This insensitivity occurs even for a CV of up to 100% - whereas most practical values for the CV of diameter will be less than 30%.

The conclusion seems to be that, unless the situation is extreme, the simpler constant size formula is quite adequate to provide an estimate for BA following the recognition and measurement of the “in” trees.

### 13.3.3 Estimating other parameters and complexities

With the sizes estimated it is possible to correct the locations of the tree centres and the ranges to the tree centres by adding  $D/2$ . With the visible trees (centre line visible) located it is possible to compute the number of trees apparently within a distance  $r$  of the EVI as described previously and test for consistency. The way to use the “In” tree data to compute a bias corrected mean and SD of diameter has also been described in Appendix 2.

It may be thought that not to use the range to each of the tree surface hits and the intensities of the collection is a waste. The span and range to a tree front centre should provide a good estimate as long as the threshold value is OK. However, the idea of using inversion of all these data – as well as the number within r in a single combined approach is tempting but maybe for the future – or at least when the time exists. At this time the variations in range are taken of some account in the development of the apparent reflectance. The data for Figure 13-6 do, however, suggest that the EVI will not resolve the variation in range for the range data to be very useful by themselves.

A complexity will occur when the site is not flat. Just as with a Relaskop, it is possible to take account of slope and topography but the way to estimate the local “DTM” needs to be fully established for this to be operational. Because the EVI scans down to a zenith angle of 108° it is possible to establish such a floor estimate. However, the processing still needs to be done. It may be necessary to undertake tree and non-tree recognition as a 3D operation to obtain the more complex measurements from the EVI data in sloping sites.

### 13.4 Basal area by size class

Total basal area is an important statistic. However, a more informative statistic is to disaggregate the BA by tree size class. Since the diameter distribution has been estimated as part of the process described this may be done in various ways. One way is to use a lognormal approximation to diameter distribution and the (bias corrected) mean and variance of the diameters obtained using the “in” trees.

Suppose that bias corrected estimates of the mean ( $\bar{D}$ ) and SD ( $S_D$ ) of the tree sizes (at EVI height) have been obtained and are consistent with changing wedge angle. We will assume that D is lognormally distributed with mean  $\bar{D}$  and coefficient of variation  $C_D$  where:

$$C_D = \frac{S_D}{\bar{D}}$$

$S_D$  is the (bias corrected) standard deviation of the distribution of D. The CV is often expressed as a percentage – i.e. the above multiplied by 100.

The lognormal distribution can also be characterised by the logarithm of D being normal with mean  $\mu_D$  and variance  $\sigma_D^2$ . We know in that case that:

$$\begin{aligned}\bar{D} &= e^{\mu_D + \sigma_D^2/2} \\ S_D &= \bar{D} \left( e^{\sigma_D^2} - 1 \right)^{1/2} \\ &= \bar{D} C_D\end{aligned}$$

That is, given the mean diameter and coefficient of variation of the diameter you can easily derive the mean and variance of the logarithm of the diameter. In terms of these, the mean cross sectional area of the trunks is:

$$\begin{aligned}\bar{A} &= \frac{\pi}{4} \left[ e^{\mu_D + \sigma_D^2} \right]^2 \\ &= \frac{\pi}{4} D_{eff}^2 \\ D_{eff} &= \bar{D} (1 + C_D^2)^{1/2}\end{aligned}$$

so that that  $D_{eff} \geq \bar{D}$ .

Conversely, to obtain the parameters of the lognormal distribution from the mean and SD of the diameters we have:

$$\begin{aligned}\sigma_D^2 &= \text{Log} (1 + C_D^2) \\ \mu_D &= \text{Log} (\bar{D}) - \sigma_D^2 / 2 \\ &= \text{Log} \left( \frac{\bar{D}}{(1 + C_D^2)^{1/2}} \right)\end{aligned}$$

This all comes together if there is a consistent estimate of basal area from the different “Relaskop” wedges and other data. It follows that:

$$\begin{aligned}BA &= \lambda \bar{A} \\ \bar{A} &= \frac{\pi}{4} \left[ e^{\mu_D + \sigma_D^2} \right]^2 \\ &= \frac{\pi}{4} \bar{D}^2 (1 + C_D^2)\end{aligned}$$

That is, the mean density of tree stems ( $\lambda$ ) can be found using this formula.

Moreover, if D is lognormally distributed as described above, the area of the cross section will also be lognormally distributed such that  $\log A$  will have mean  $\log \pi / 4 + 2\mu_D$  and SD of  $2\sigma_D$ .

It is therefore possible to estimate a set of N mean sizes such that size classes have mean size between given limits. The proportions of the trees within the limits ( $p_j$ ) can be computed as can the mean area and we have:

$$\begin{aligned}
BA &= \sum_{j=1}^N BA_j \\
&= \sum_{j=1}^N \lambda_j \bar{A}_j \\
&= \lambda \sum_{j=1}^N p_j \bar{A}_j
\end{aligned}$$

This allows the basal area to be disaggregated by size class.

If  $F(h)$  is the Form Height then the timber volume for the  $j$ 'th size class will be:

$$\begin{aligned}
V_j &= \lambda_j F(h_j) \bar{A}_j \\
&= \lambda (p_j F(h_j) \bar{A}_j) \\
V &= \sum_{j=1}^N V_j
\end{aligned}$$

That is, the density and partitioning of the density by size class can be done and the volumes by size class can be done as well. In the future, if the species of the “In” trees are known or can be inferred from EVI profiles then a species by size class frequency diagram – or Stand Table - can also be developed for the site. The accuracy, of course, is yet to be established.

The form height can be driven by a Stand Height curve (a height/DBH relationship) for the forest or estimated from EVI data as described below. The Stand Height provides what foresters mean by “structure” if size and age are related. This adds some complexity but nothing that cannot be accommodated with simple computing that can be done once and re-used. EVI may also be able to estimate tree height for the “In” trees as described before. If that works well then predominant height can be computed for the stand and allometry completed. Possibly the Stand Height curve may be estimated as well.

### 13.5 Taper and stem form

The form or shape of the tree stem can obviously be very complex. However, since much of forestry deals with even age plantations where defect and multiple branching is minimised by management it is possible to simplify the equations and approaches for this case.

The simple approach is to assume that trees are basically straight and that departures from “straight” (or sweep) are local shearing that do not affect the simple volume formulae being used in the following (like a stack of plates that can individually move by small steps horizontally without changing the amount of “plate”).

The main tree stem is assumed to form the central “spine” of the tree from base to its tip at the tree height. Branches are lesser stems that are supported by the primary

stem. Obviously this is not always the case! It is also usual to parameterise the stem form in terms of proportional distance from the ground to the tip or vice versa. I will use a parameter “s” ( $s = z/h$ ) that is zero at the base and 1.0 at the tip of the stem at tree height.

The main specification is that at any height “z” or value of “s” there is a diameter of the trunk  $d(z)$  or  $d(s)$ . The way this changes with position in the stem is the “taper function” and the basis for the form factor.

The form factor is important as it relates basal area, tree height and tree or stand volume. For an individual tree the general volume equation is that:

$$v = A_r \times h \times ff$$

where  $v$  the volume of the tree (main) stem,  $A_r$  is the cross sectional area at breast (or reference) height and  $ff$  is the stem form factor which will be defined more specifically later. For a stand the corresponding volume density (eg per ha) becomes:

$$V = BA_r \times \bar{h} \times FF$$

where  $V$  is stem volume per ha,  $BA_r$  is the basal area ( $\lambda \bar{A}_r$ ) at reference height,  $\bar{h}$  is the mean height of the trees (some care must be taken to accommodate predominant height or other forms of height measurement) and  $FF$  is the stand form factor.

Form Factors can be simple or complex. Many have been derived for both specific purposes and general use. The simplest choice is to assume the tree stem is a cone with apex at the tree height and the diameter  $d_r$  at the reference height. The form factor is roughly 1/3 in this case. More complex form factors can be based on sample trees where diameter is measured at key places on the stem and the shape assumed to be linear between these locations. This forms the basis for the Pressler Normal Form Factor. In many cases, the highest significant point is at the green level or bole height and the upper section of the stem assumed to taper linearly to the tip of the tree.

Expressed in a general form, the Pressler equation for a single tree can be written:

$$\begin{aligned} v &= \frac{\pi}{4} \int_0^h d^2(z) dz \\ &= \frac{\pi}{4} d_r^2 h \int_0^1 e^2(s) ds \\ &= A_r \times h \times ff \\ e(s) &= d(s) / d_r \\ ff &= \int_0^1 e^2(s) ds \end{aligned}$$

The Pressler method is to estimate  $ff$  from measurements at a number of levels. The form factor must be scaled up to stand level for stand volume estimation and obviously we have skimmed over a few statistical issues that keep statisticians employed by the forestry industry.

In terms of stand volume we can write the Pressler equation in a different way:

$$\begin{aligned}
 V &= \int_0^{\bar{h}} BA(z) dz \\
 &= BA_r \bar{h} \int_0^1 g(s) ds \\
 &= BA_r \times \bar{h} \times FF \\
 g(s) &= \bar{e}^2(s) = \frac{BA(s)}{BA_r} \\
 FF &= \int_0^1 g(s) ds
 \end{aligned}$$

In this definition it is assumed that the basal area is that of the primary stems and that they can be identified as connected objects from the ground up to the tips of the trees. Note also that some people combine  $\bar{h}$  and  $FF$  into another variant on “form factor”.

Above the green level it may be hard to measure the form factor but (as always) there are approximations. It could well be that if the BA is separated into size classes and the height/DBH correlation used to modify the heights then the volume has also been divided into size classes – a very powerful analysis. If the integral is taken up to the mean green level (bole height) then the statistic is for volume of trunks (by size class). Again this is a very useful dis-aggregation of the data.

### 13.6 Deriving Form Factor from EVI data

However the form factor is expressed, there is a good potential for a stand (and possibly later individual tree) form factors to be derived from EVI data. In order to do this we need to look at how the EVI diameter and BA estimation change as we change the level of the analysis.

The first thing to note is that much of the problem has been solved already by cylindrical projection program and so I am assuming that this is the base data format for the work. For example, the other projections present trees that seem to “taper” due to perspective but this projection issue is overcome in the re-projecting to the Cylindrical format. The main issues are magnitude and the threshold value for tree angular width. Assuming the previous work and diagram for the horizontal case, the more general situation is shown in the following Figure 13-13:

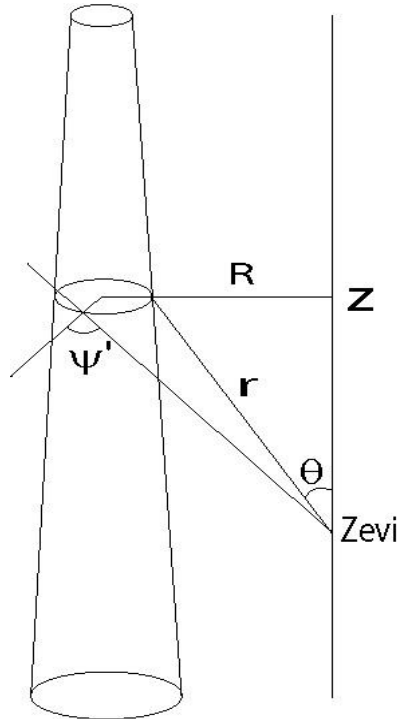


Figure 13-13: Geometry of EVI range and hits at height slice “z”.

The radial distance (R) and height above the ground (z) are the primary coordinates in the re-projected image. The actual range to a hit on the trunk is related to the new coordinates simply by:

$$r = \sqrt{R^2 + (z - z_{evi})^2}$$

In this equation,  $z_{evi}$  is the height of the EVI position above the ground level. This kind of information is contained in the EVI file headers. The original zenith angle of the shot is shown in the Figure 13-13 and can also be calculated (although in practice it is stored in a more accurate form for use) as:

$$\tan \theta = \frac{R}{z}$$

Recalling the expression for the intensity of the data returns around the tree trunk at the height “z” we have:

$$I_t(r) = \frac{K(R)}{R^2} \Phi_0 (r - R) \rho_{app}$$

$$\rho_{app} = P_{int} \langle \cos \psi' \rangle \rho_t$$

I have written the angle as  $\psi'$  for reasons that will become clear soon. That is, provided the value for “r” is modified as above and the new angle computed for the way the intensity will change across the trunk the method is the same. In fact, the new angle can be shown to be:

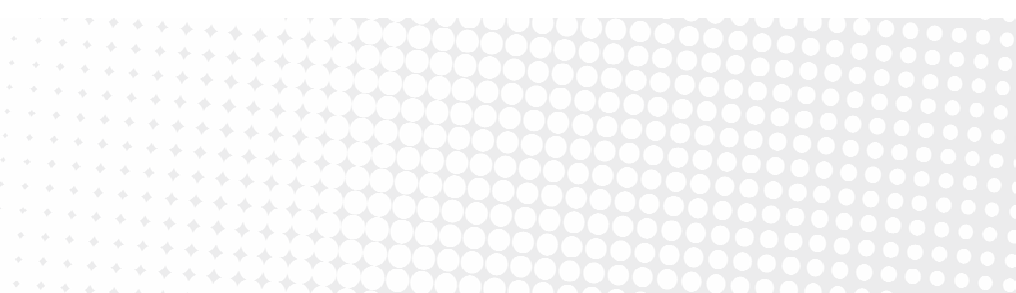
$$\cos \psi' = \sin \theta \cos \psi$$

$$\langle \cos \psi' \rangle = \sin \theta \langle \cos \psi \rangle$$

where now  $\psi$  is the angle as previously calculated for the horizontal case. In addition, since the zenith angles and range change very little over the hits from a single trunk on the same horizontal level, the ratio to the central (maximum) value is identical with the previous case. The main change is to take account of the absolute value (due to changes in both range and zenith angle) when finding the stems.

With this approach, the same basic steps are used at all levels to measure diameters and estimate BA by “Relaskop” principles. There will be added complexity due to the increasing amount of branch and bending as the height increases so that trees stems will need to incorporate more complex measures of continuity with height.

If we thereby obtain basal area as a function of height at points up to the mean green level and assume that above the green level the primary stem tapers linearly to the tip then we have a form factor and information needed for the volume density – possibly by size class as measured by DBH. Obviously, tree branching, multi-stems, sweep and our capacity to separate out the basal area of the primary stems will make this difficult. However, it provides a pathway to the analysis discussed above and to the effective measurement of taper (or form factor) from an ECHIDNA® instrument in a way no other instrument has been able to do on more than a single tree basis.



## Contact Us

Phone: 1 300 363 400

+61 3 9545 2176

Email: [enquiries@csiro.au](mailto:enquiries@csiro.au)

Web: [www.csiro.au](http://www.csiro.au)

## Your CSIRO

Australia is founding its future on science and innovation. Its national science agency, CSIRO, is a powerhouse of ideas, technologies and skills for building prosperity, growth, health and sustainability. It serves governments, industries, business and communities across the nation.